U.S. Department
of Transportation
**Research and
Special Programs
Administration**

Soil Reinforcement in Soft Ground Tunneling

Office of
University Research

EPORT
CONTRACT
81-C-00024

JANUARY 1983
DOT/RSPA/DMA-50/83/15

Technical Report Documentation Page

1. Report No.	2. Government Accession No.	3. Recipient's Catalog No.
DOT/RSPA/DMA-50/83/15		

4. Title and Subtitle	5. Report Date
Soil Reinforcement in Soft Ground Tunneling	December 1982
	6. Performing Organization Code
	8. Performing Organization Report No.
7. Author(s)	
Drs. Sangchul Bang and Chih-Kang Shen	
9. Performing Organization Name and Address	10. Work Unit No. (TRAIS)
Department of Civil Engineering University of Notre Dame Notre Dame, IN 46556	11. Contract or Grant No. DTRS5681-C-00024
	13. Type of Report and Period Covered Final Report
12. Sponsoring Agency Name and Address	
U. S. Department of Transportation Office of University Research 400 7th Street, S. W. Washington, D. C. 20590	14. Sponsoring Agency Code DMA-50

15. Supplementary Notes

Technical Monitor: Andy Sluz

16. Abstract A new technique of reinforcing earth masses around tunnels, known as the spiling reinforcement technique, is illustrated. The system consists of a series of radially installed reinforcing spiles spaced between 2 and 5 ft. with an angle of approximately 30° to the tunnel axis. The spiles are formed by inserting 1-1.5 in. diameter rebars into the holes with subsequent grout.

The principal of this system is to stabilize a weak mass by installing reinforcing elements into the in-situ mass as excavation proceeds. A reinforced mass adjacent to the opening is therefore formed. This method minimizes not only the instantaneous instability but also the permanent deformation. The system has been primarily used in reinforcing tunnels in weak rock formations and proven very successful. The application also involves reinforcing tunnels in soft grounds but in limited occasions due to the lack of proven design methodology.

This report presents the results of the preliminary investigation of the spiling reinforcement system in soft ground tunneling. It includes the development of the analytical method of analysis, the major findings from the parametric study, and the development of the centrifuge model testing program. The analytical method of analysis includes the development of a computer finite element program with the generalized plane strain approach. The model testing program includes the modeling process of tunneling and spiling reinforcement, and the simulation of the excavation procedure in flight.

The objective of this research is to conduct a preliminary study of the spiling reinforcement system regarding its behavior through theoretical and experimental investigations. It is hoped that the research would result in a better understanding of the soft ground tunneling reinforcement technique and the formation of a rational desigh approach for this technique.

17. Key Words	18. Distribution Statement
	Document is available to the U. S. public through the National Technical Information Service, Springfield, Virginia 22161

19. Security Classif. (of this report)	20. Security Classif. (of this page)	21. No. of Pages	22. Price
Unclassified	Unclassified		

METRIC CONVERSION FACTORS

Approximate Conversions to Metric Measures

Symbol	When You Know	Multiply by	To Find	Symbol
	LENGTH			
in	inches	*2.5	centimeters	cm
ft	feet	30	centimeters	cm
yd	yards	0.9	meters	m
mi	miles	1.6	kilometers	km
	AREA			
in^2	square inches	6.5	square centimeters	cm^2
ft^2	square feet	0.09	square meters	m^2
yd^2	square yards	0.8	square meters	m^2
mi^2	square miles	2.6	square kilometers	km^2
	acres	0.4	hectares	ha
	MASS (weight)			
oz	ounces	28	grams	g
lb	pounds	0.45	kilograms	kg
	short tons (2000 lb)	0.9	tonnes	t
	VOLUME			
tsp	teaspoons	5	milliliters	ml
Tbsp	tablespoons	15	milliliters	ml
fl oz	fluid ounces	30	milliliters	ml
c	cups	0.24	liters	l
pt	pints	0.47	liters	l
qt	quarts	0.95	liters	l
gal	gallons	3.8	liters	l
ft^3	cubic feet	0.03	cubic meters	m^3
yd^3	cubic yards	0.76	cubic meters	m^3
	TEMPERATURE (exact)			
°F	Fahrenheit temperature	5/9 (after subtracting 32)	Celsius temperature	°C

*1 in = 2.54 (exactly). For other exact conversions and more detailed tables, see NBS Misc. Publ. 286, Units of Weights and Measures, Price $2.25, SD Catalog No. C13.10:286.

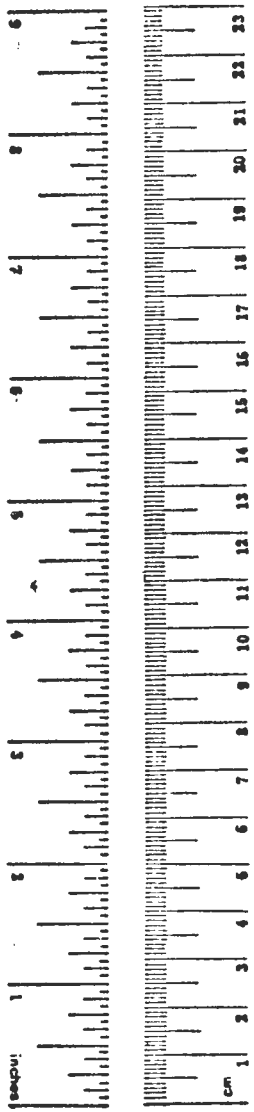

Approximate Conversions from Metric Measures

Symbol	When You Know	Multiply by	To Find	Symbol
	LENGTH			
mm	millimeters	0.04	inches	in
cm	centimeters	0.4	inches	in
m	meters	3.3	feet	ft
m	meters	1.1	yards	yd
km	kilometers	0.6	miles	mi
	AREA			
cm^2	square centimeters	0.16	square inches	in^2
m^2	square meters	1.2	square yards	yd^2
km^2	square kilometers	0.4	square miles	mi^2
ha	hectares (10,000 m^2)	2.5	acres	
	MASS (weight)			
g	grams	0.035	ounces	oz
kg	kilograms	2.2	pounds	lb
t	tonnes (1000 kg)	1.1	short tons	
	VOLUME			
ml	milliliters	0.03	fluid ounces	fl oz
l	liters	2.1	pints	pt
l	liters	1.06	quarts	qt
l	liters	0.26	gallons	gal
m^3	cubic meters	35	cubic feet	ft^3
m^3	cubic meters	1.3	cubic yards	yd^3
	TEMPERATURE (exact)			
°C	Celsius temperature	9/5 (then add 32)	Fahrenheit temperature	°F

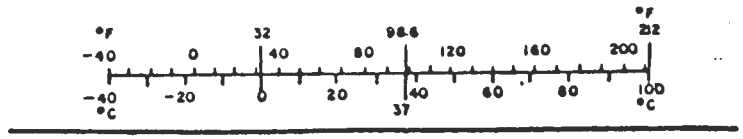

ACKNOWLEDGEMENTS

The work presented in this report is based upon research supported by U.S. Department of Transportation under Contract No. DTRS-5681-C-00024. The authors are extremely grateful for this support. A deep appreciation is extended to the Office of University Research and to Mr. Andrew Sluz, Project Technical Monitor, for providing the opportunity to work on this problem. Mr. Sluz provided direction and helpful comments throughout the study.

Many University personnel contributed to this report. The authors are indebted to Dr. Michael Katona, University of Notre Dame, and Dr. Leonard Herrmann, University of California, Davis, for their help and constructive discussions. The manuscript was typed by Ms. Maureen Miller.

CONTENTS

CHAPTER I

INTRODUCTION

1.1 General

In recent years, the application of earth reinforcement technique has been quite popular and used in a variety of geotechnical engineering structures. In Italy, micro-piles, which are formed by inserting tubular metal linings into drilled holes and filled with compressed mortar, have been successfully used to contain the pressure of the ground against the tunnel face (13). These micro-piles, which essentially reinforce the soil property and thereby increase its strength, make it possible to reduce the soil pressure on the wall of the tunnel excavation. However, since many micro-piles have to be driven from the ground surface to the depth of the projected tunnel, it has limited practical application in populated areas.

Alternatively the reinforcement of soil mass can be performed from the tunnel opening. The New Austrian Tunneling Method is such an example (3). The brief description of the NATM is as follows. A thin layer of shotcrete reinforced by wire mesh and light steel ribs is sprayed immediately after excavation. Soil anchors are then installed to reinforce the surrounding soil mass, which is followed by a construction of a permanent lining. This method reduced the the surface settlement to as little as 1/2 in., compared to approximately 4 in. of settlement in shield method. The construction also resulted in a minimum employment of machines and therefore a reduction in costs. The application involved the subway construction of Metro Nuremburg (D = 32 ft. in soft sandstone formation) and Metro Bochum (D = 38 ft. in medium marl formation) in West Germany (9).

A similar technique has been successfully used in the United States to reinforce weak rock formation on several occasions (8). Fig-1 shows a typical cross section of this system known as the "Spiling Reinforcement" technique.

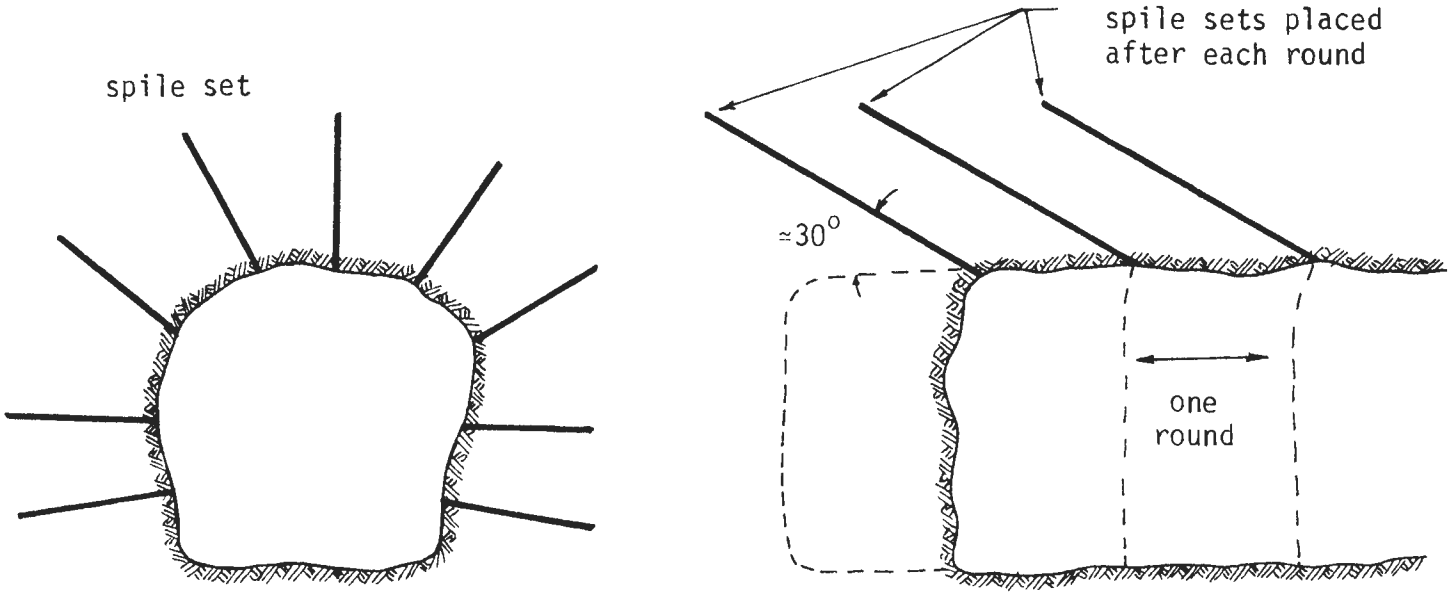

Fig-1 Spiling reinforcement ahead of the face

It consists of a series of radially installed 15-20 ft. long reinforcing spiles spaced between 2 and 5 ft. with an angle of approximately 30° to the horizontal. The reinforcing spiles are formed by inserting 1 - 1.5 in. diameter rebars into the holes with subsequent grout.

The general underlying principle of this system is to stabilize a weak mass by installing reinforcing elements into the in-situ mass as excavation proceeds. A reinforced mass adjacent to the tunnel opening is therefore formed. This reinforcement technique is similar in concept to the rock bolt technique in mining practive. However, when this system is used in soft-ground tunneling, the mechanism becomes quite different from that of rock bolt, since the principal resistance of this system is mobilized by the friction betwen the reinforcing element and the surrounding soil mass. The application of this technique serves to stiffen the soil, to induce higher strength, to make it more resistant to stresses around the opening, and therefore to limit the movement of the soil. The ultimate goal is to improve the ground by preventing loosening (immediate stabilization) and to contribute to the permanent stabilization of the opening by limiting deformations.

By adopting the spiling reinforcement technique in soft ground tunneling, advantages over conventional methods of stabilization may be expected. However the spiling reinforcement technique can not be utilized in pure cohesionless soils (sands and gravels) without additional measures such as grouting, since an excavation has to preceed the installation of any suport system. This system nevertheless could be utilized safely and economically in silty and clayey deposits, as well as glacial tils and weathered rocks which have some stand-up time.

The objective of this research is to conduct a preliminary study of this system regarding its behavior through theoretical and experimental

investigations. It is hoped that the research would result in a better understanding of the soft ground tunneling reinforcement technique and the formation of a rational design aproach for this technique.

1.2 Scope

The investigation covers a period of seventeen months (June 1981 - October 1982). Following is the brief description of the tasks conducted in this investigation.

Task 1: Develop a tool capable of identifying and assessing the parameters that influence the effectiveness of the spiling technique of soil reinforcement as applied to tunneling excavation.

Task 2: Perform a parametric study using the tool developed in Task 1 to identify the pertinent parameters controlling the behavior of the spiling reinforcement system.

Task 3: Conduct preliminary centrifuge scale model tests to develop the capability of the modeling technique to:

a) Model the process of tunneling and spiling reinforcement

b) Simulate tunneling excavation procedure in flight.

c) Develop an optimized plan for conducting scale model tests of the behavior of reinforced and unreinforced tunnels in soft grounds

This report includes the development, the results, and the findings of each task; the description of the analytical method of analysis, the results of the preliminary investigation, the findings from the parametric study, and the development of the centrifuge model testing.

CHAPTER II

DESCRIPTION OF THE ANALYTICAL METHOD OF ANALYSIS

This chapter presents a description of the analytical finite element method of analysis adopted in the study of spiling reinforcement in soft grounds.

2.1 General

The method of analysis to be used in this study must have a capability of closely incorporating the incremental excavation and the soil-reinforcement composite behavior. These factors, which greatly influence the performance of the spiling reinforcement system, favor the use of the finite element method of analysis.

To investigate the behavior of the spiling reinforcement system, an existing two-dimensional plane strain computer finite element program has been expanded to cover the "generalized plane strain" problem. The "generalized plane strain" condition assumes that the plane strain directional strain (ε_z) is zero instead of displacement (δ_z) being zero as commonly used in the conventional plane strain approach. In this way, three dimensional stresses and displacements can be calculated while the finite element grid remains in two dimensions. The generalized plane strain approach was adopted mainly due to the facts that the inclination of the reinforcing spiles can not be modeled effectively by conventional two dimensional approach, and that truly three dimensional analysis is prohibitively expensive and time-consuming. A detailed description of the generalized plane strain approach is included in the subsequent section.

A computer program has been modified and used for the study. A new subroutine, which generates a composite element stiffness matrix for the

generalized plane strain approach, has been developed. The size of the element stiffness matrix is 12 x 12 for quadrilateral elements, since each node has three displacement components. This subroutine requires input of geometric and material properties of the reinforcing spiles (and the shotcrete lining for the elements adjacent to the tunnel opening). The element stiffness matrix of any spile reinforced elements with various degree of reinforcement is then automatically generated and added into a system stiffness matrix. The detailed description of the composite element is included in section 2.3.

2.2 Generalized Plane Strain Condition

The generalized plane strain condition simply requires that no displacement is dependent on z, where z is the coordinate along the plane strain direction. Let's denote u, v and w displacements along x, y and z directions. The generalized plane strain condition leads to

$$\varepsilon_x = \frac{\partial u}{\partial x}$$

$$\varepsilon_y = \frac{\partial v}{\partial y}$$

$$\varepsilon_z = \frac{\partial w}{\partial z} = 0$$

$$\gamma_{xy} = \frac{\partial u}{\partial y} + \frac{\partial v}{\partial x}$$

$$\gamma_{xz} = \frac{\partial u}{\partial z} + \frac{\partial w}{\partial x} = \frac{\partial w}{\partial x}$$

$$\gamma_{yz} = \frac{\partial v}{\partial z} + \frac{\partial w}{\partial y} = \frac{\partial w}{\partial y}$$

The usual constitutive relationship in x-y-z coordinate is

$$\{\sigma\} = [C]\{\varepsilon\}$$

Using linear approximation of displacements between nodes, one can obtain the approximate solution of displacements

$$\hat{u} = \sum_{i=1}^{4} u_i N_i$$

$$\hat{v} = \sum_{i=1}^{4} v_i N_i$$

$$\hat{w} = \sum_{i=1}^{4} w_i N_i$$

where u_i, v_i and w_i are approximate nodal displacements and N_i is a first order shape function.

The strain components are then

$$\varepsilon_x = \frac{\partial u}{\partial x} \simeq \frac{\partial \hat{u}}{\partial x} = \frac{\partial}{\partial x}\left[\sum_{i=1}^{4} u_i N_i\right] = \sum_{i=1}^{4} u_i F_i$$

where

$$F_i = \frac{\partial N_i}{\partial x}$$

Similarly, one can obtain

$$\varepsilon_y = \sum_{i=1}^{4} v_i G_i$$

$$\gamma_{xy} = \sum_{i=1}^{4} [u_i G_i + v_i F_i]$$

$$\gamma_{xz} = \sum_{i=1}^{4} w_i F_i$$

and

$$\gamma_{yz} = \sum_{i=1}^{4} w_i G_i$$

where

$$G_i = \frac{\partial N_i}{\partial y}$$

After some manipulation, one can obtain

$$\frac{\partial U}{\partial u_i} = \int_{-1}^{1}\int_{-1}^{1} \left\{ \sum_{j=1}^{4} [C_{11}F_iF_j + C_{44}G_iG_j + C_{14}(F_iG_j + F_jG_i)]\, u_j \right.$$

$$+ \sum_{j=1}^{4} [C_{44}F_jG_i + C_{12}F_iG_j + C_{14}F_iF_j + C_{24}G_iG_j]\, v_j$$

$$\left. + \sum_{j=1}^{4} [C_{15}F_iF_j + C_{16}F_iG_j + C_{45}F_jG_i + C_{46}G_iG_j]\, w_j \right\} |J| d\xi d\eta$$

$$\frac{\partial U}{\partial v_i} = \int_{-1}^{1}\int_{-1}^{1} \left\{ \sum_{j=1}^{4} [C_{12}G_iF_j + C_{24}G_iG_j + C_{14}F_iF_j + C_{44}F_iG_j]\, u_j \right.$$

$$+ \sum_{j=1}^{4} [C_{22}G_iG_j + C_{24}(F_jG_i + F_iG_j) + C_{44}\, F_iF_j]\, v_j$$

$$\left. + \sum_{j=1}^{4} [C_{25}G_iF_j + C_{26}G_iG_j + C_{45}F_iF_j + C_{46}F_iG_j]\, w_j \right\} |J| d\xi d\eta$$

$$- \sum_{n=1}^{N}\sum_{m=1}^{M} \{F_y\, N_i\}_{n,m}\, |J|_{n,m}\, W_n\, W_m$$

$$\frac{\partial U}{\partial w_i} = \int_{-1}^{1}\int_{-1}^{1} \left\{ \sum_{j=1}^{4} [C_{15}F_iF_j + C_{45}F_iG_j + C_{16}F_jG_i + C_{46}G_iG_j]\, u_j \right.$$

$$+ \sum_{j=1}^{4} [C_{25}F_jG_j + C_{45}F_iF_j + C_{26}G_iG_j + C_{46}G_iF_j]\, v_j$$

$$\left. + \sum_{j=1}^{4} [C_{55}F_iF_j + C_{56}(F_iG_j + G_iF_j) + C_{66}G_iG_j]\, w_j \right\} |J| d\xi d\eta$$

where U = total strain energy

C_{ij} = coefficients of matrix [C]

$|J|$ = determinant of Jacobian matrix

ξ, η = local coordinates

and F_y = body force

This leads to the element stiffness matrix $[S]_{12 \times 12}$ and the element load vector $\{R\}_{12}$ of the quadrilateral element in the generalized plane strain condition.

2.3 Composite Element

The representation of the reinforced system in this study is an expansion of the composite element model proposed by Romstad (14). This model expresses the orthotropic composite material properties as functions of the properties of each of the constituent materials, i.e., the soil and the reinforcement, and their geometric arrangement.

The composite element approach is based on the concept of "unit cell", which is an isolated small unit of the material that completely exhibits its composite characteristics. The schematic diagram of the unit cell is shown in Fig-2. The average values of the stresses distributed over the cell faces, in this approach, are equal to the stresses in the equivalent composite material, and the average values of the strains for the cell are those of the composite. The desired composite properties may therefore be calculated from a detailed consideration of the behavior of the unit cell. These composite properties may then be used in the analysis of the composite structure. Such an analysis yields the composite stress and strain throughout the system; once the composite stress state is determined at a particular point in the system, the corresponding constituent stress states, e.g., the soil and the reinforcement, may be determined by returning to the analysis of the unit cell.

The constitutive relationship for the composite element developed by Romstad is as follows

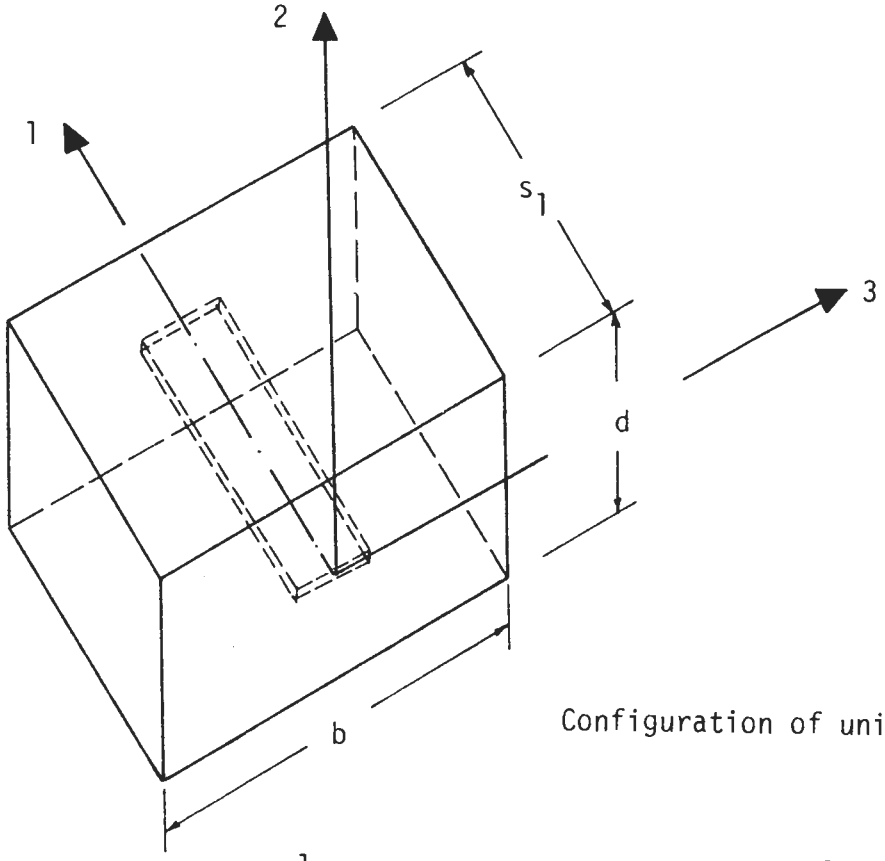

Configuration of unit cell

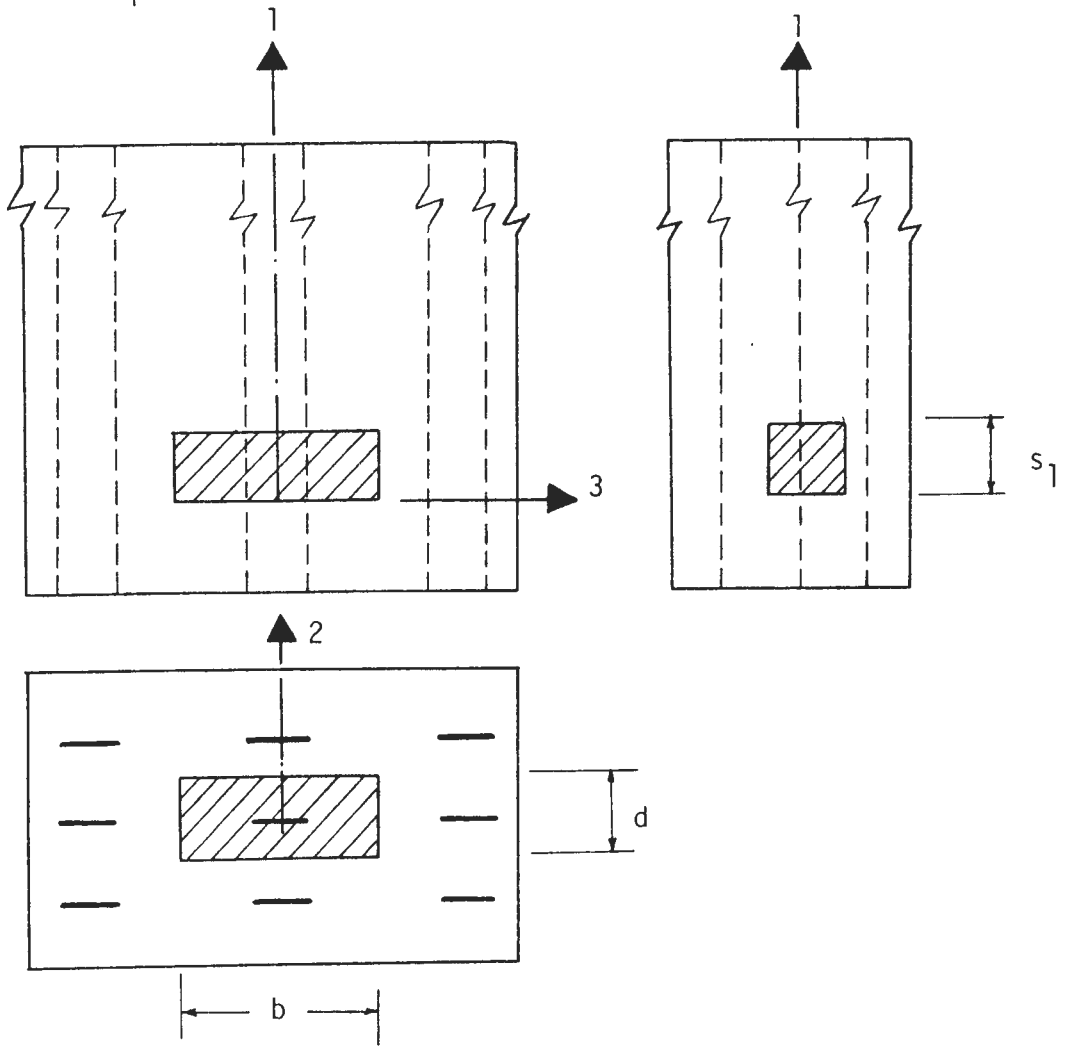

Fig-2 Unit cell

$$\begin{Bmatrix} \varepsilon_1 \\ \varepsilon_2 \\ \varepsilon_3 \\ \gamma_{12} \\ \gamma_{13} \\ \gamma_{23} \end{Bmatrix} = \begin{bmatrix} S_{11} & S_{12} & S_{13} & 0 & 0 & 0 \\ S_{21} & S_{22} & S_{23} & 0 & 0 & 0 \\ S_{31} & S_{32} & S_{33} & 0 & 0 & 0 \\ 0 & 0 & 0 & S_{44} & 0 & 0 \\ 0 & 0 & 0 & 0 & S_{55} & 0 \\ 0 & 0 & 0 & 0 & 0 & S_{66} \end{bmatrix} \begin{Bmatrix} \sigma_1 \\ \sigma_2 \\ \sigma_3 \\ \tau_{12} \\ \tau_{13} \\ \tau_{23} \end{Bmatrix}$$

where $S_{11} = \dfrac{1}{E^{SO}(1+\alpha)}$

$S_{12} = -\nu^{SO} S_{11}$

$S_{13} = S_{12} = S_{21} = S_{31}$

$S_{22} = \{1 + \alpha(1 - \nu^{SO^2})\} S_{11}$

$S_{23} = -\nu^{SO} \{1 + \alpha(1 + \nu^{SO})\} S_{11}$

$S_{32} = S_{23}$

$S_{33} = S_{23}$

$S_{44} = S_{55} = S_{66} = \dfrac{1}{G^{SO}}$

$\alpha = \dfrac{A^{SP} E^{SP}}{A^{C} E^{SO}}$

E^{SO} = modulus of the soil

ν^{SO} = Poisson's ratio of the soil

G^{SO} = shear modulus of the soil

A^{SP} = cross-sectional area of the reinforcement

E^{SP} = modulus of the reinforcement

A^{C} = composite cross-section

The unit cell for spiling reinforcement system is shown in Fig-3. The 1-axis in the figure is chosen parallel to the spile and the 2-axis passes through the center of the tunnel. A plane defined by the 2 and 3 axes is perpendicular to the spile axis. For a given reinforcing pattern, all spiles in the 1-2 plane are assumed to be equally spaced.

The incorporation of the proposed constitutive relationship in local coordinates into global coordinates (x,y and z) requires two transformations; first, rotation from 1-2-3 coordinates to 3-T-z coordinates and second from 3-T-z coordinates to x-y-z coordinates. The former is a rotation about the 3-axis whereas the latter is a rotation about the z-axis. In matrix notation,

$$\{\sigma\}_{xyz} = [B]\ \{\sigma\}_{3Tz}$$

$$\{\sigma\}_{3Tz} = [A]\ \{\sigma\}_{123}$$

where [A] and [B] are transformation matrices.

$$[A] = \begin{bmatrix} 0 & 0 & 1 & 0 & 0 & 0 \\ \sin^2\phi' & \cos^2\phi' & 0 & \sin 2\phi' & 0 & 0 \\ \cos^2\phi' & \sin^2\phi' & 0 & -\sin 2\phi' & 0 & 0 \\ 0 & 0 & 0 & 0 & \sin\phi' & \cos\phi' \\ 0 & 0 & 0 & 0 & \cos\phi' & -\sin\phi' \\ \frac{\sin 2\phi'}{2} & -\frac{\sin 2\phi'}{2} & 0 & \cos 2\phi' & 0 & 0 \end{bmatrix}$$

$$[B] = \begin{bmatrix} \cos^2\alpha & \sin^2\alpha & 0 & -\sin 2\alpha & 0 & 0 \\ \sin^2\alpha & \cos^2\alpha & 0 & \sin 2\alpha & 0 & 0 \\ 0 & 0 & 1 & 0 & 0 & 0 \\ \frac{\sin 2\alpha}{2} & -\frac{\sin 2\alpha}{2} & 0 & \cos 2\alpha & 0 & 0 \\ 0 & 0 & 0 & 0 & \cos\alpha & -\sin\alpha \\ 0 & 0 & 0 & 0 & \sin\alpha & \cos\alpha \end{bmatrix}$$

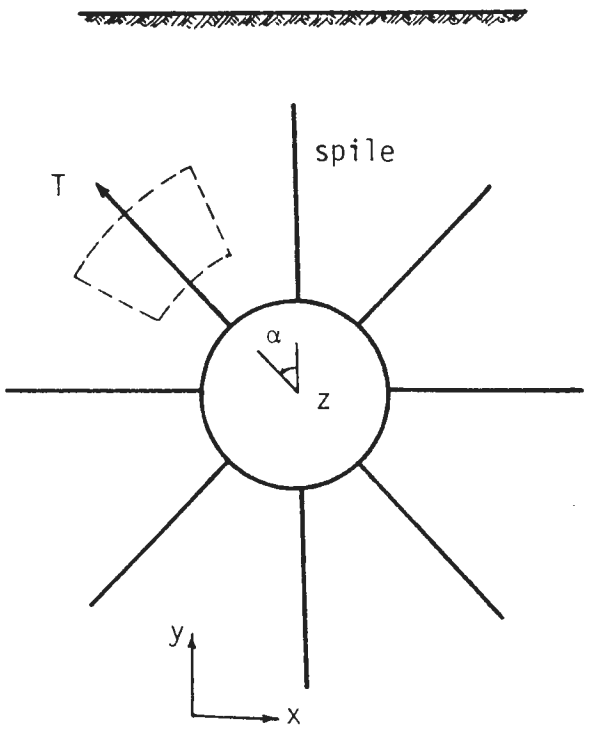

α: measured CCW from crown

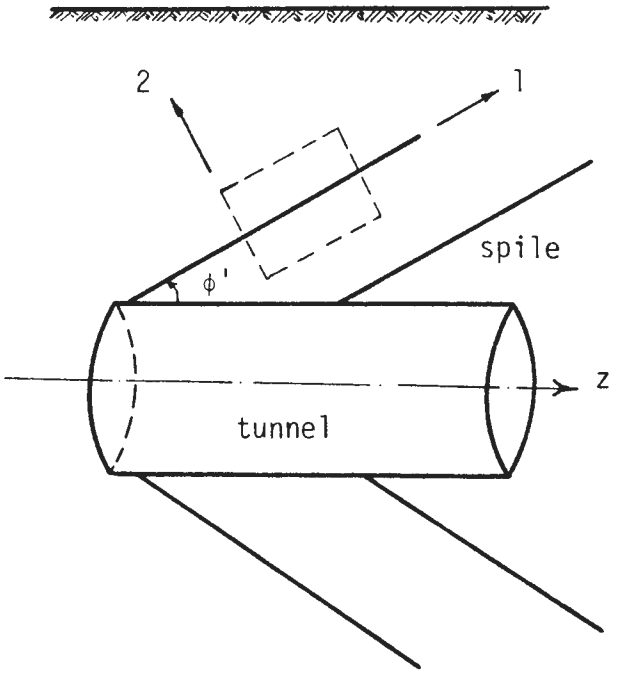

φ': spile inclination angle

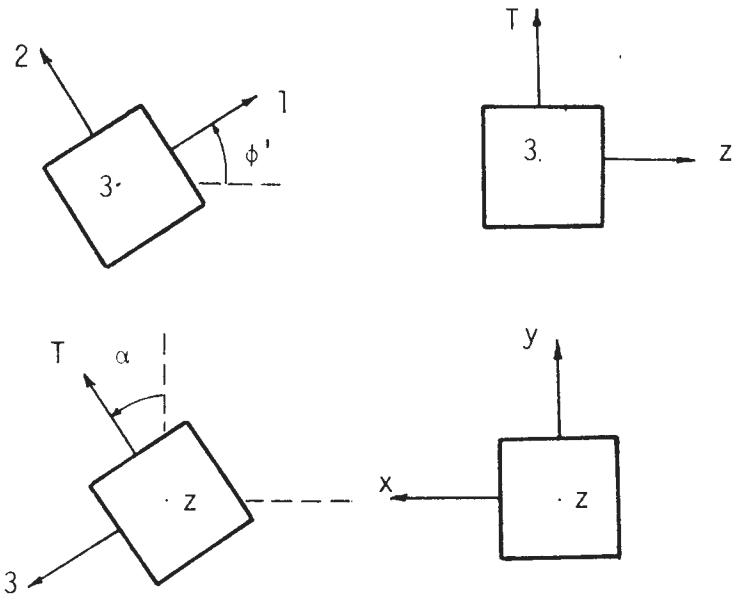

Fig-3 Unit cell for spiling reinforcement system

Once matrices [A] and [B] are formed, the constitutive relationship in x-y-z coordinates can be obtained.

$$\{\sigma\}_{xyz} = [B]\,[A]\,\{\sigma\}_{123}$$

$$= [B]\,[A]\,[S]^{-1}\{\varepsilon\}_{123}$$

$$= [B]\,[A]\,[S]^{-1}\,[A']^{-1}\,[B']^{-1}\{\varepsilon\}_{xyz}$$

since $[A]^T = [A']^{-1}$ and $[B]^T = [B']^{-1}$,

$$\{\sigma\}_{xyz} = [BAS^{-1}A^TB^T]\,\{\varepsilon\}_{xyz}$$

$$= [E]\,\{\varepsilon\}_{xyz}$$

The developed stress within the reinforcing spile can be obtained from the "unit cell" formulation, once the stresses $\{\sigma\}_{xyz}$ are obtained. The calcluation involves the following steps.

$$\{\sigma\}_{xyz} = [B]\,[A]\,\{\sigma\}_{123}$$

and $$\{\varepsilon\}_{123} = [A']^{-1}\,[B']^{-1}\,\{\varepsilon\}_{xyz}$$

where $[A]^T = [A']^{-1}$ and $[B]^T = [B']^{-1}$

Therefore $$\{\varepsilon\}_{123} = [A]^T\,[B]^T\,\{\varepsilon\}_{xyz}$$

$$= [BA]^T\,\{\varepsilon\}_{xyz}$$

or $$\varepsilon_1 = \sum_{j=1}^{6} [BA]_{j,1}\,\{\varepsilon\}_{\substack{xyz \\ j}}$$

where ε_1 is a composite strain along the axial direction of the spile. The developed spile stress can therefore be easily obtained by

$$\sigma_{spile} = E_{spile}\,\varepsilon_1$$

2.4 Shotcrete Lining

The shotcrete concrete lining reinforced with re-bars is modeled in the analysis by membrane elements. This is mainly due to the fact that the shotcrete

lining is relatively thin and flexible. It is also much easier and economical to be included in the finite element formulation, since no separate elements for the shotcrete lining are necessary in the analysis. The effect of the shotcrete lining can be directly added to the element stiffness matrix of the composite element adjacent to the shotcrete lining. Following is a brief description of the membrane element model adopted in the study.

Fig-4 shows a general membrane element with thickness "t" and length "ℓ". General constitutive relationship for the membrane element is

$$\begin{Bmatrix} \sigma_{x'} \\ \sigma_{z'} \\ \tau_{x'z'} \end{Bmatrix} = \begin{bmatrix} C_{11} & C_{12} & 0 \\ C_{12} & C_{22} & 0 \\ 0 & 0 & C_{33} \end{bmatrix} \begin{Bmatrix} \varepsilon_{x'} \\ \varepsilon_{z'} \\ \gamma_{x'z'} \end{Bmatrix} \qquad (1)$$

where

$$\left.\begin{aligned} \varepsilon_{x'} &= \frac{\partial u'}{\partial x'} \\ \varepsilon_{z'} &= \frac{\partial w'}{\partial z'} = 0 \\ \text{and } \gamma_{x'z'} &= \frac{\partial u'}{\partial z'} + \frac{\partial w'}{\partial x'} = \frac{\partial w'}{\partial x'} \end{aligned}\right\} \qquad (2)$$

Note that $\frac{\partial}{\partial z'} = 0$ due to generalized plane strain condition. From the figure, it is obvious that

$$x' = x_0 + \xi \frac{\ell}{2}$$

$$\text{and } \frac{\partial}{\partial x'} = \frac{\partial}{\partial \xi} \frac{\partial \xi}{\partial x'} = \frac{2}{\ell} \frac{\partial}{\partial \xi}$$

Also

$$u' = \frac{1}{2} u_1' (1-\xi) + \frac{1}{2} u_2' (1+\xi)$$

$$= \frac{1}{2}[(u_2' + u_1') + \xi (u_2' - u_1')]$$

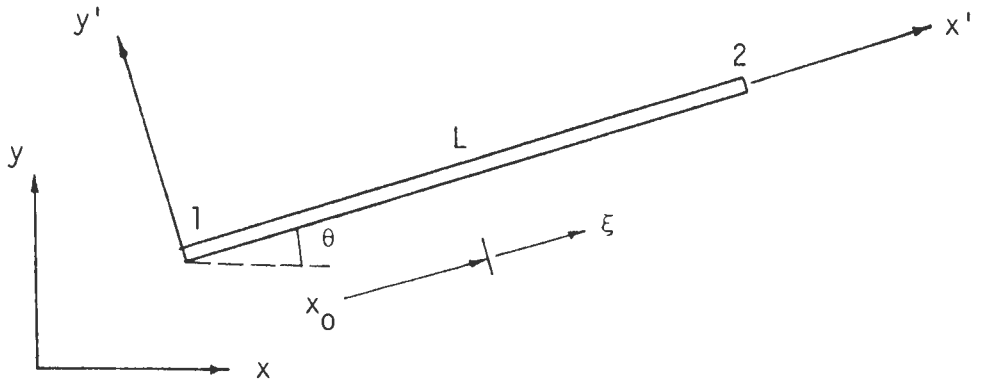

x,y : global coordinates

x',y' : local coordinates

ξ : distance along x' measured from middle of the element

Fig-4 Membrane element representation

and $w' = \frac{1}{2} w'_1 (1-\xi) + \frac{1}{2} w'_2 (1+\xi)$

$$= \frac{1}{2}\left[(w'_2 + w'_1) + \xi (w'_2 - w'_1)\right]$$

where $u'_1 = x'_1$ directional displacements of node 1, etc.

Since
$$\left.\begin{aligned} u'_1 &= u_1 \cos\theta + v_1 \sin\theta \\ v'_1 &= -u_1 \sin\theta + v_1 \cos\theta \\ w'_1 &= w_1 \\ u'_2 &= u_2 \cos\theta + v_2 \sin\theta \\ v'_2 &= -u_2 \sin\theta + v_2 \cos\theta \\ \text{and} \quad w'_2 &= w_2 \end{aligned}\right\} \qquad (3)$$

where u,v and w are the displacements on x-y-z coordinates.

Substituting equations (3) into (2), equations (2) into (1), and equation (1) into the strain energy expression yields

$$U = \frac{t}{4\ell} \int_{-1}^{1} [C_{11} \{(u_2 - u_1) \cos\theta + (v_2 - v_1) \sin\theta\}^2 + C_{33}(w_2 - w_1)^2] d\xi$$

To obtain the element stiffness matrix, one must differentiate the strain energy with respect to nodal unknowns, i.e.,

$$\frac{\partial U}{\partial u_{n1}} = \frac{t}{4\ell} \int_{-1}^{1} 2C_{11}\{(u_{n2} - u_{n1}) \cos\theta + (v_{n2} - v_{n1}) \sin\theta\}(-\cos\theta) d\xi$$

$$= \frac{-tC_{11} \cos\theta}{\ell} [-u_{n1} \cos\theta + u_{n2} \cos\theta - v_{n1} \sin\theta + v_{n2} \sin\theta]$$

$$\frac{\partial U}{\partial u_{n2}} = \frac{tC_{11} \cos\theta}{\ell} [-u_{n1} \cos\theta + u_{n2} \cos\theta - v_{n1} \sin\theta + v_{n2} \sin\theta]$$

$$\frac{\partial U}{\partial v_{n1}} = \frac{t}{4\ell} \int_{-1}^{1} 2C_{11}\{(u_{n2} - u_{n1})\cos\theta + (v_{n2} - v_{n1})\sin\theta\}(-\sin\theta)d\xi$$

$$= \frac{-tC_{11}\sin\theta}{\ell}[-u_{n1}\cos\theta + u_{n2}\cos\theta - v_{n1}\sin\theta + v_{n2}\sin\theta]$$

$$\frac{\partial U}{\partial v_{n2}} = \frac{tC_{11}\sin\theta}{\ell}[-u_{n1}\cos\theta + u_{n2}\cos\theta - v_{n1}\sin\theta + v_{n2}\sin\theta]$$

$$\frac{\partial U}{\partial w_{n1}} = \frac{t}{4\ell} \int_{-1}^{1} 2C_{33}(w_{n2} - w_{n1})(-1)d\xi$$

$$= \frac{-tC_{33}}{\ell}(-w_{n1} + w_{n2})$$

$$\frac{\partial U}{\partial w_{n2}} = \frac{tC_{33}}{\ell}(-w_{n1} + w_{n2})$$

Finally the following element stiffness matrix of the membrane element is obtained.

$$\begin{bmatrix} S_{11} & S_{12} & 0 & -S_{11} & -S_{12} & 0 \\ S_{12} & S_{22} & 0 & -S_{12} & -S_{22} & 0 \\ 0 & 0 & S_{33} & 0 & 0 & -S_{33} \\ -S_{11} & -S_{12} & 0 & S_{11} & S_{12} & 0 \\ -S_{12} & -S_{22} & 0 & S_{12} & S_{22} & 0 \\ 0 & 0 & -S_{33} & 0 & 0 & S_{33} \end{bmatrix}$$

where $S_{11} = \frac{t}{\ell} C_{11}\cos^2\theta$

$S_{12} = \frac{t}{\ell} C_{11}\cos\theta\sin\theta$

$S_{22} = \frac{t}{\ell} C_{11}\sin^2\theta$

and $S_{33} = \frac{t}{\ell} C_{33}$

To completely define the element stiffness matrix of the membrane element, C_{11} and C_{33} need to be defined. Since the shotcrete lining is reinforced with small diameter re-bars in both directions as shown in Fig-5, it may be reasonable to assume that the re-bars have no resistance against shear. This leads to

$$A_C \tau_{x'z'} = A_T G_C \gamma_{x'z'}$$

where

A_C = area of the shotcrete concrete in the unit cell

A_T = total area

G_C = shear modulus of the shotcrete concrete

Since $C_{33} = \dfrac{\tau_{x'z'}}{\gamma_{x'z'}}$ from the constitutive relationship,

$$C_{33} = \frac{A_T G_C}{A_C}$$

$$= \frac{A_T E_C}{2A_C(1+\nu_C)}$$

where E_C and ν_C are the modulus and the Poisson's ratio of the shotecrete concrete.

Coefficient C_{11} can be obtained simply from the equilibrium along the x' axis, $F_{total} = F_{re\text{-}bar} + F_{concrete}$.

Or

$$A_T \sigma_{x'} = A_S E_S \varepsilon_{x'} + A_C \frac{E_C}{1-\nu_C^2} \varepsilon_{x'}$$

therefore $C_{11} = \dfrac{\sigma_{x'}}{\varepsilon_{x'}}$

$$= \frac{A_S}{A_T} E_S + \frac{A_C}{A_T} \frac{E_C}{1-\nu_C^2}$$

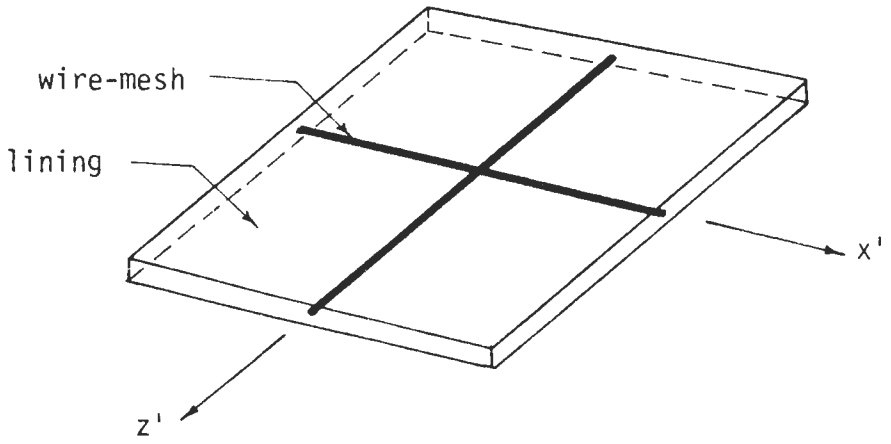

Fig-5 Unit cell of shotcrete concrete lining

where E_S = modulus of the re-bar

A_S = area of the re-bar in the unit cell

2.5 Simulation of Field Conditions

The finite element computer program consists of two increments; first for the simulation of in-situ stress conditions, and second for the installation of the reinforcing spiles and the shotcrete lining as well as the tunnel excavation. Note that no displacement is allowed in the first increment.

The soil model employed in the study is a characterization proposed by Duncan et al.(5). This nonlinear inelastic model has been used to describe the constitutive behavior of the soil. It assumes that the soil does not experience stress or strain induced anisotropy, i.e., the soil may at all times be described by instantaneous values of modulus E_S and poisson's ratio ν. The equation used for expressing E_S as a function of the soil type and the stress state (i.e., the stress state for the midpoint of the increment) is given in the form:

$$E_S = \left[1 - \frac{R_f(1 - \sin\phi)(\sigma_1 - \sigma_3)}{2\,C\cos\phi + 2\sigma_3 \sin\phi}\right]^2 KP_a \left\{\frac{\sigma_3}{P_a}\right\}^n$$

In order to ensure numerical stability, the property is not allowed to fall below $0.001\,KP_a$. In the study, however, a constant Poisson's ratio of 0.3 has been adopted to avoid any unrealistic ground surface movements. The summary of the parameters in the characterization is listed in Table -1.

The values of the principal stresses σ_1 and σ_3 are established by the iteration process. For the first iteration of the first increment, the state of stress is estimated as follows: σ_1 is taken to be $0.5\,\gamma h$, where h is the depth to the center of the element below the surface and $\sigma_3 = 0.43\,\sigma_1$; as iteration proceeds, this estimate is of course modified.

Table 1. Summary of the Hyperbolic Parameters

Parameter	Name	Function
K, K_{ur}	Modulus number-loading, unloading	Relate E_i and E_{ur} to σ_3
n	Modulus exponent	
c	Cohesion intercept	Relate $(\sigma_1 - \sigma_3)_f$ to σ_3
ϕ	Friction angle	
R_f	Failure ratio	Relates $(\sigma_1 - \sigma_3)_{ult}$ to $(\sigma_1 - \sigma_3)_f$

Duncan's characterization is based on the generalized Hooke's law and therefore, most suitable for analysis of stresses and deformations prior to failure. For many situations it is capable of predicting nonlinear relationships between loads and movements in a stable earth mass. In addition, it has been found that the finite element predictions based on Duncan's characterization are in reasonable agreement with experimental measurements for failure and near failure conditions.

CHAPTER III

PRELIMINARY INVESTIGATION

This chapter presents the results of the comparison between the spile reinforced and the unreinforced tunnels. It also provides the effect of the spile inclination angle to the performance of the system.

3.1 General

To develop an understanding of the spiling reinforcement system in soft grounds, first a quantitative comparison was made between the performance of the spile reinforced tunnel and that of the unreinforced tunnel. Second the effect of the spile inclination was investigated in detail. The study was performed using the developed generalized plane strain computer program.

The investigation was limited to the study of a single horizontal circular tunnel. Typical finite element mesh used in the study was as shown in Fig-6. The soil elements are isoparametric quadrilateral elements (triangular elements for those to be excavated). The shaded portion in the figure represents the soil elements reinforced with spiles, and the shotcrete lining is indicated by thick lines.

For the purpose of this investigation, two soil types were chosen; namely silty clay and low plasticity clay. Their pertinent properties in terms of Duncan's characterization are listed in Table-2. In addition, the following geometrical parameters were used:

Depth to the tunnel center (H) = 50 ft.

Diameter of the tunnel (D) = 20 ft.

Length of the reinforcing spiles (L) = 20 ft.

Spacing of the reinforcing spiles (S) = 5 ft.

Diameter of the reinforcing spiles (d) = 4 in.

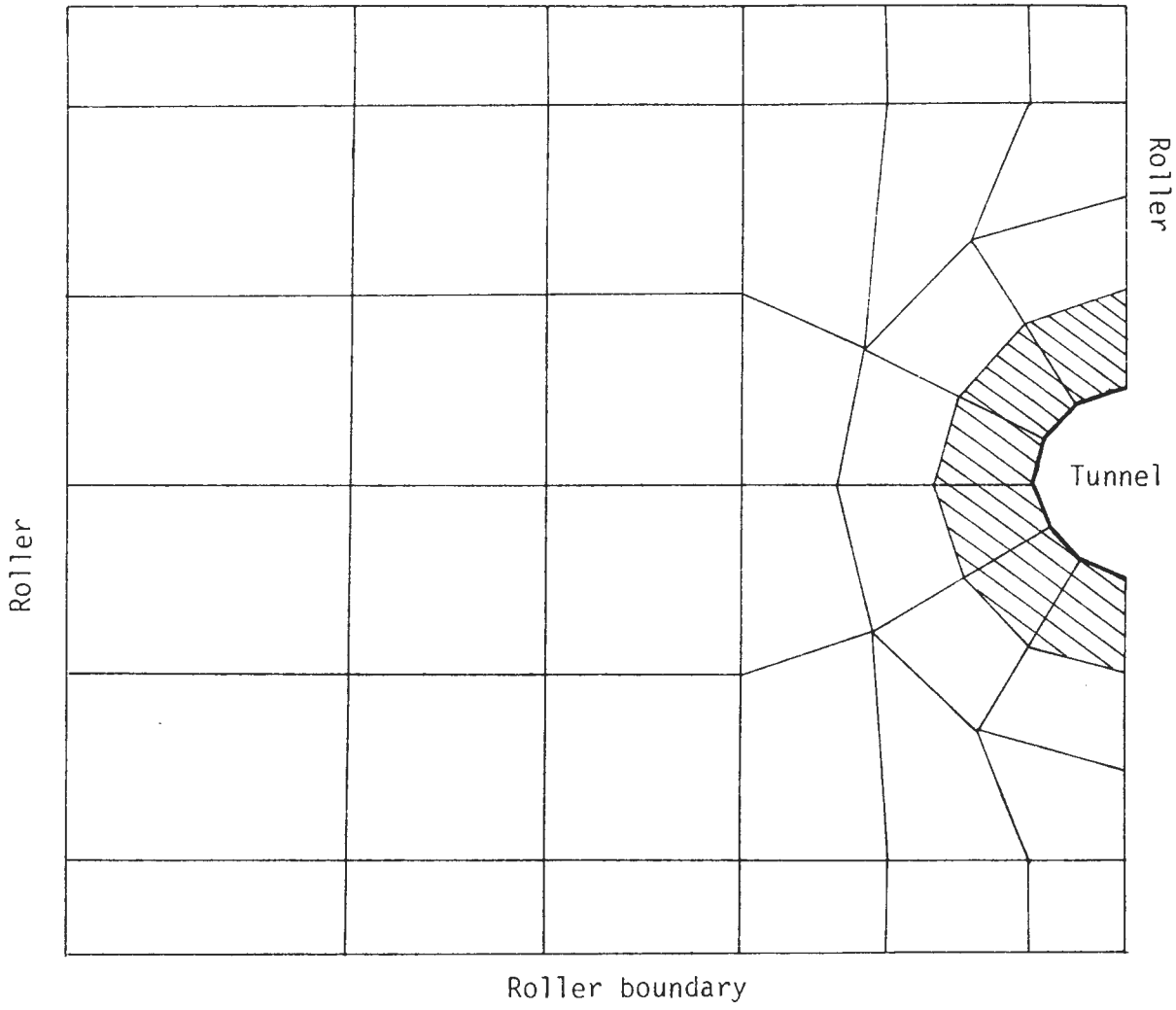

Fig-6 Typical finite element grid

TABLE-2

Soil Properties

	Soil #1	Soil #2
Description	SM	CL
Loading modulus (K)	200	120
Unloading modulus* (K_{ur})	330	198
Modulus exponent (n)	0.6	0.45
Failure ratio (R_f)	0.7	0.7
Cohesion (C) in psi	2.778	2.083
Friction angle (ϕ) in degrees	33	30
Poisson's ratio (ν)	0.3	0.3

*For soil #1, K_{ur} = 1.5 K

For soil #2, K_{ur} = 1.65 K

These values were chosen based on the following observations:

1. The depths to the tunnel center in most shallow tunneling projects - Washington, D.C. Metro (1975), Frankfurt (1975), Brussel Metro (1969), etc. - are approximately 50 ft. (4).
2. The diameter of the tunnels in most projects ranges from 16 ft. to 25 ft.
3. Korbin (7) reported that the region most susceptible to deterioration is within one-half radius from the opening where approximately two thirds of the total deformation occurs. Further than one radius from the opening the strains are low and the confinement is high such that any increase in strength related to the presence of the reinforcement is small. Length of the reinforcing spiles equal to the diameter of the tunnel with an inclination of 30° is equivalent to reinforced zone of one radius from the opening.
4. In practice, grouted reinforcing spiles have spacings between 2 and 5 ft. (2).

The rest of the parameters defining the entire system including the properties of the shotcrete lining are indicated in Table-3.

3.2 Comparison Between Reinforced and Unreinforced Tunnels

Using the spile inclination angle of 30°, the following observations were obtained.

3.2.1 Tunnel Deformation

In comparison with the unreinforced tunnel, the reinforced tunnel produces very small deformations as expected. Fig-7 shows the results of tunnel deformations for soil #1. To indicate the effectiveness of the spiling reinforcement in soft ground tunneling, the percentage reduction in total displacement is

TABLE-3

Additional Parameters

Thickness of the lining:	4 in.
Spacing of the re-bars in the lining:	4 in.
Diameter of the re-bars in the lining:	$\frac{1}{6}$ in.
Modulus of the lining material:	2,000 ksi
Modulus of the re-bars:	30,000 ksi
Composite modulus of the spiles:	1,875 ksi
Composite yield stress of the spiles:	3,125 psi

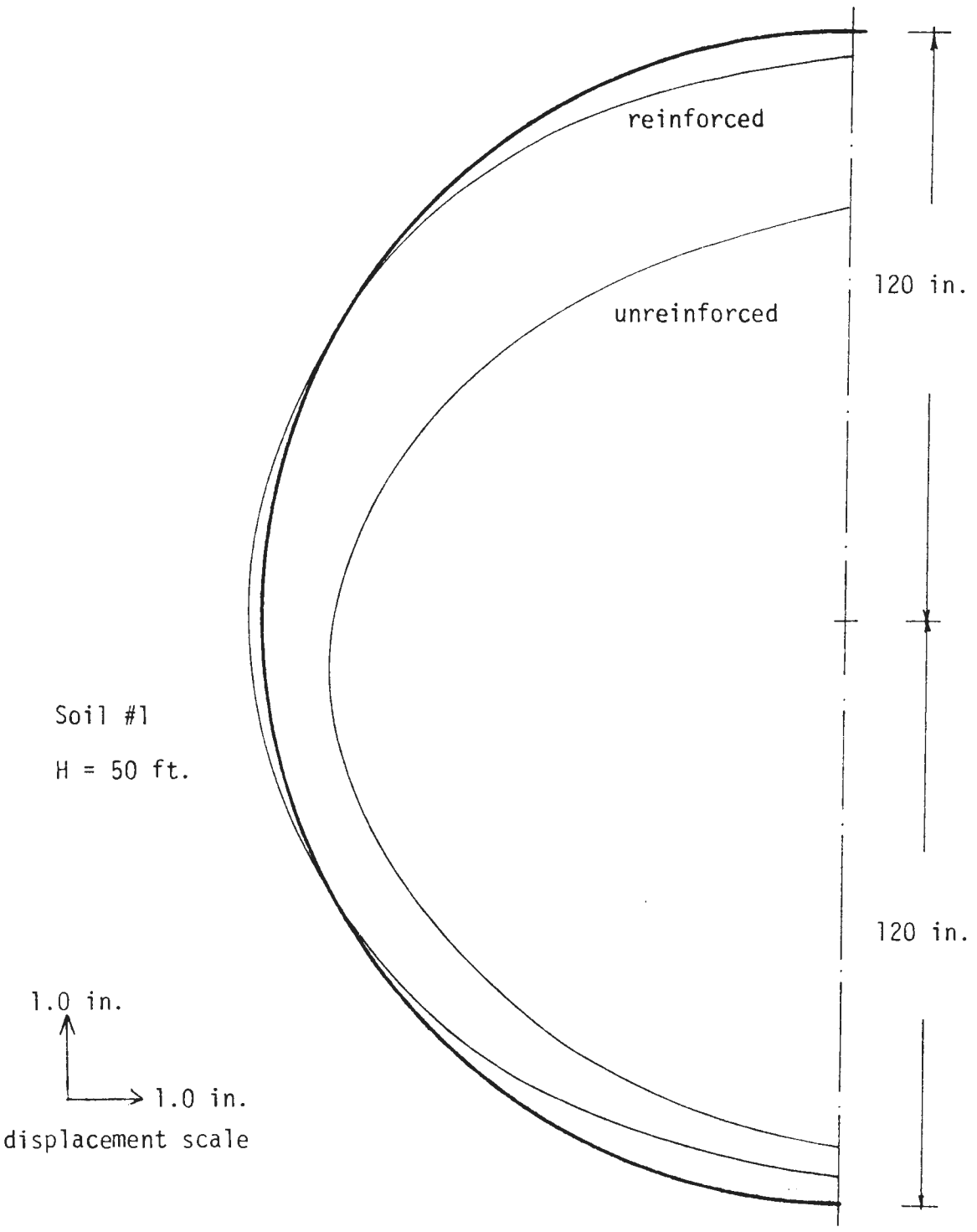

Fig-7 Deformation of the tunnel

calculated for the crown and bottom of the tunnels and included in Table-4, where

$$\% \text{ reduction} = \frac{\delta_{\text{unreinforced}} - \delta_{\text{reinforced}}}{\delta_{\text{unreinforced}}} \times 100$$

From this analysis, it is quite obvious that the spiling reinforcement reduces the crown settlement and the bottom heave by approximately 90% and 50% respectively.

3.2.2 Ground Surface Displacements

The vertical and horizontal ground surface displacements are also significantly reduced by the presence of spiling reinforcement. Fig-8 and 9 show the vertical displacements for soil #1 and #2 respectively. The magnitude of the surface displacements both in vertical and horizontal directions of reinforced system is approximately one tenth of those of unreinforced systems, as can be seen in Table-5.

Another way of interpreting the ground surface displacements is in terms of distortions; vertical distortion and horizontal distortion. Vertical distortion is the differential vertical movements between two adjacent points divided by the distance separating them. Horizontal distortion is defined in a similar manner for the differential horizontal movements. Previous studies indicate that the surface distrotions are the main causes of the damage of the structures near the excavation (6,10,12,15). The detailed damage criteria of various types of structures due to surface distortions can be found in the reference (1).

Fig-10 shows one of the example plots of the vertical distortion of the ground surface for soil #2. As can be seen from the figure, it is obvious that the maximum vertical distortion does not take place directly above the tunnel center, but at some distance away from the center line. This is due to the shape of the surface settlement trough (Fig-8 and 9), in which maximum

TABLE-4

Comparison of Tunnel Deformations

Soil #1

	Unreinforced Tunnel	Reinforced Tunnel	% Reduction
Crown Settlement	-4.44 in.	-0.57 in.	87%
Bottom Heave	1.40 in.	0.72 in.	48%

Soil #2

	Unreinforced Tunnel	Reinforced Tunnel	% Reduction
Crown Settlement	-8.85 in.	-0.79 in.	91%
Bottom Heave	2.53 in.	1.25 in.	51%

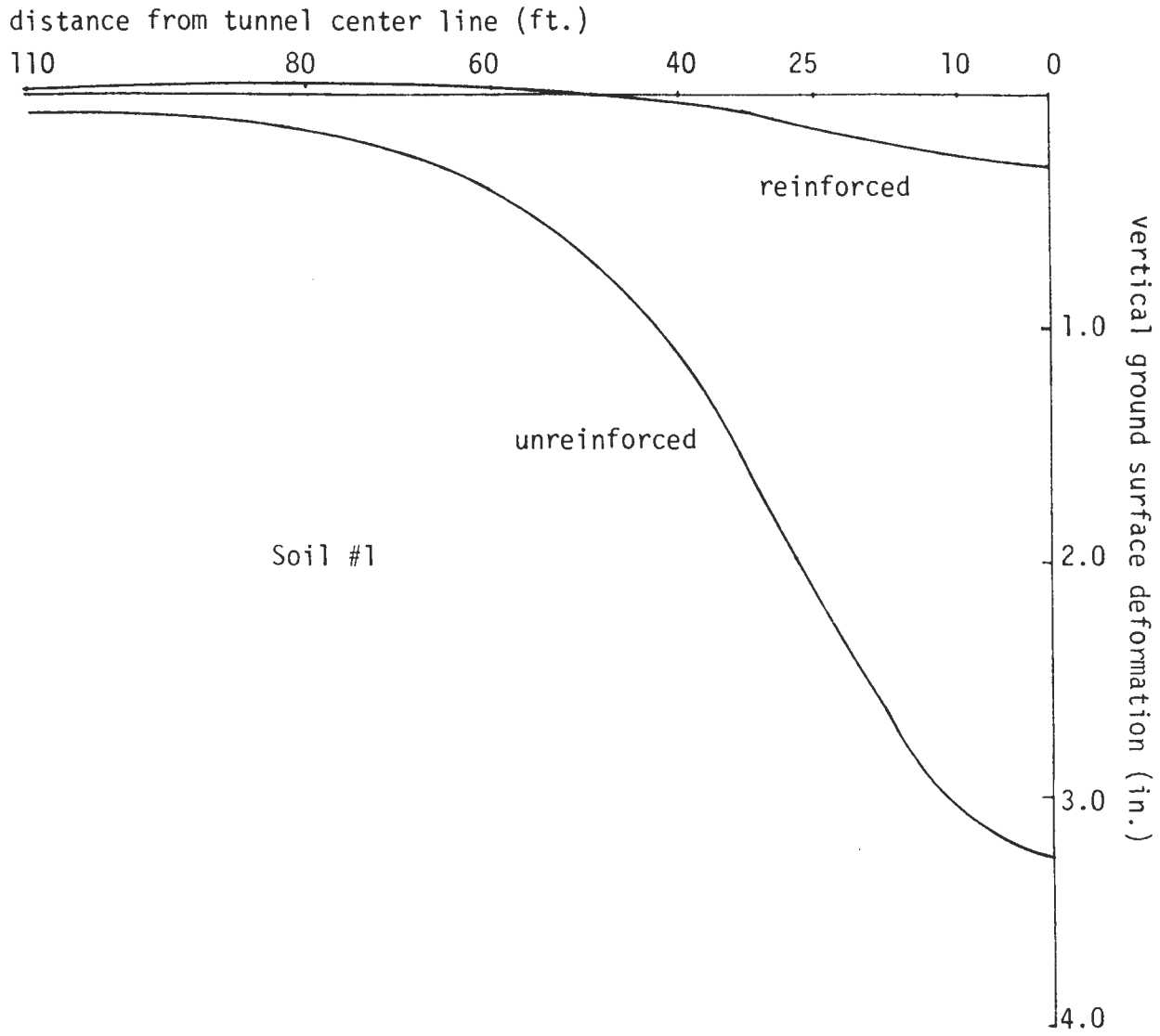

Fig-8 Vertical ground surface movement

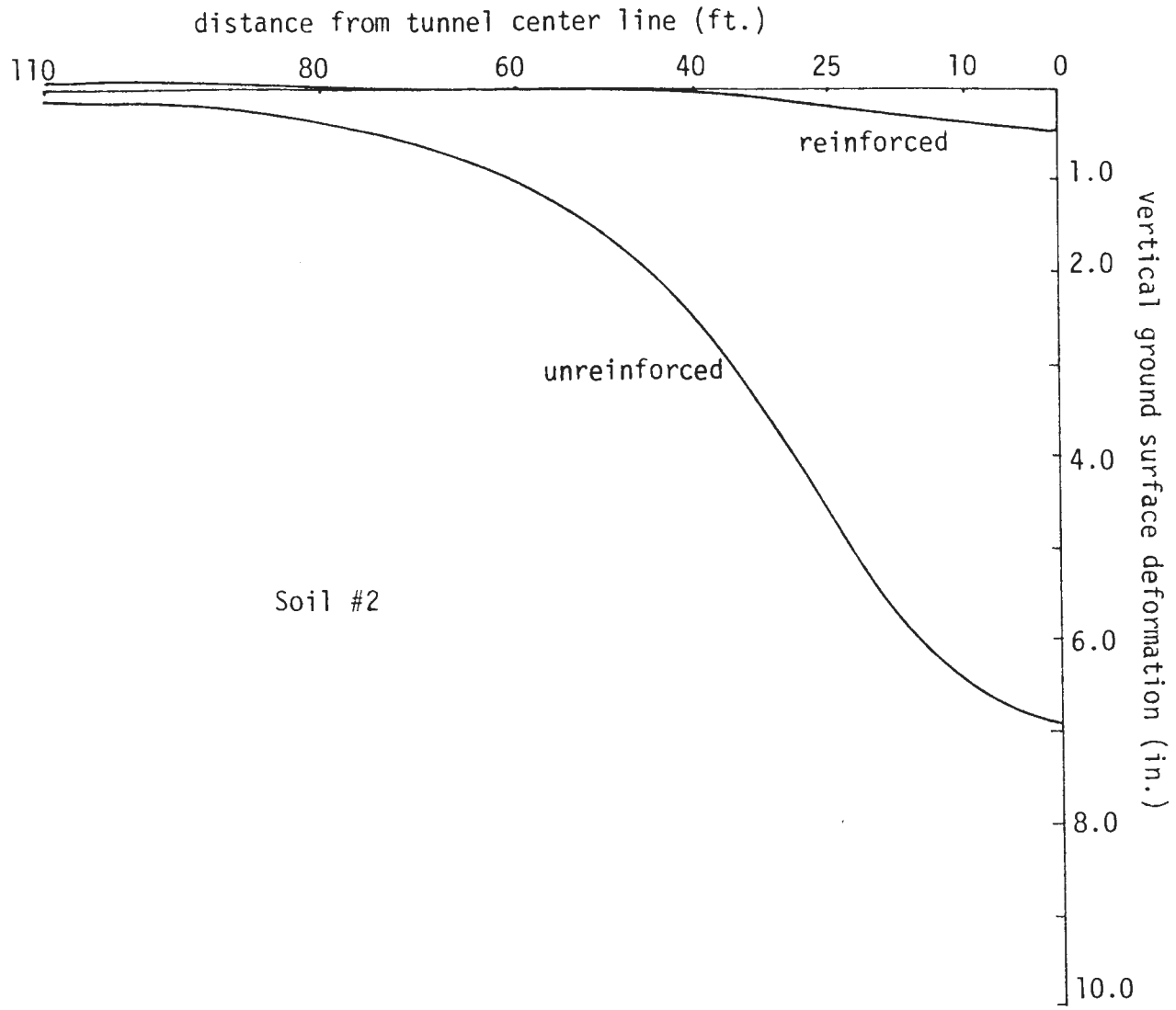

Fig-9 Vertical ground surface deformation

TABLE-5

Comparison of Maximum Displacements
on the Ground Surface

Soil #1

	Unreinforced Tunnel	Reinforced Tunnel	% Reduction
Max. vertical displacement	-3.25 in.	-0.32 in.	90%
Max. horizontal displacement	0.89 in.	0.09 in.	90%

Soil #2

	Unreinforced Tunnel	Reinforced Tunnel	% Reduction
Max. vertical displacement	-6.92 in.	-0.46 in.	93%
Max. horizontal displacement	1.78 in.	0.12 in.	93%

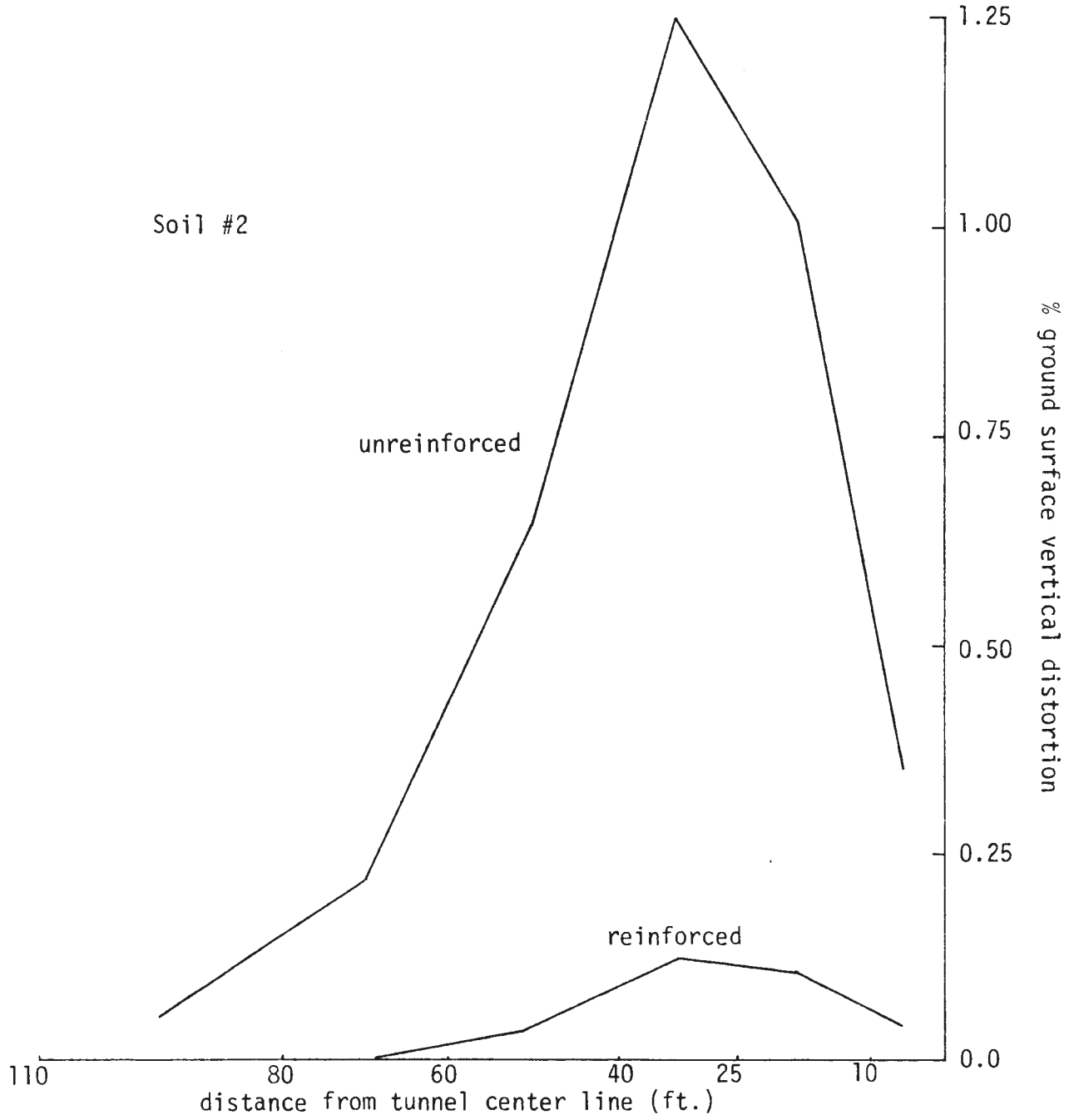

Fig-10 Vertical ground surface distortion

vertical distortion occurs at the inflection point. The maximum vertical and horizontal distortions obtained from the analysis are indicated in Table-6. It shows that the reduction in surface distortions is significant (in the order of 10), indicating the effectivness of the spiling reinforcement in soft ground tunneling.

3.3 Effect of Spile Inclination

In order to investigate the effect of the spile inclination to the performance of the system, three different spile inclination angles to the tunnel axis (20°, 30° and 40°) with two previously described representative soils were analyzed.

The effect of the spile inclination to the tunnel movements are shown in Fig-11 and 12, for soil #1 and soil #2, respectively. For soil #1, which is relatively stronger than soil #2, there exists virtually no difference. However, significant changes in tunnel deformation are obvious for soil #2. It also indicates that the angle of the spile inclination of 30° produced minimum inward and outward movements of the tunnel lining due to the excavation. Similar observations can be drawn from Fig-13 and 14 (resulting vertical ground settlements) and from Fig-15 and 16 (resulting horizontal ground movements). The resulting surface vertical distortions and horizontal distortions for soil #2 are also plotted in Fig-17 and 18.

From the results of this investigation, an important observation can be made. The angle of spile inclination of 30° to the tunnel axis produces least tunnel deformation, ground surface displacements, and distortions in the weaker soils. The effect of the spile inclination however diminishes as the soil becomes stronger. The parametric study was therefore conducted using this 30° of spile inclination angle.

TABLE-6

Comparison of Ground Surface Distortions

Soil #1

	Unreinforced Tunnel	Reinforced Tunnel	% Reduction
Max. vertical distortion (%)	0.585	0.076	87%
max. horizontal distortion (%)	0.370	0.050	87%

Soil #2

	Unreinforced Tunnel	Reinforced Tunnel	% Reduction
Max. vertical distortion (%)	1.247	0.122	90%
Max. horizontal distortion (%)	0.790	0.066	92%

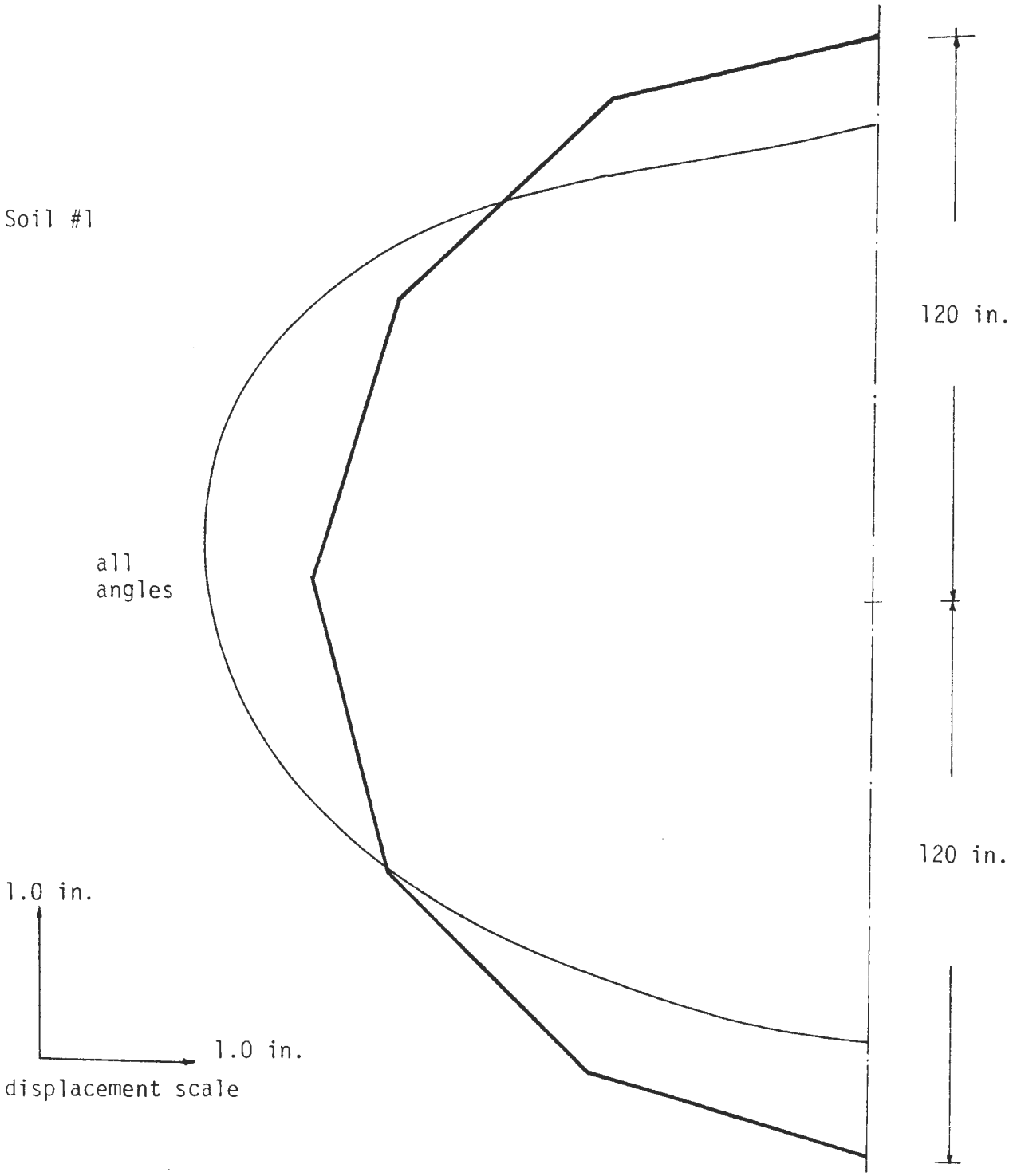

Fig-11 Tunnel deformation of soil #1

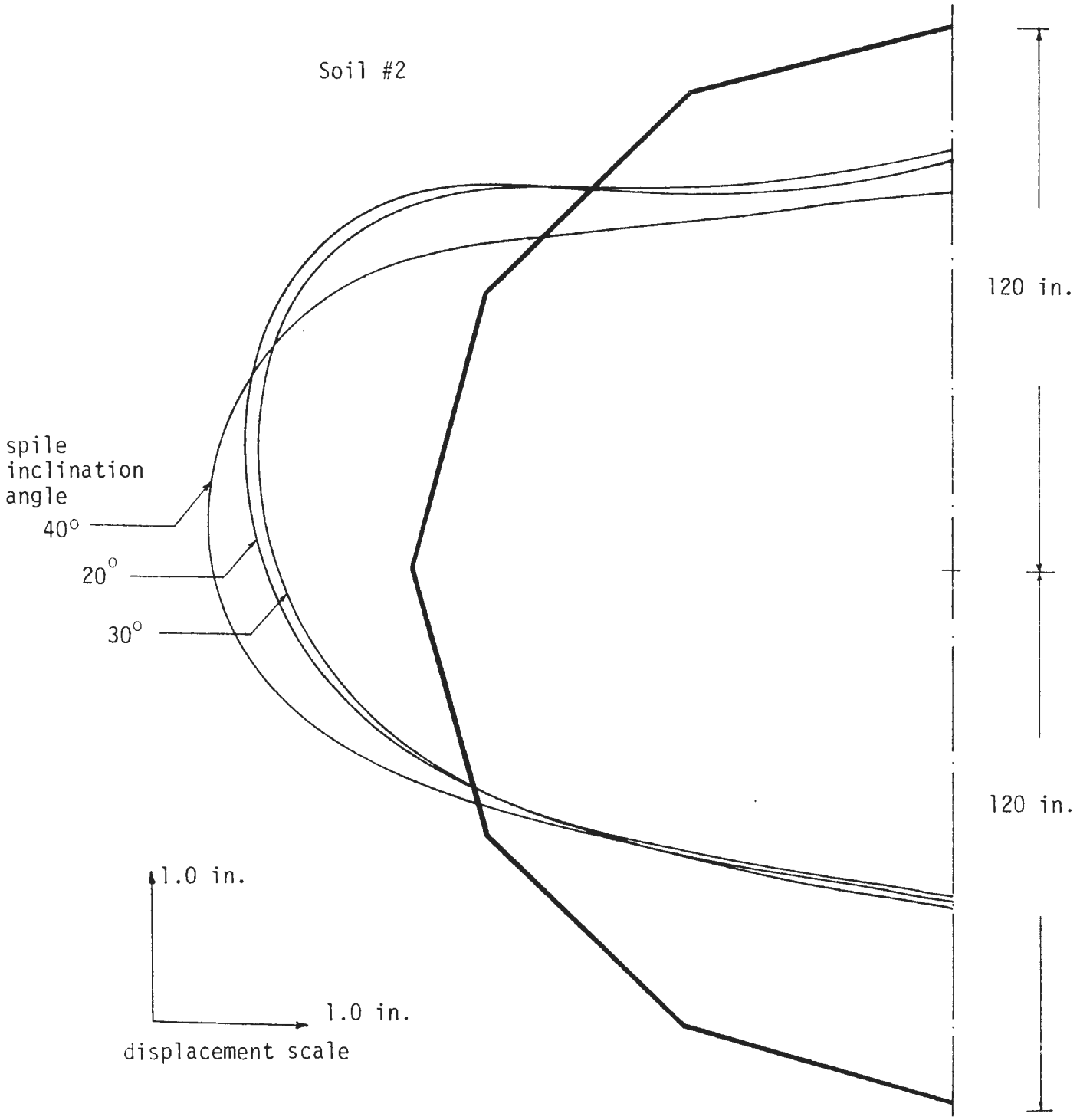

Fig-12 Tunnel deformation of soil #2

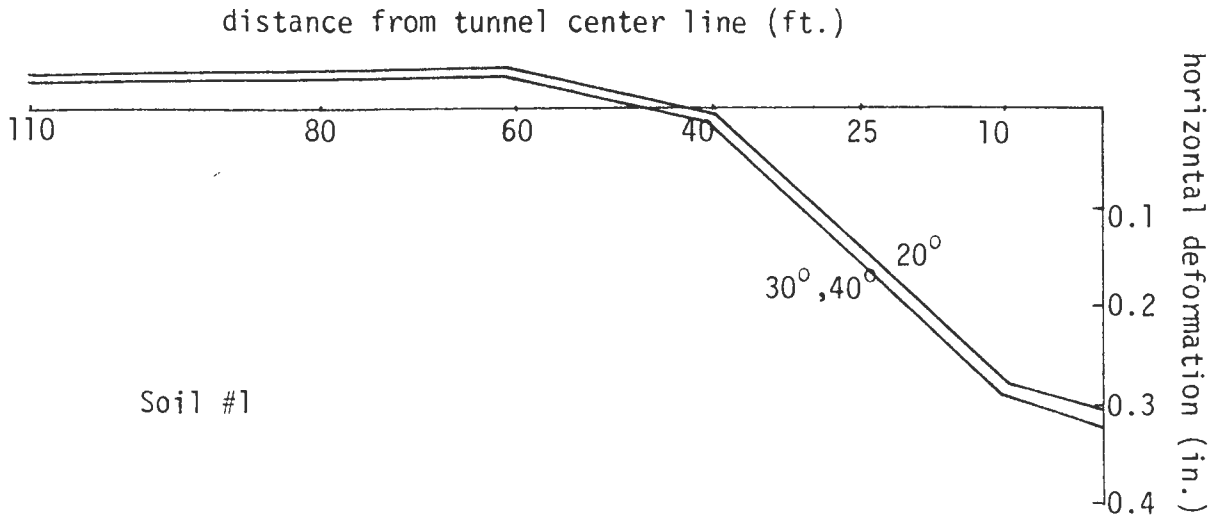

Fig-13 Vertical ground surface deformation (soil #1)

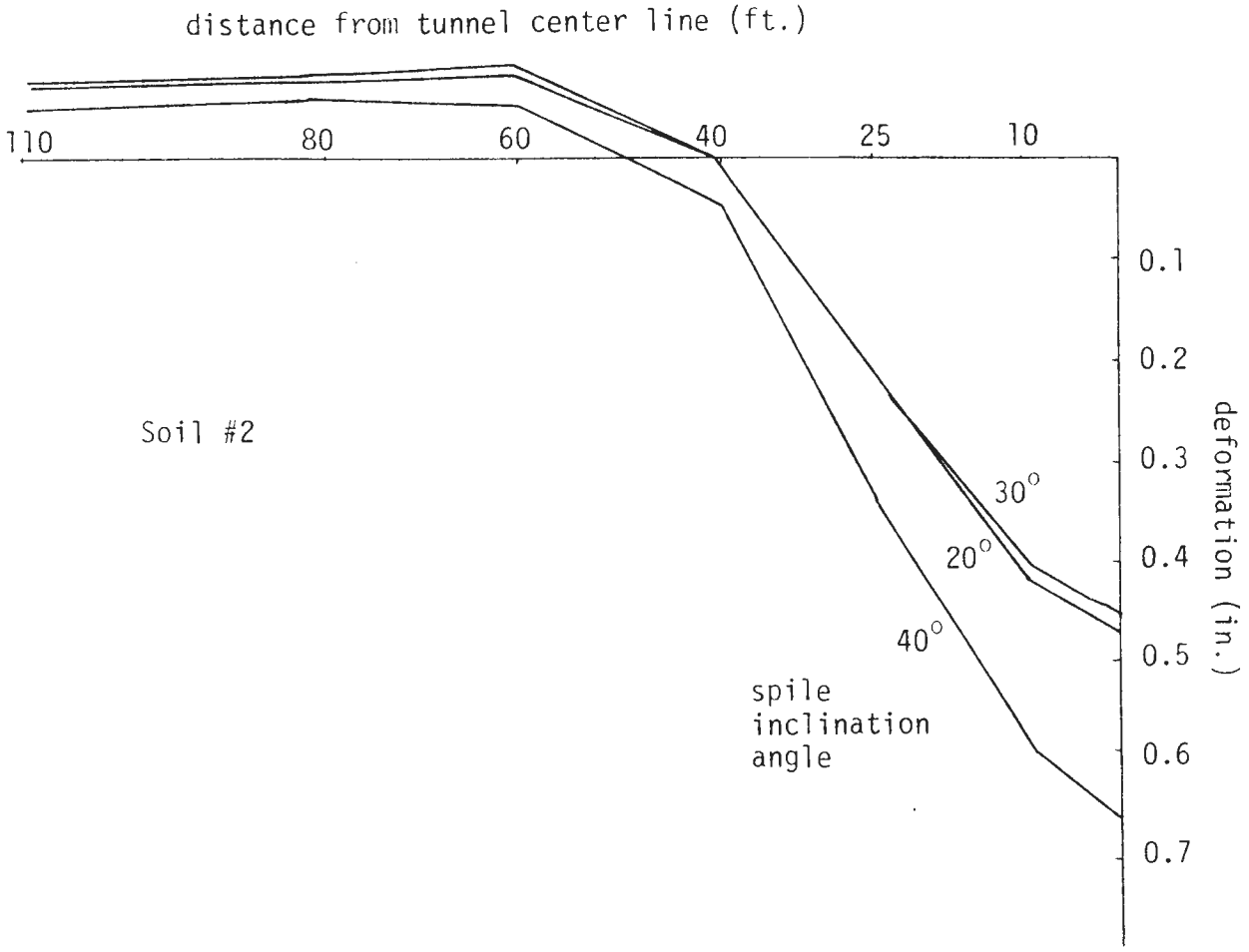

Fig-14 Vertical ground surface deformation (soil #2)

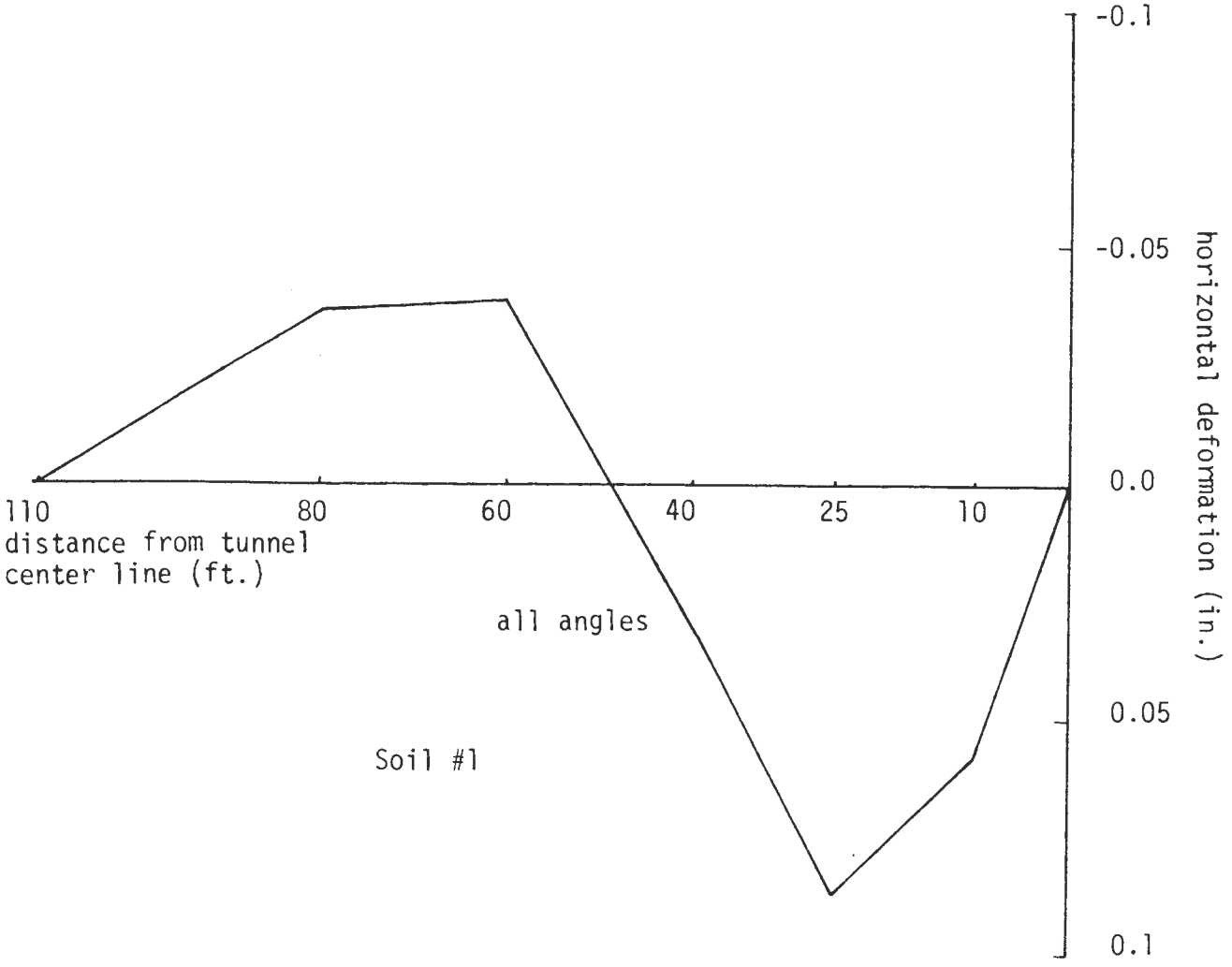

Fig-15 Horizontal ground surface deformation (soil #1)

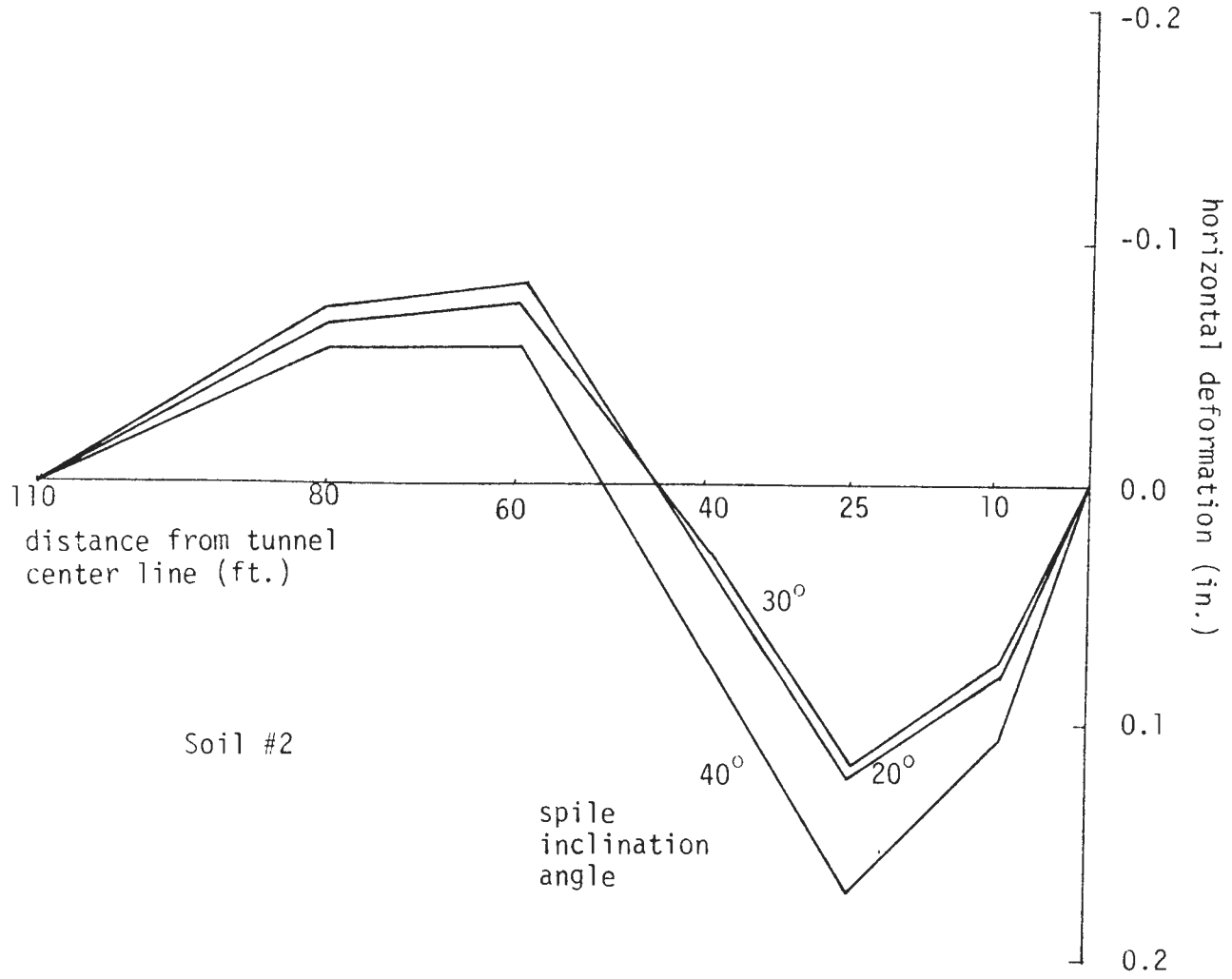

Fig-16 Horizontal ground surface deformation (soil #2)

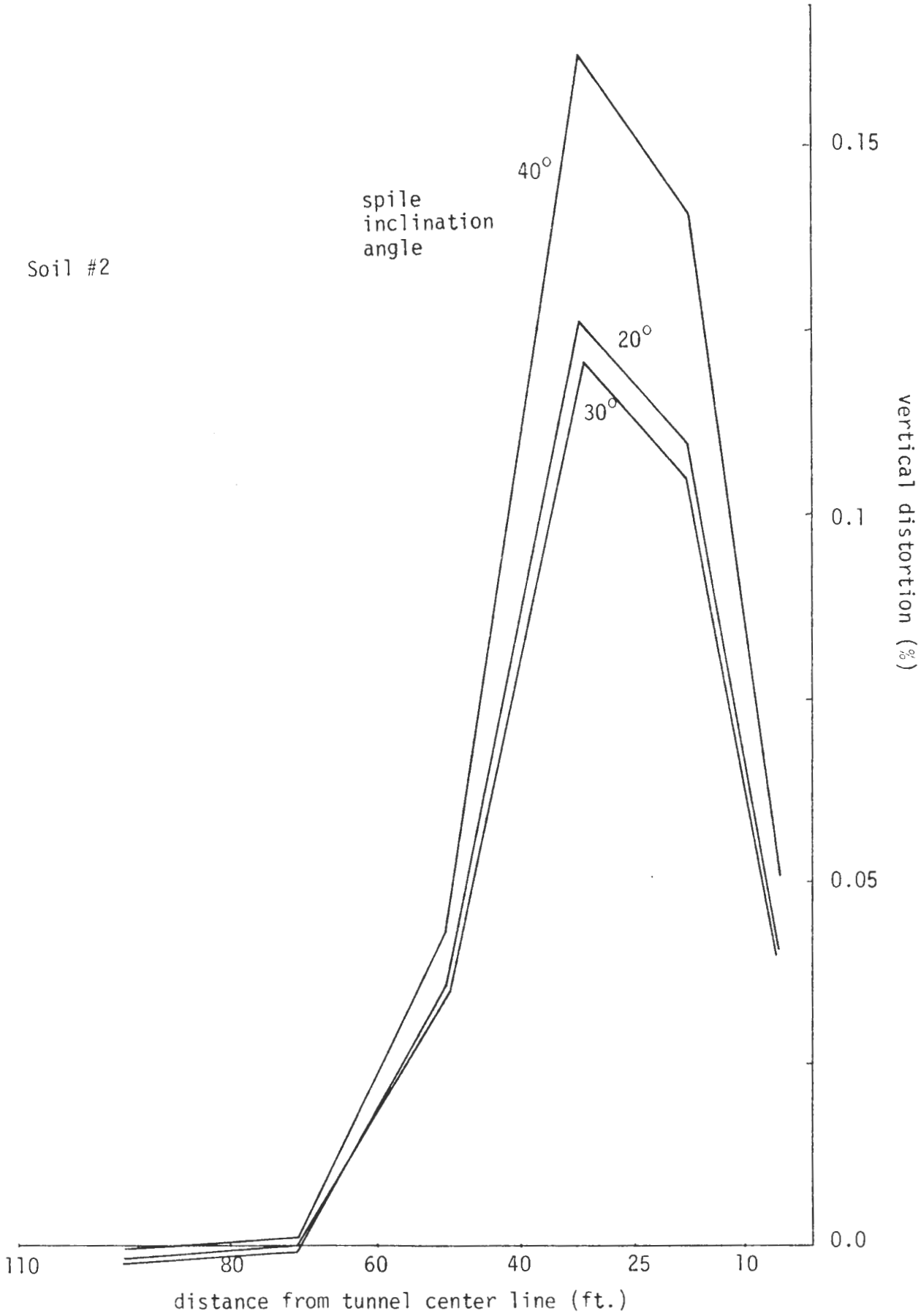

Fig-17 Vertical ground surface distortion (soil #2)

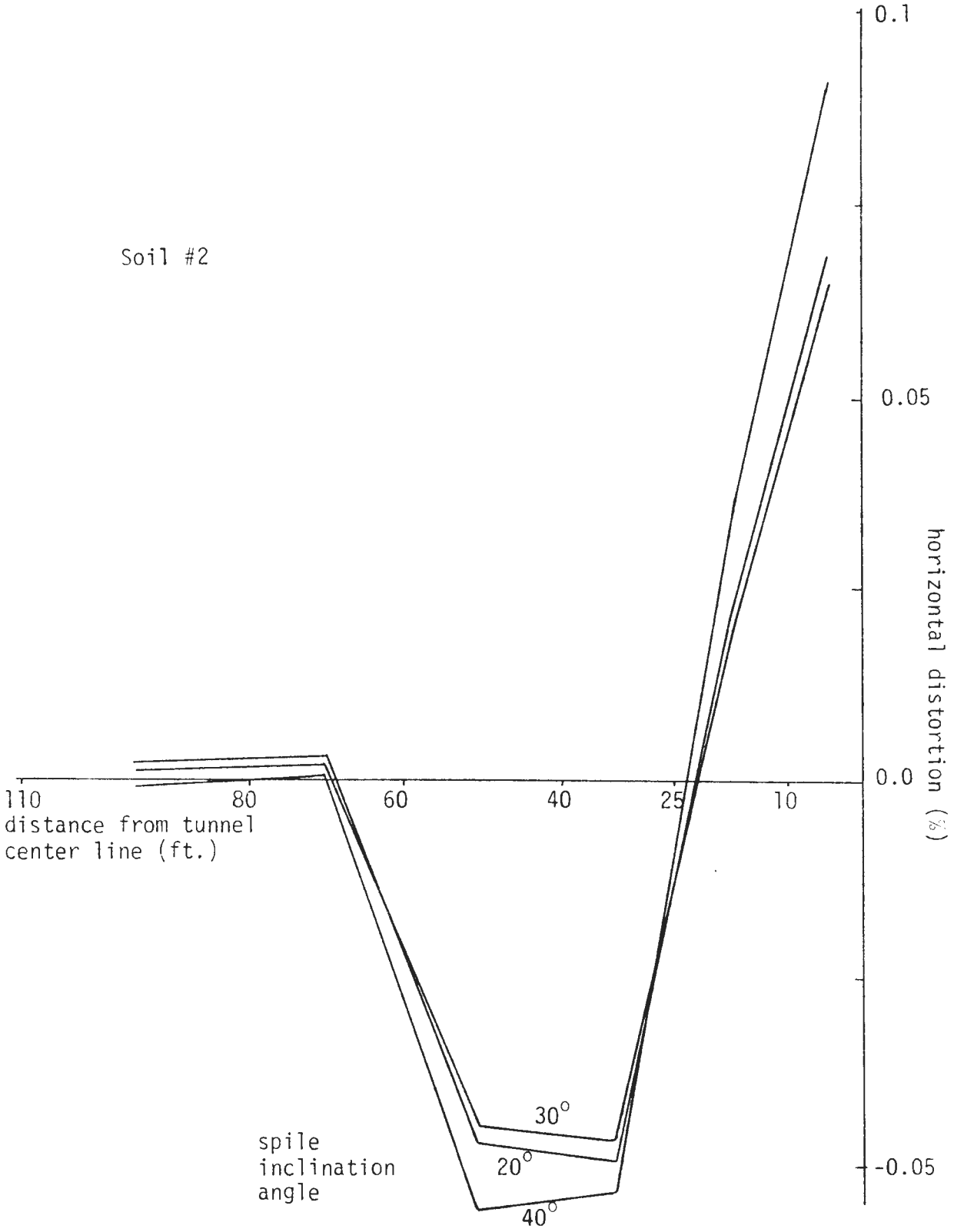

Fig-18 Horizontal ground surface distortion (soil #2)

CHAPTER IV

PARAMETRIC STUDY

The results of the parametric study of the spiling reinforcement in soft ground tunneling are presented in this chapter. It provides the effect of each of the parameters consisting the spiling reinforcement system on the overall performance.

4.1 General

To analyze the field behavior of the system including the tunnel deformation and the resulting ground surface movements, all the relevent elements in the spiling reinforcement system must be considered in the analysis. The comprehensive parametric study took an orientation toward the investigation of the effect of the soil type, the depth of the tunnel, and the spacing of the spiling reinforcement. The rest of the parameters involved in the spiling reinforcement system have constant values as indicated in Chapter III.

Two types of soil, whose pertinent properties are described in Table-7, were considered. The depths of the tunnel adopted in the study were 30, 40, 50 and 60 ft. and the spacings of the spiles were 2, 3, 4 and 5 ft. A total of 32 computer runs were therefore necessary to obtain the desired results.

The study was limited to a single spiling reinforced horizontal circular tunnel in soft ground. Using the developed generalized plane strain computer program, the following observations were made.

4.2 Effect of the Soil Type

Fig-19 and 20 show the typical deformed shapes of the tunnel, after the installation of the spiles and the excavation are completed, for the spiling

TABLE-7

Soil Properties

	Soil #1	Soil #3
Description	SM	CL
Loading modulus (K)	200	60
Unloading modulus* (K_{ur})	330	153
Modulus exponent (n)	0.6	0.45
Failure ratio (R_f)	0.7	0.7
Cohesion (C) in psi	2.778	0.695
Friction angle (ϕ)	33	30
Poisson's ratio (ν)	0.3	0.3

*For soil #1, $K_{ur} = 1.15 \times K$ and $K_{ur} = 2.55 \times K$ for soil #3

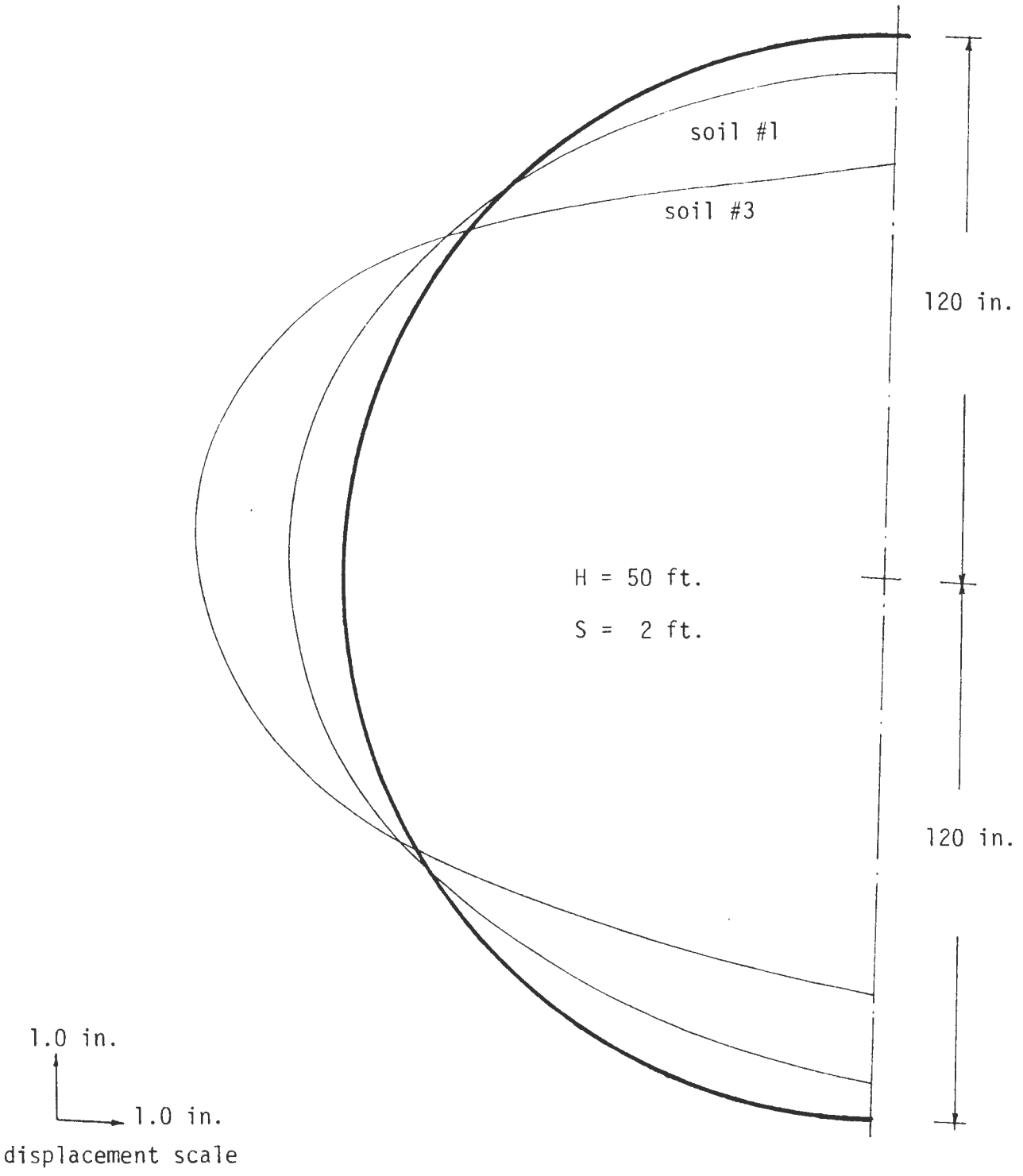

Fig-19 Effect of soil type on tunnel deformation (S = 2 ft.)

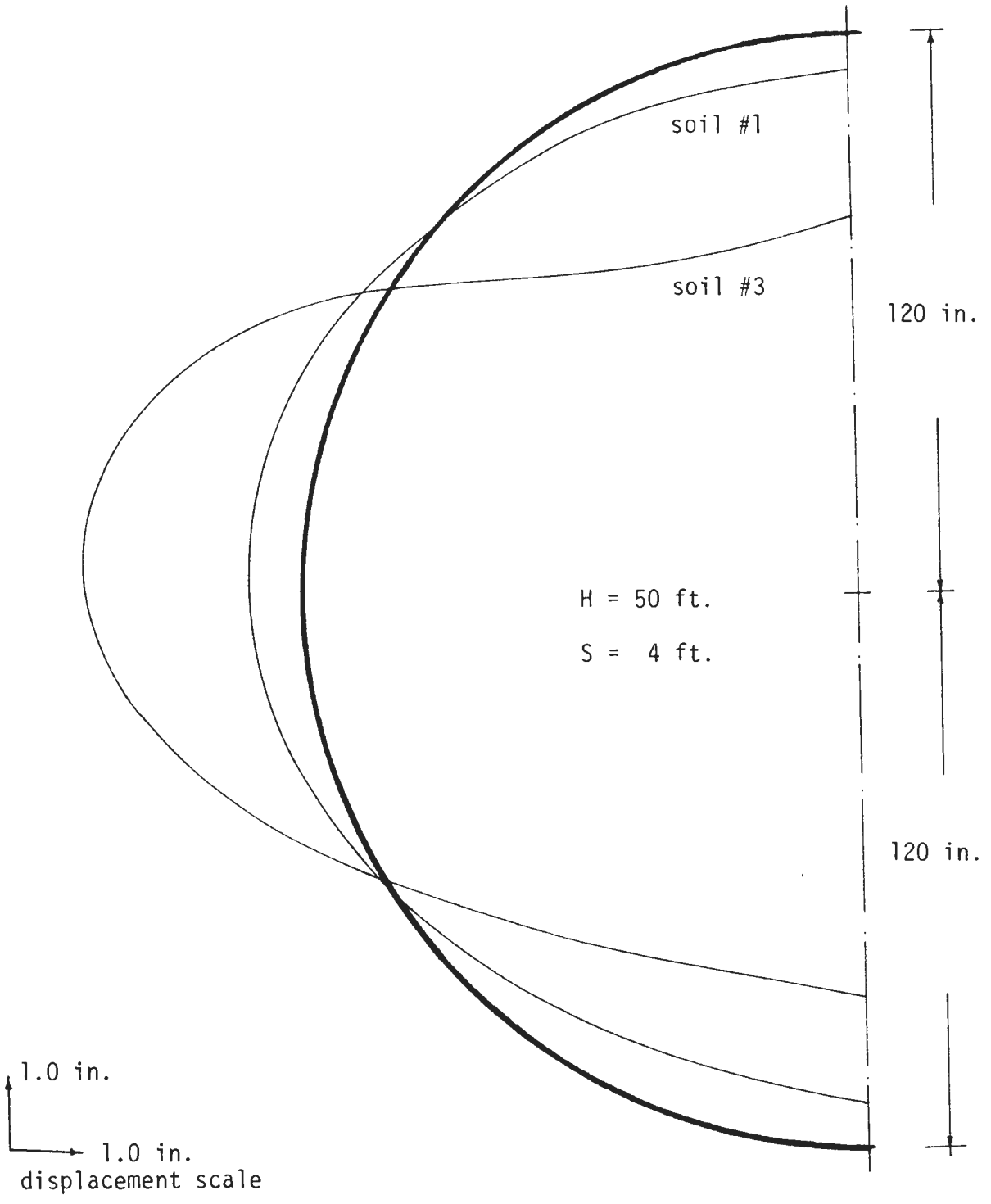

Fig-20 Effect of soil type on tunnel deformation (S = 4 ft.)

reinforcement spacing of 2 ft. and 4 ft., respectively. The depth of the tunnel in both cases is 50 ft. Note that different scales are used for the tunnel diameter and for the deformation. The general pattern of the deformation is inward movement of the crown and bottom of the tunnel and outward movement of the sides of the tunnel; inward movements in every direction were obtained for unreinforced system in Chapter III. Clearly, the weaker soil (soil #3) has more crown settlement, bottom heave, and lateral movement. However, the effect of spiling reinforcement is much greater in weaker soil, i.e., more percentage improvement can be expected from the spiling reinforcement in weaker soils. 87% reduction in the tunnel crown settlement and 48% reduction in the tunnel bottom heave due to the spiling reinforcement in soil #1 are resulted, whereas 91% and 51% are obtained in soil #2 (Table -4).

Fig-21 shows the resulting tunnel crown settlements for soil #1 and #3 with different depths of the tunnel. It is apparent from the figure that the tunnel crown movement is much more sensitive in soil #3. For instance, an increase in tunnel depth from 30 ft. to 60 ft. results in additional 0.5 in. of the crown settlement in soil #1 and additional 1.8 in. in soil #3. This could be explained by the fact that the load transfer due to arching action is greater in dense and strong soils. Similar observations can be made in Fig-22, which indicates the resulting vertical ground surface movement (for the depth of the tunnel of 50 ft. and the spiling reinforcement spacing of 4 ft.). The percentage ground loss, defined as $\delta_{max} \cdot W/V_{tunnel}$, where δ_{max} is the maximum ground surface settlement directly above the tunnel center and W is the horizontal distance from the tunnel center line to the zero vertical ground surface displacement, is calculated to be approximately 0.3% and 2.5% for soil #1 and #3, respectively, for this particular example. This indicates that the soil #1 experiences much smaller ground surface settlement trough volume, about 1/8 of the soil #3, due to the

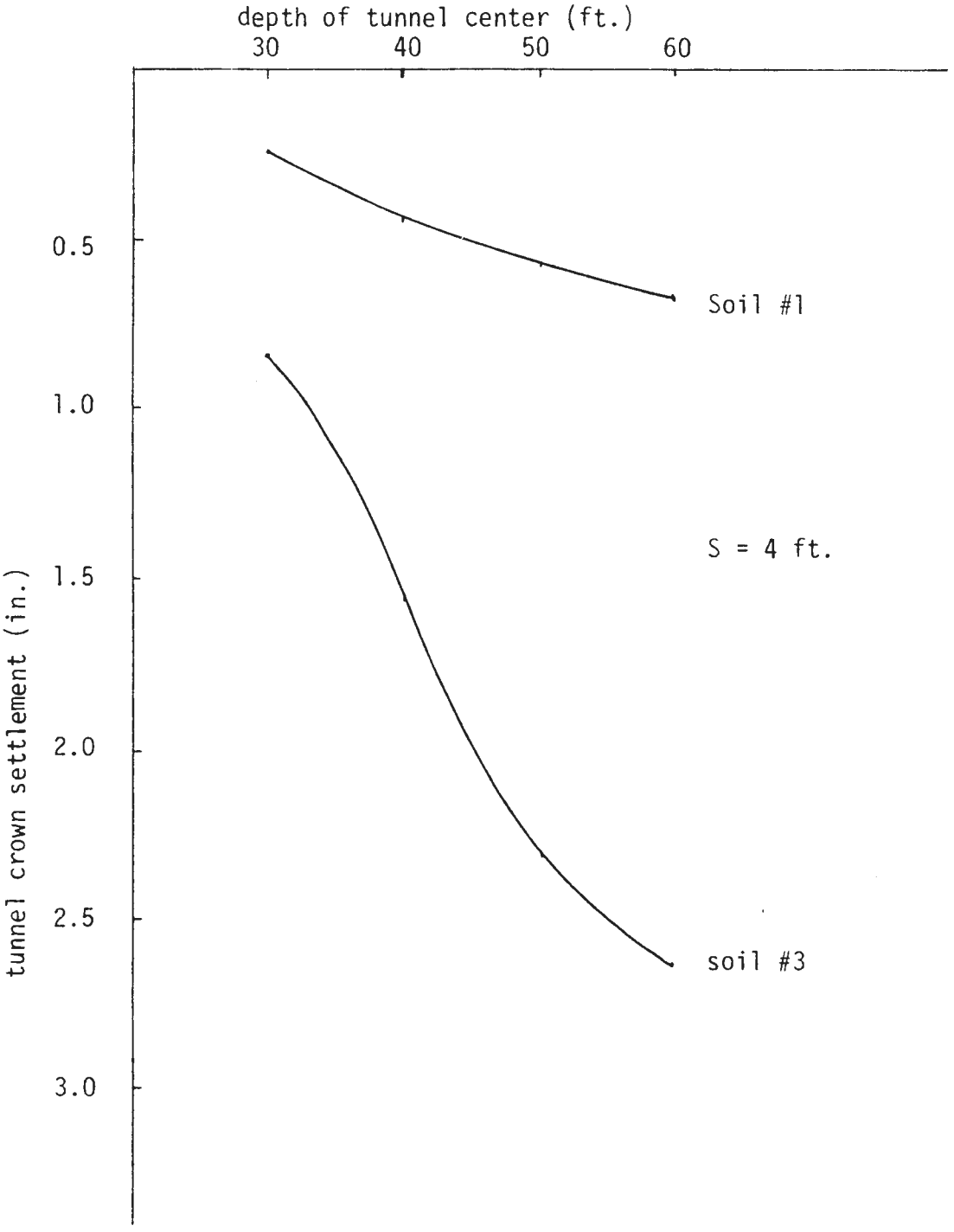

Fig-21 Tunnel crown settlement

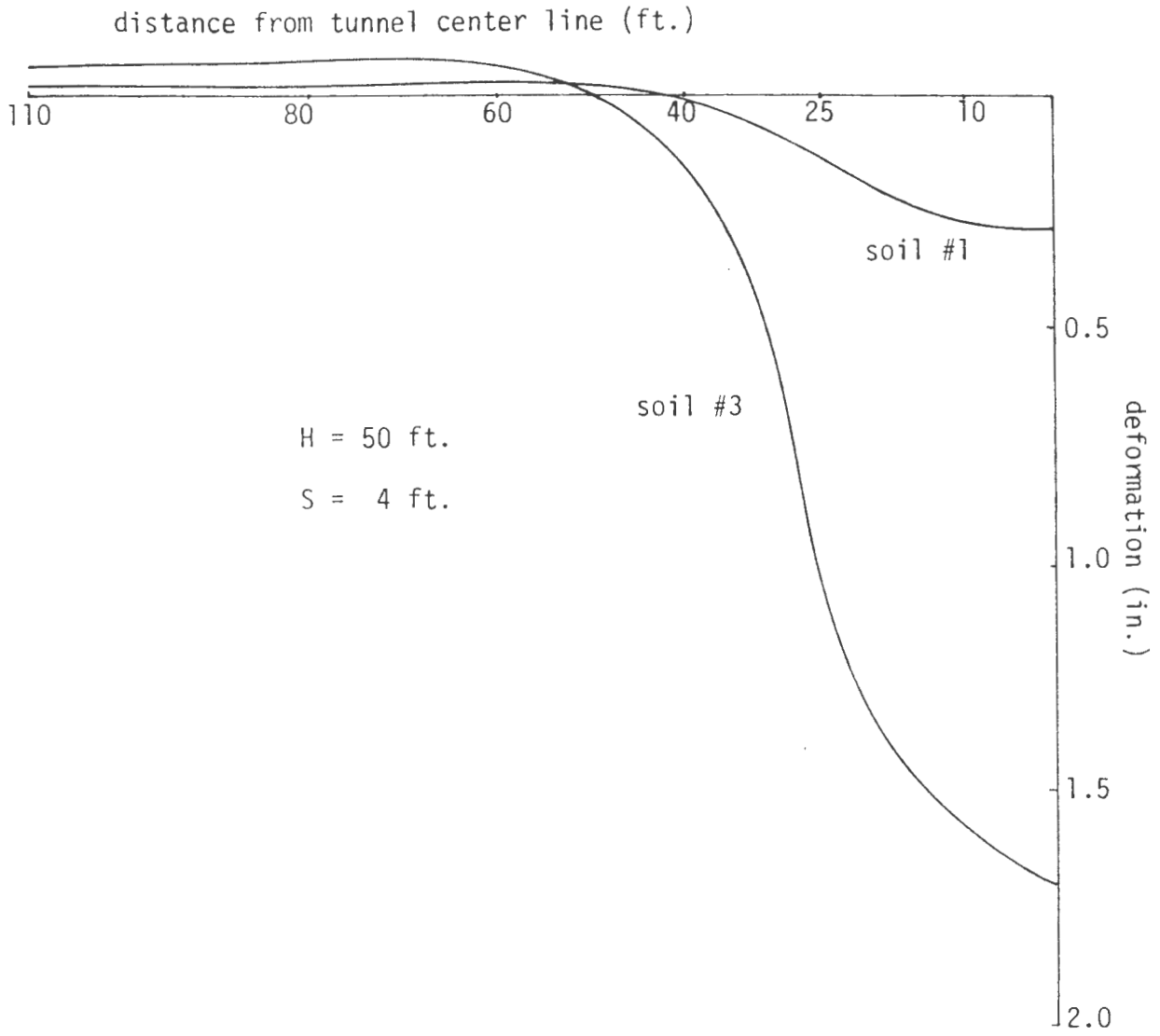

Fig-22 Vertical ground surface movement

tunnel excavation. For comparison, the percentage ground loss for an unreinforced tunnel with the same diameter and depth is approximately 10%. Fig-23 shows the effect of the soil type on the maximum ground surface settlement for various depths of the tunnel.

4.3 Effect of the Depth of the Tunnel

The depths (from the ground surface to the center of the tunnel) considered in the study were in the range of 1.5 to 3.0 times the tunnel diameter. It must be noted that within this range of tunnel depth full arching action does not take place.

Fig-24 and 25 show the deformed shapes of the tunnels with spiling reinforcement spacing of 4 ft. and with various tunnel depths for soil #1 and soil # 3 respectively. As expected, the deeper the tunnel, the larger the deformation. The rate of increment in deformation however decreases as the depth increases due to the increasing arching effect. As indicated previously the increase in tunnel deformation is less sensitive in stronger soil (#1). For soil #1, the crown settlement is approximately 0.25 in. for the depth of the tunnel of 30 ft., while 0.6 in. of settlement takes place for the depth of the tunnel of 50 ft. The corresponding settlements for soil #3 are 0.8 in. and 2.3 in., respectively.

Fig-26 and 27 represent the resulting vertical and horizontal ground surface movements for soil #1 with the spiling reinforcement spacing of 4 ft. As can be seen from the figure, the vertical movements follow the general deformation pattern; the deeper the tunnel, the larger the settlement with decreasing rate. The horizontal movement toward the tunnel center (indicated as positive in Fig-27) increases as the depth of the tunnel increases, while the horizontal movement away from the tunnel center (negative in Fig-27) decreases as the depth

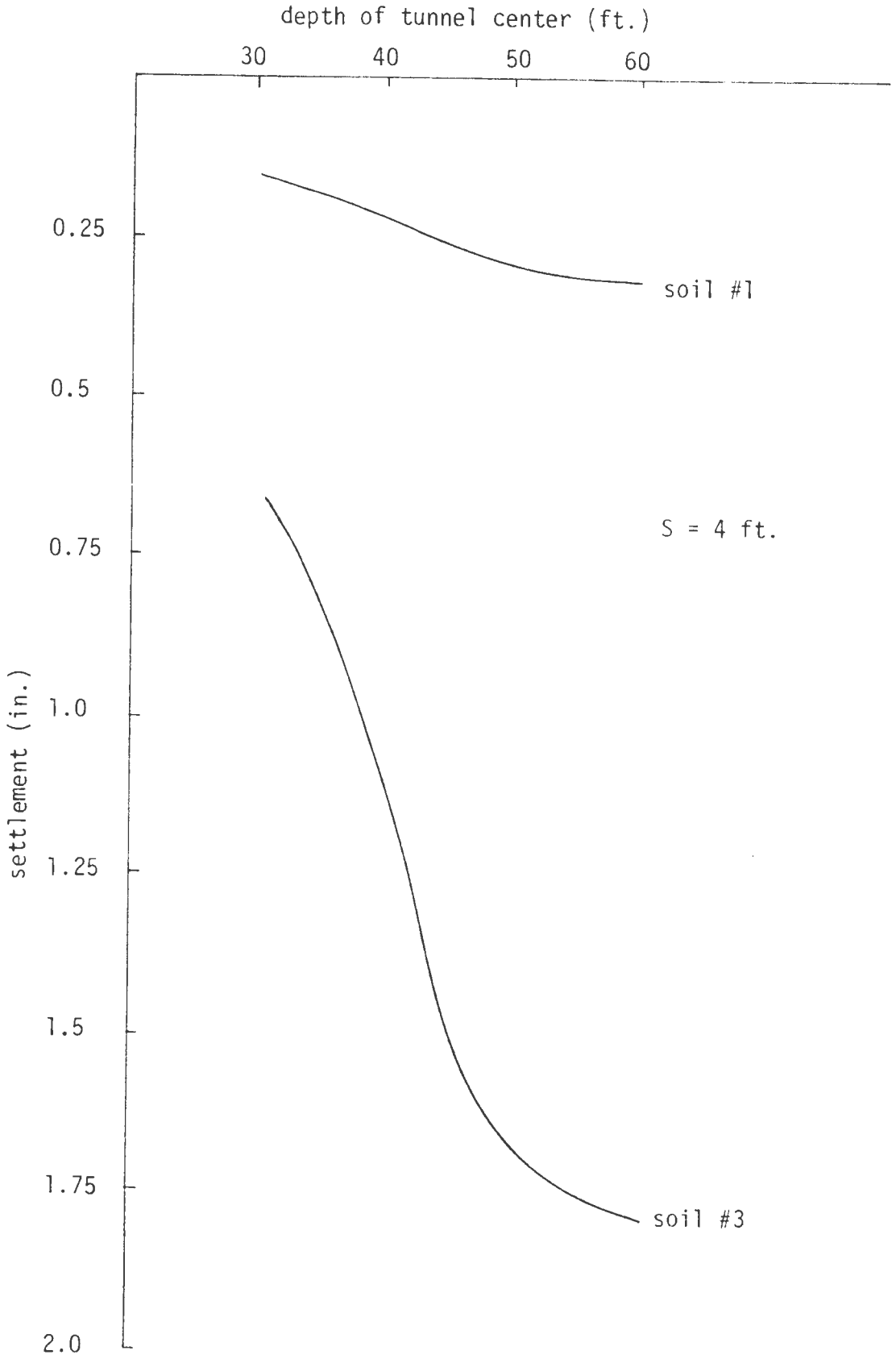

Fig-23 Maximum ground surface settlement

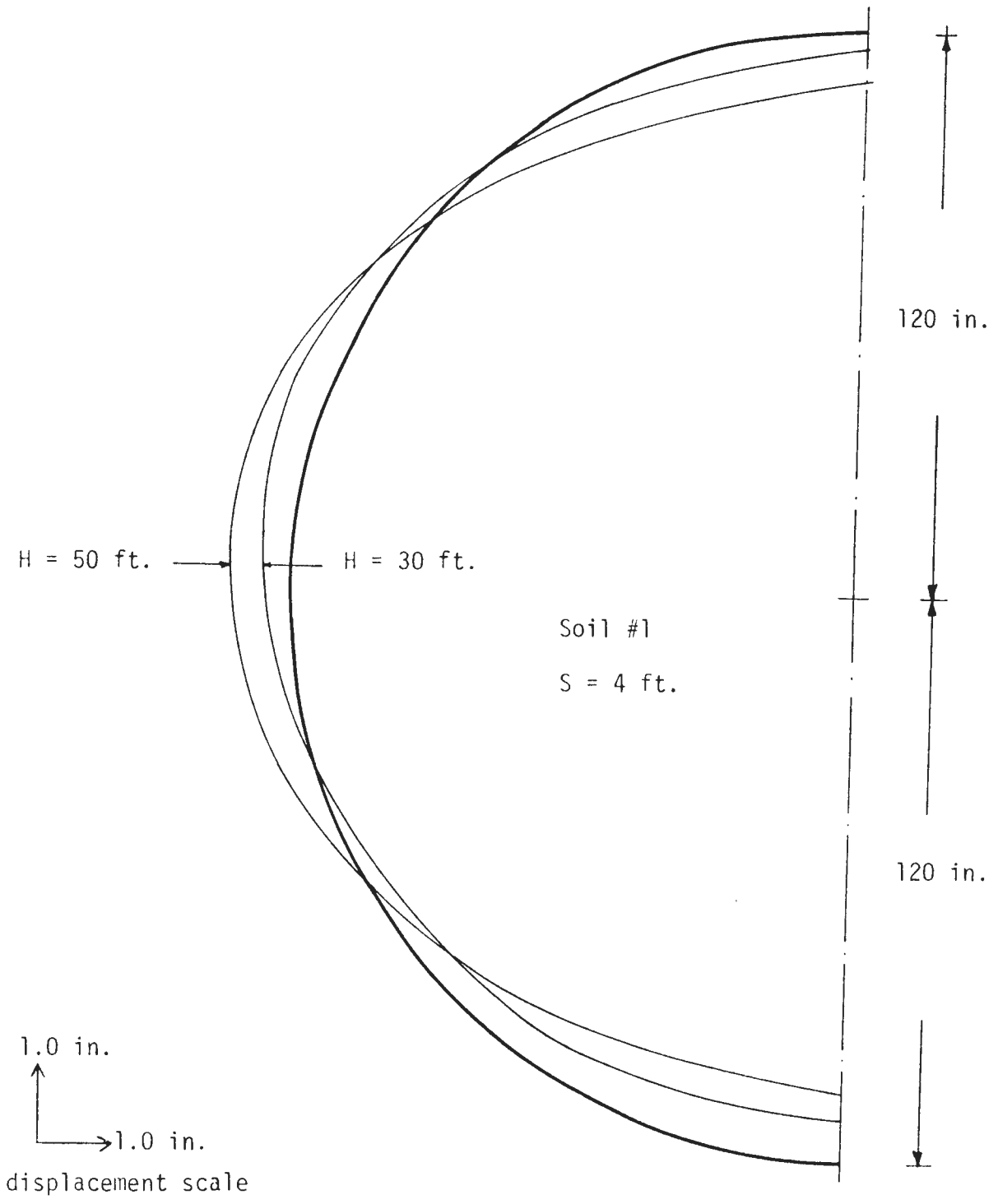

Fig-24 Effect of tunnel depth on tunnel deformation (soil #1)

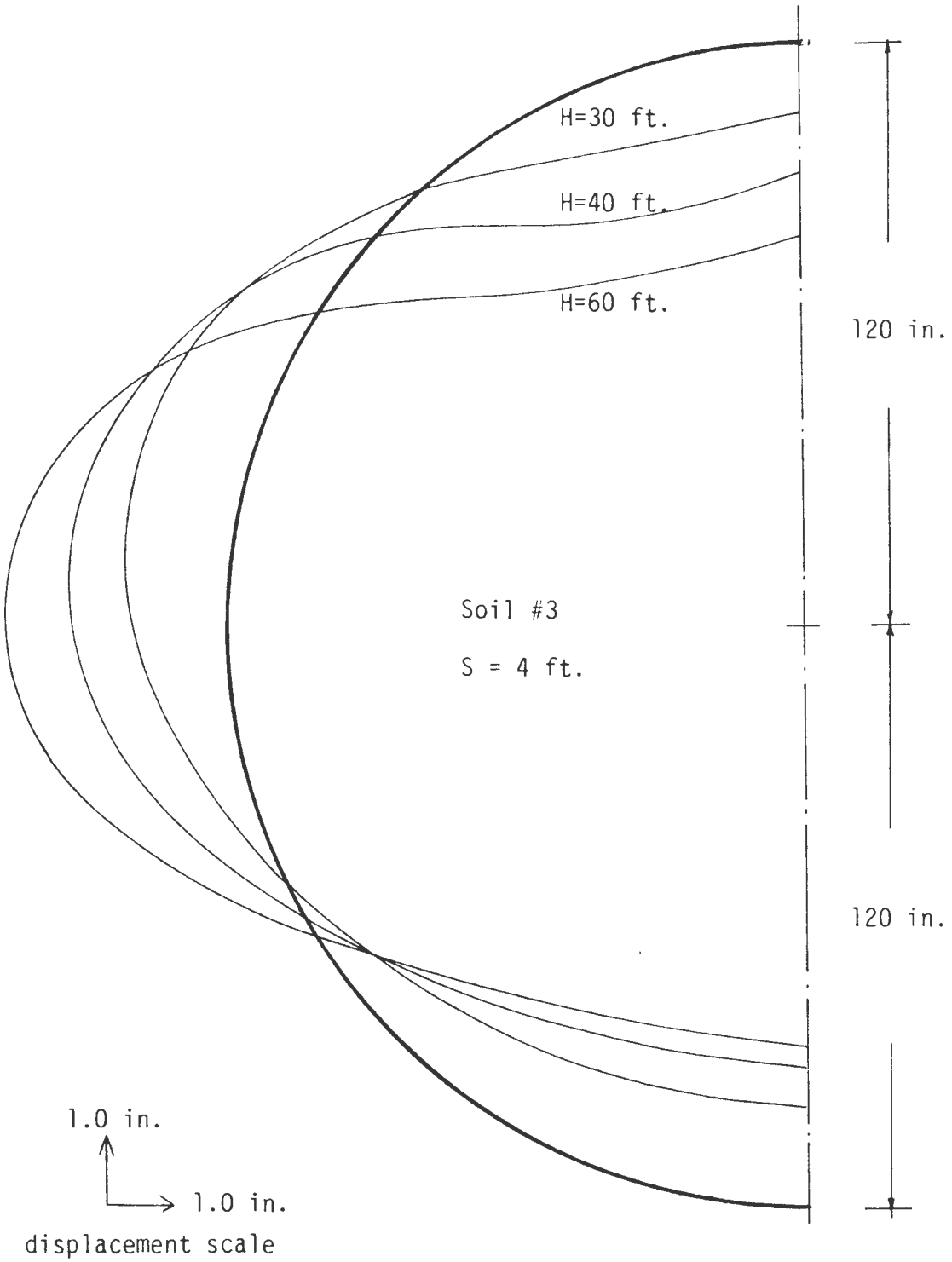

Fig-25 Effect of tunnel depth on tunnel deformation (soil #3)

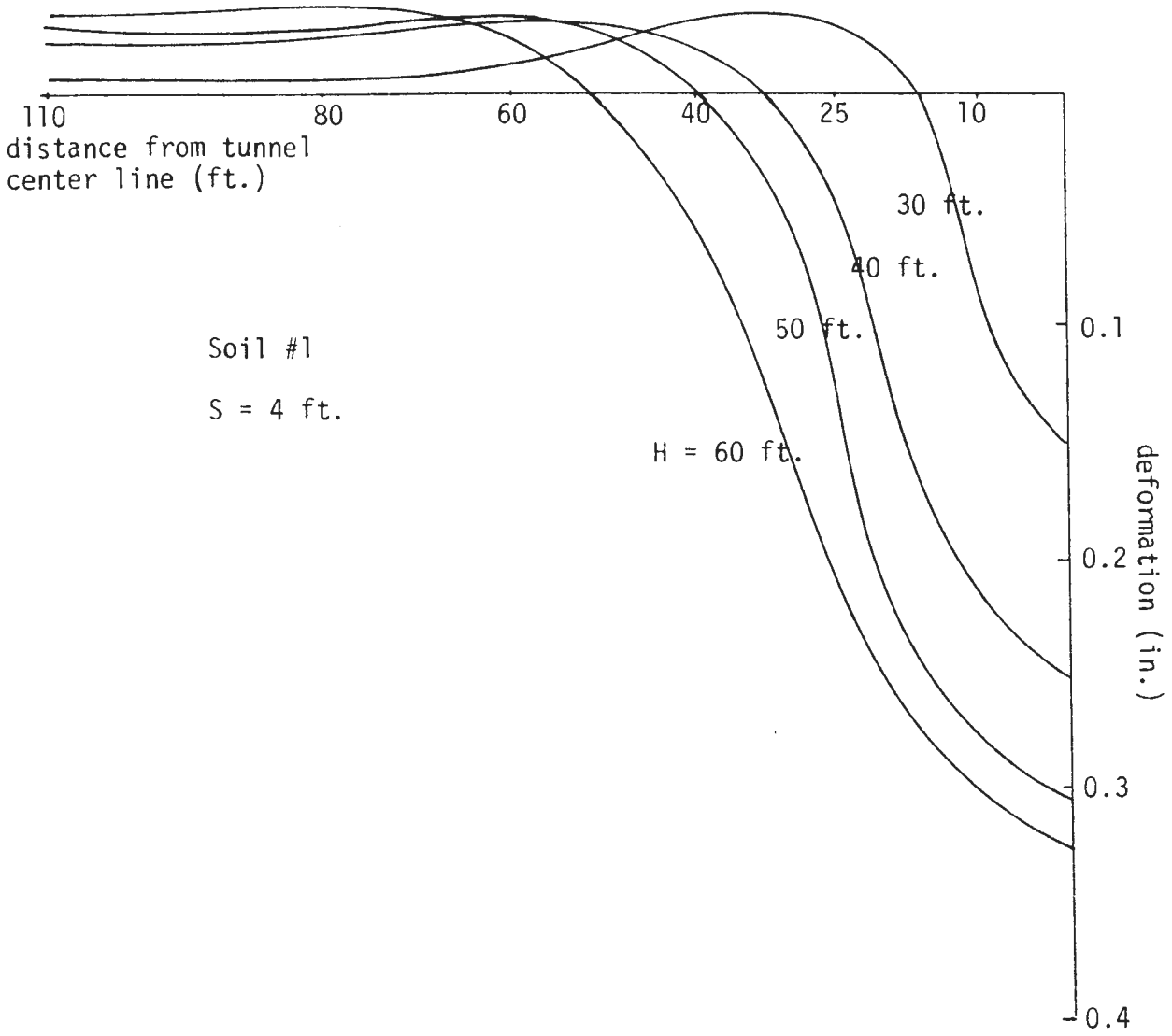

Fig-26 Vertical ground surface movement

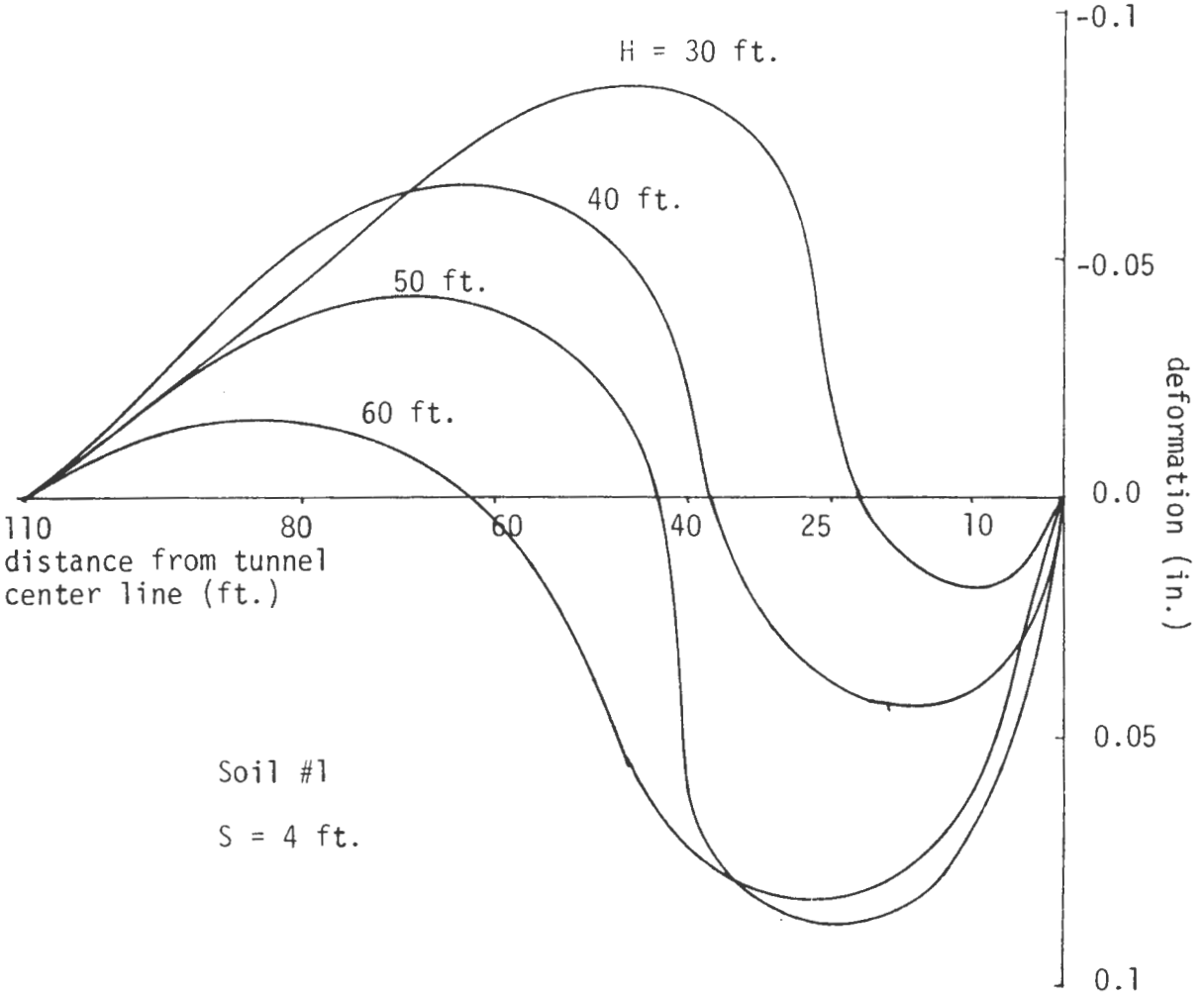

Fig-27 Horizontal ground surface movement

of the tunnel increases. The reason of this horizontal ground surface displacement pattern is not yet clear. It may be suspected that the limited extent of the finite element grid used in the analysis has some influence on this. This requires more study including the literature survey and the comparison with the more detailed model test results.

The ratios between the maximum ground surface settlement and the tunnel crown settlement are also calculated and listed in Table-8 for the spiling reinforcement spacing of 4 ft. In general the ratio decreases as the depth to the tunnel center increases for both soils, indicating that the percentage volume change on the ground surface with respect to the volume change on the tunnel face decreases as the depth of the tunnel increases, i.e., the effect of the depth of the tunnel on the ground surface settlement diminishes as the depth increases.

4.4 Effect of the Spile Spacing

This is probably the most important factor influencing the effectiveness of the reinforcement and the performance of the system. It directly indicates the percentage reinforcement in the soil. Four different values of the spiling reinforcement spacing were analyzed and the results are discussed briefly below. As indicated previously a constant spiling reinforcement inclination angle of 30° was used throughout the study.

Table-9 indicates the calculated crown and bottom movements of the tunnel for soil #1 and soil #3 with different spiling reinforcement spacing, and Fig-28 shows an example of the deformed shape of the tunnel obtained from the analysis. In general the effect of the spiling reinforcement spacing on the deformations of the system, including the crown settlement, the bottom heave and the lateral movement of the tunnel, and the ground surface movements,

TABLE- 8

Ratio of $\frac{\delta_{surface,\ max}}{\delta_{crown}}$

spile spacing = 4 ft.

Soil #1

H	Ratio
30'	0.645
40'	0.588
50'	0.549
60'	0.493

Soil # 3

H	Ratio
30'	0.794
40'	0.758
50'	0.741
60'	0.685

TABLE- 9

Tunnel Crown and Bottom Deformation

H = 50'

Spile Spacing	Crown Settlement		Bottom Heave	
	soil #1	soil #3	soil #1	soil #3
2'	0.539 in.	1.648 in.	0.720 in.	1.654 in.
3'	0.541	2.192	0.719	1.740
4'	0.552	2.287	0.730	1.760
5'	0.559	2.370	0.735	1.776

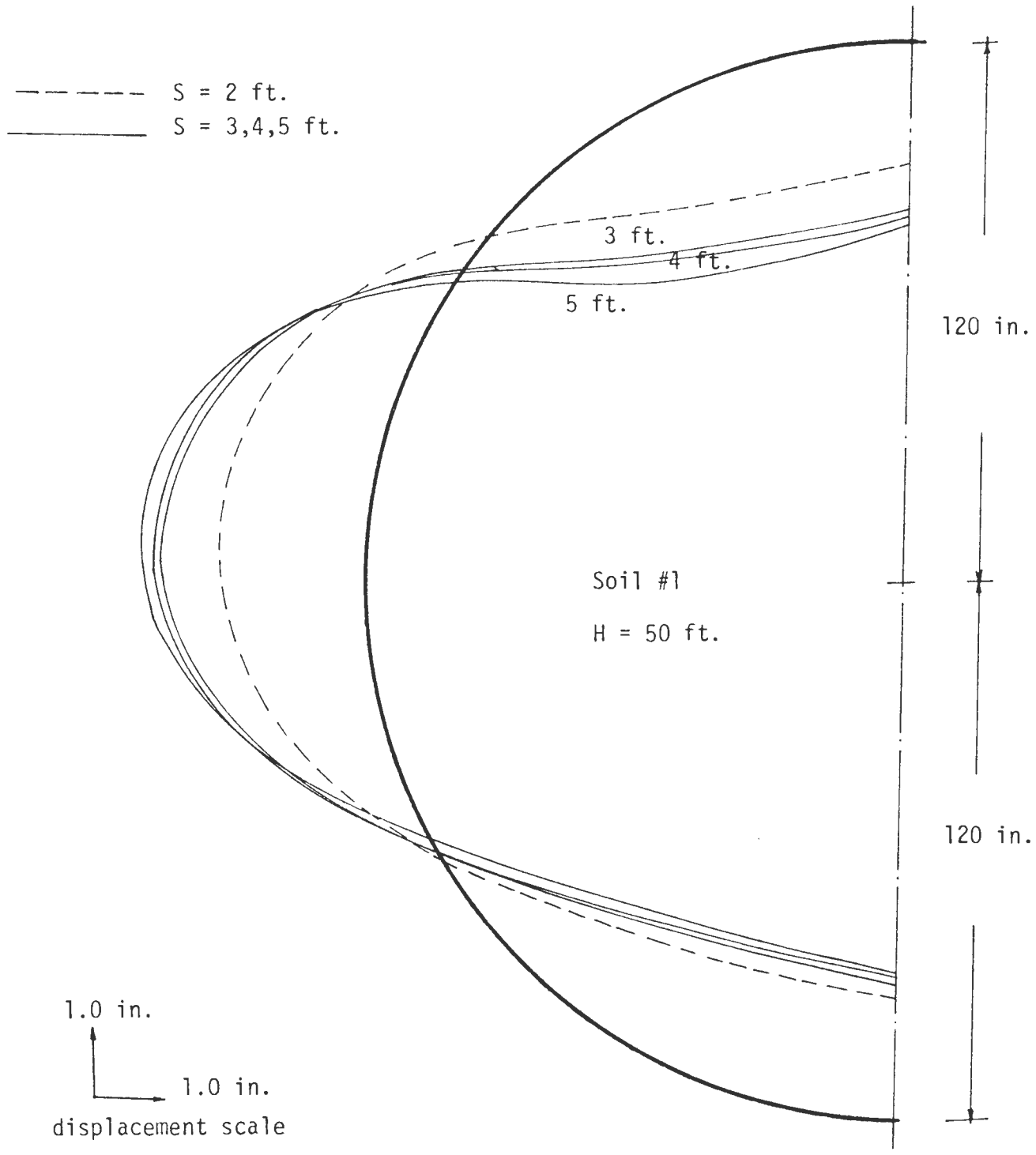

Fig-28 Effect of spile spacing on tunnel deformation

is much greater in weaker soil. It must be noted that even though the effect of the spiling reinforcement spacing is much smaller in stronger soils, the effect of the spiling reinforcement is still remarkable when the behavior of the spiling reinforcement system is compared with that of the unreinforced system (Chapter III).

Similar observations can be made in the horizontal ground surface displacement as for the effect of the depth of the tunnel; the denser the spiling reinforcement, the smaller the movement toward the tunnel center line and the larger the movement away from the tunnel center line (Fig-29). Again this observation must be further investigated and checked in detail through the comparison with the model test results.

4.5 Summary

The results of the individual study for the effect of each of the parameters were described in the previous sections. However, it is much more useful when they are synthesized so that the overall performance of the spiling reinforcement system with various design parameters can be evaluated.

Fig-30 through Fig-33 show the summary of the parametric study. They indicate the effect of each parameter, i.e., the soil type, the spiling reinforcement spacing and the depth of the tunnel, on the ground surface movements and the tunnel crown settlement for soil #1 and soil #3. The effect of the spile inclination angle is included separately in Chapter III. These figures can be used for the prediction of the movements of the spiling reinforcement system in soft grounds as well as for the stability analysis of the existing structures above the tunnel by comparing the expected ground movement/distortion with the allowable movement/distortion of the existing structures.

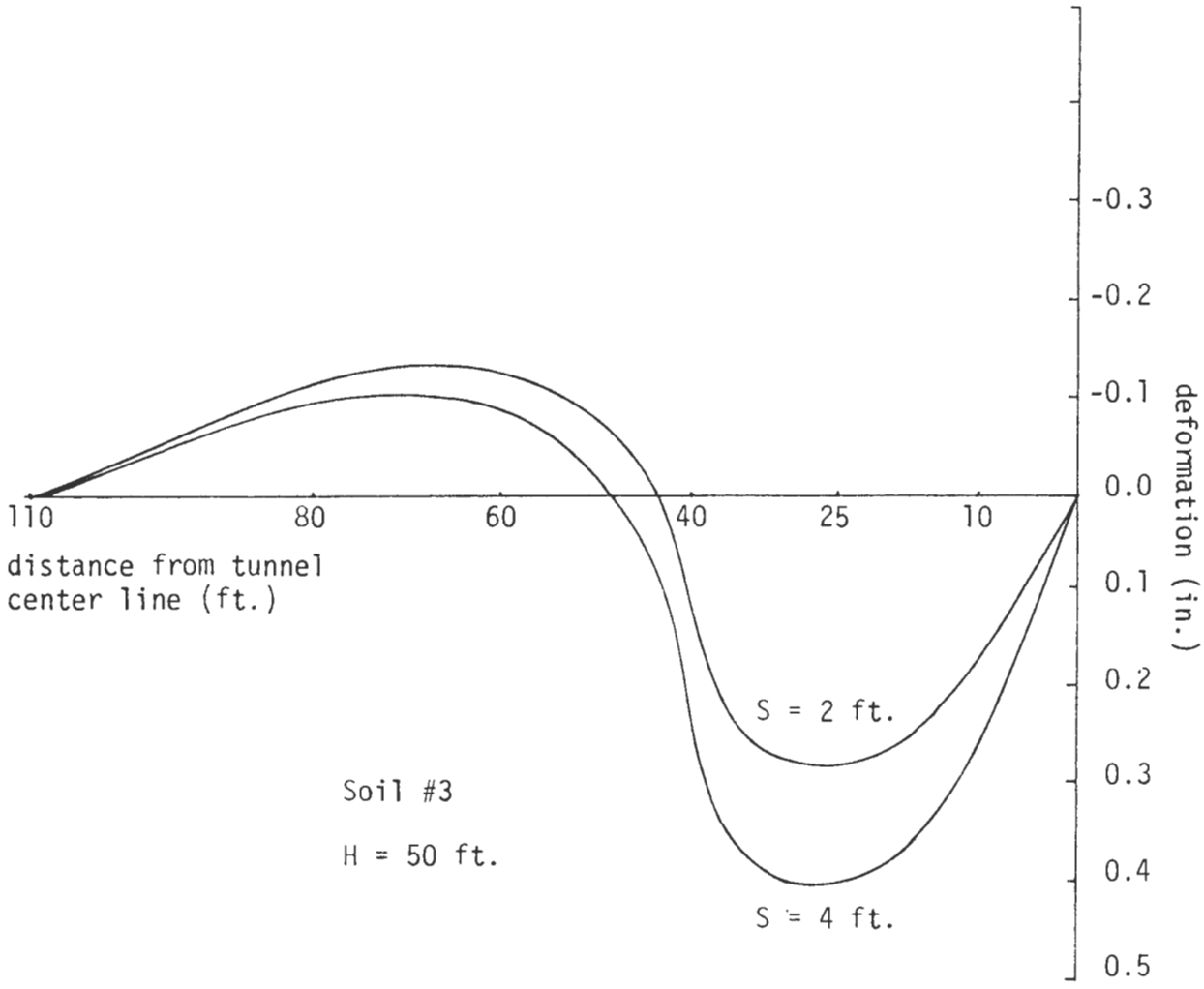

Fig-29 Horizontal ground surface movement

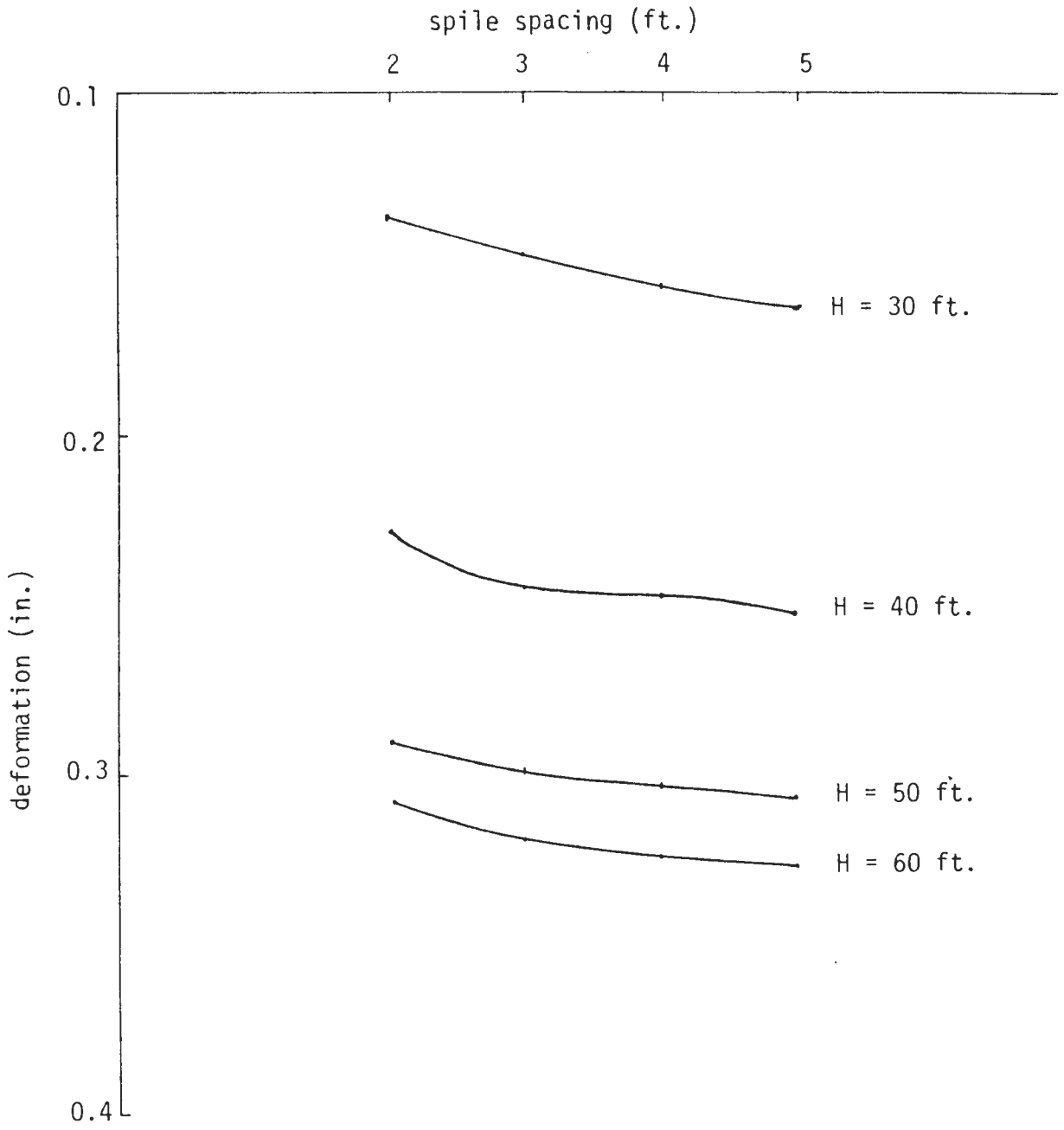

Fig-30 Maximum vertical ground surface movement (soil #1)

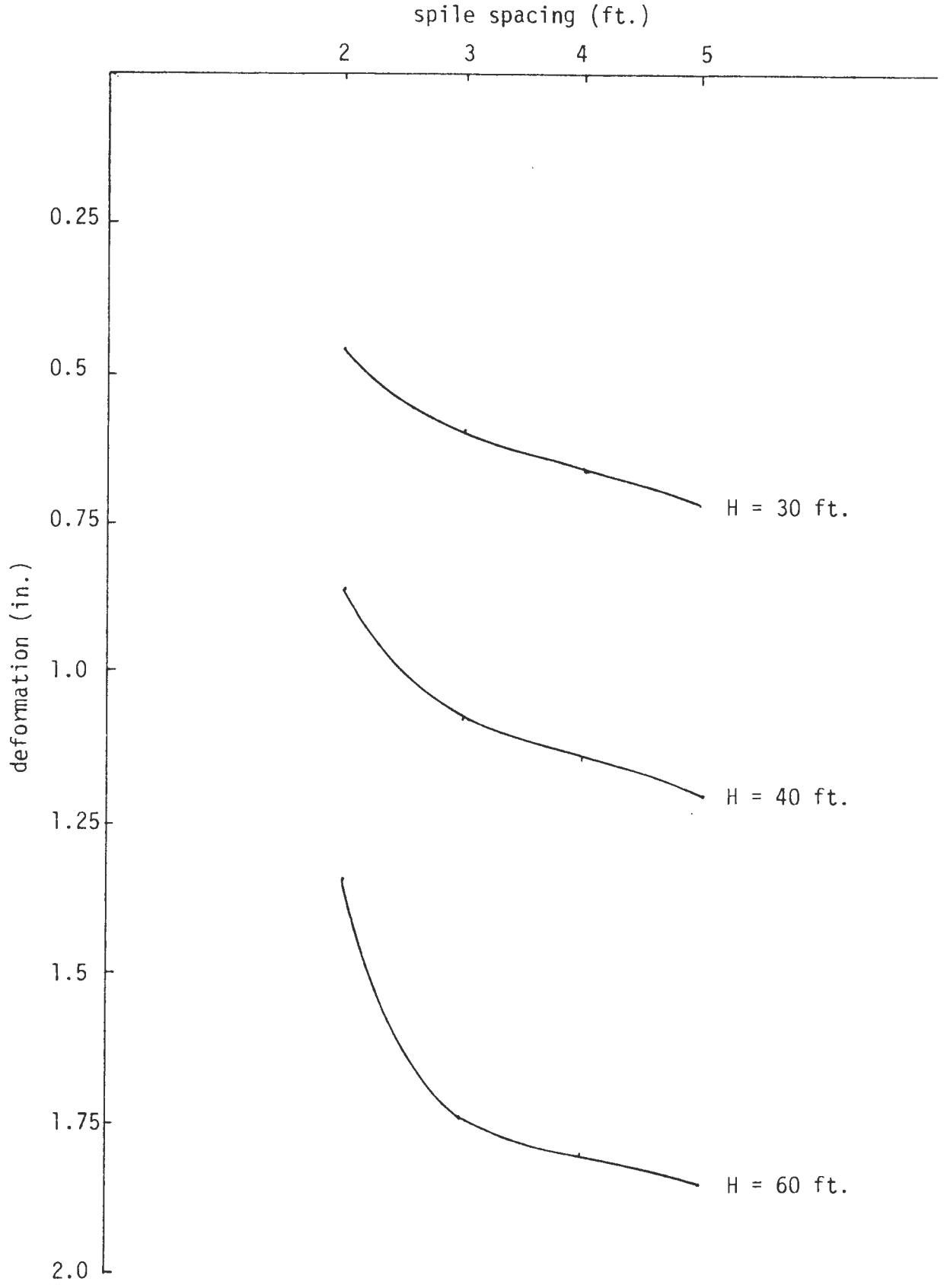

Fig-31 Maximum vertical ground surface movement (soil #3)

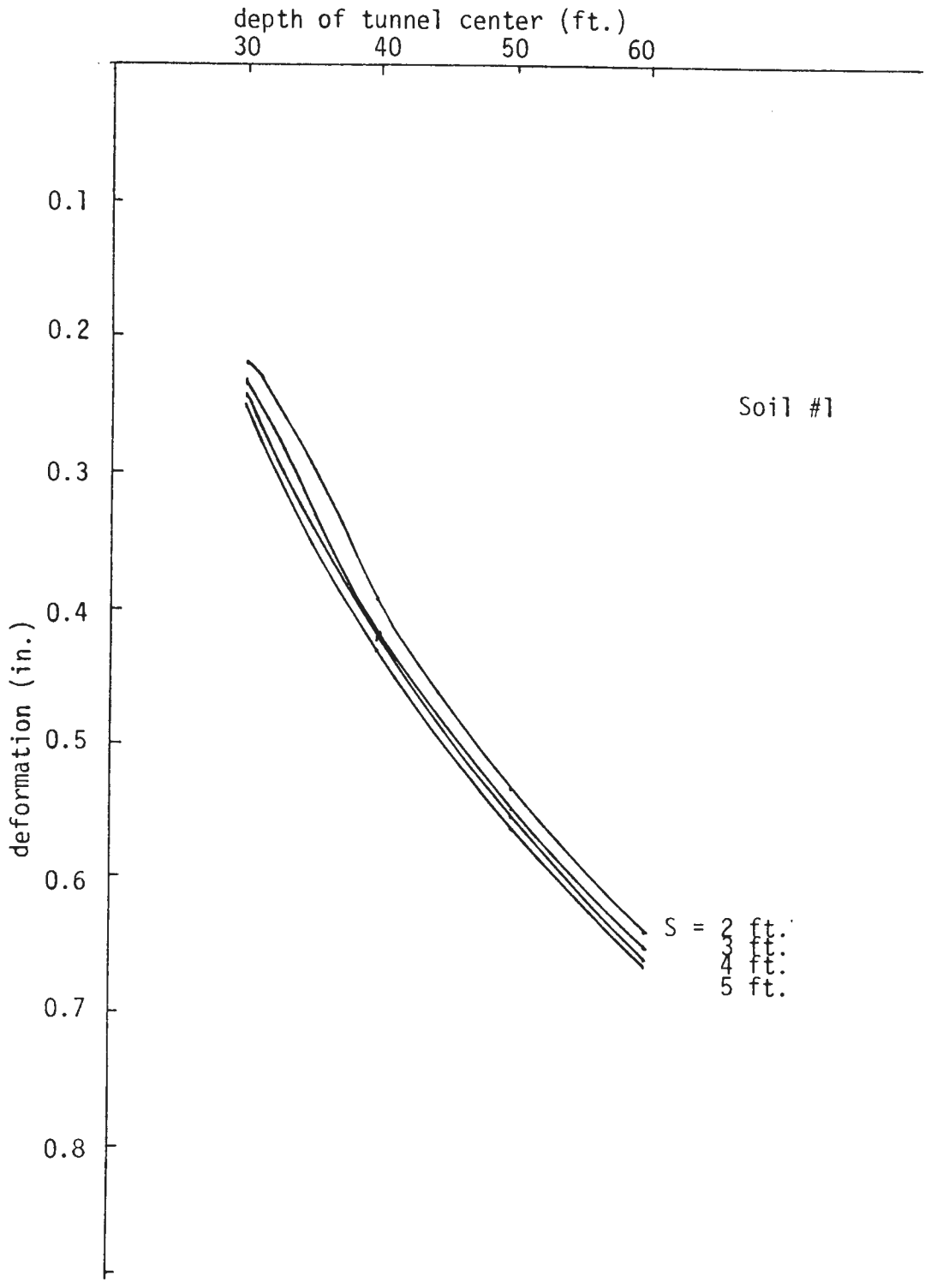

Fig-32 Tunnel crown settlement (soil #1)

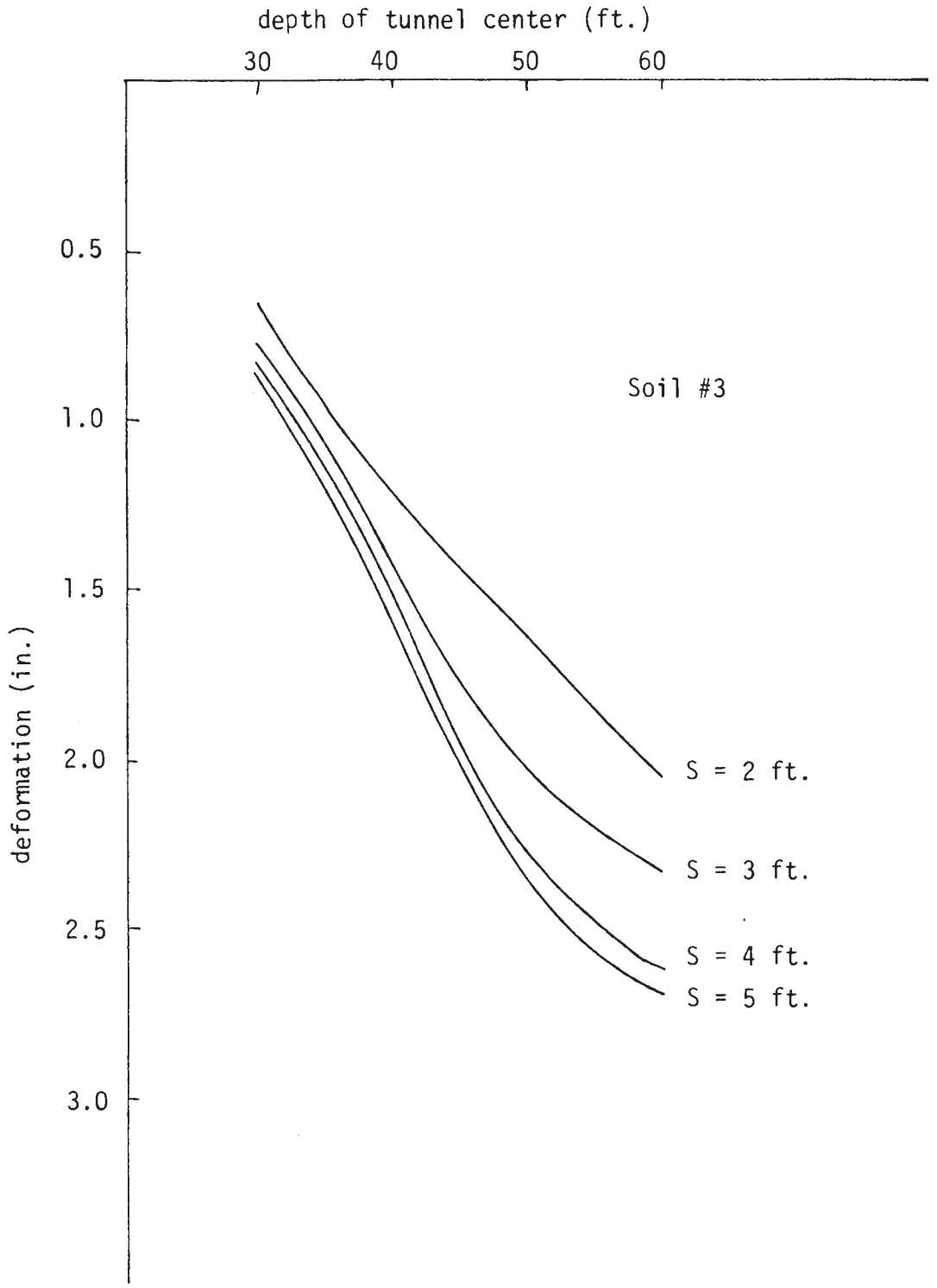

Fig-33 Tunnel crown settlement (soil #3)

The described parametric study is solely based on the results from the analytical finite element method of analysis. The validity of the developed finite element method of analysis therefore must be checked and modified, if necessary, through the comparisons with the model test results and/or field instrumentation.

CHAPTER V

PRELIMINARY CENTRIFUGE MODEL TESTS

Preliminary scale models have been tested in the University of California, Davis geotechnical centrifuge at 60 gravities to simulate a prototype 60 times as large as the model. Various spile configurations were studied to provide insight to the effects that the spile spacing, the length, and the inclination angle have on the serviceability and safety of the tunnel.

This chapter describes: 1) the apparatus used in the tests, 2) methods used in the preparation and execution of tests, 3) preliminary tests and, 4) observations noted in the preliminary tests.

5.1 Apparatus

The apparatus used in the tests to date is composed of the strong sample box that contains the soil model, the excavation system used to form the tunnel, and measurement devices used to monitor the model's deformation.

A) Sample Box

The box which had been used in a prior investigation at University of California, Davis was modified to fit the requirements of the soft ground tunneling study. The box consisted of 3/8 in. aluminum plates on the back, two sides, and bottom, with a 1 in. thick gridded plexiglas front. Room was needed at one side to allow for excavation, so the box's original 17 1/4-inch long dimension was reduced to 13 inches. Mounting holes were drilled in the bottom for use with the fixed bucket, and holes were milled in the sides for the excavation. A safety analysis of the box was required due to the altered geometry and conditions of edge restraint. The nature of centrifuge work, with the high velocities and large momenta imparted to rotated parts, makes it imperative that equipment rupture be utterly avoided.

The safety analysis showed the box to have minimum safety factor of 2.7 at an acceleration of 100 g. The box has since given adequate performance in the centrifuge with all soil conditions at accelerations up to 100 g.

The 45-degree mirror used to view the soil through the plexiglas face was also modified to give a better picture. Early in the study, it was decided that the tunnel should be made adjacent to the plexiglas face so that soil deflections above the tunnel could be monitored.

B) Excavation System

This system consists of wooden blocks embedded in the model. The blocks are pulled by a cable out of the model to simulate the forming of a tunnel cavity. The blocks drop to the bottom of the centrifuge bucket after they exit the box. The cable is wound on a spool turned by a motor-gearbox system (Fig-34).

The excavation system was originally conceived as using pneumatic pressure to provide support for the tunnel section. Pressurized rubber cells along the tunnel were to have been deflated to simulate the excavation. A discussion and preliminary design with this idea showed that: 1) the pressure cells would be hard to make, 2) considerable pneumatic "plumbing" would be required, which would take excessive set-up and dismantling time for each test, and 3) the cost of remote valves, tubes, fittings, and fabrication would have been high. The block-and-cable system was then investigated and found to be practicable using readily available hardware and equipment already acquired for the University of California, Davis centrifuge facility.

The variable speed D.C. motor, 1750:1 stepdown gearbox, and their mounting plate had been used in prior research, and were modified only slightly. The speed control available from the D.C. motor could be useful in future tests to study the effect of tunnel advance rate on deformation.

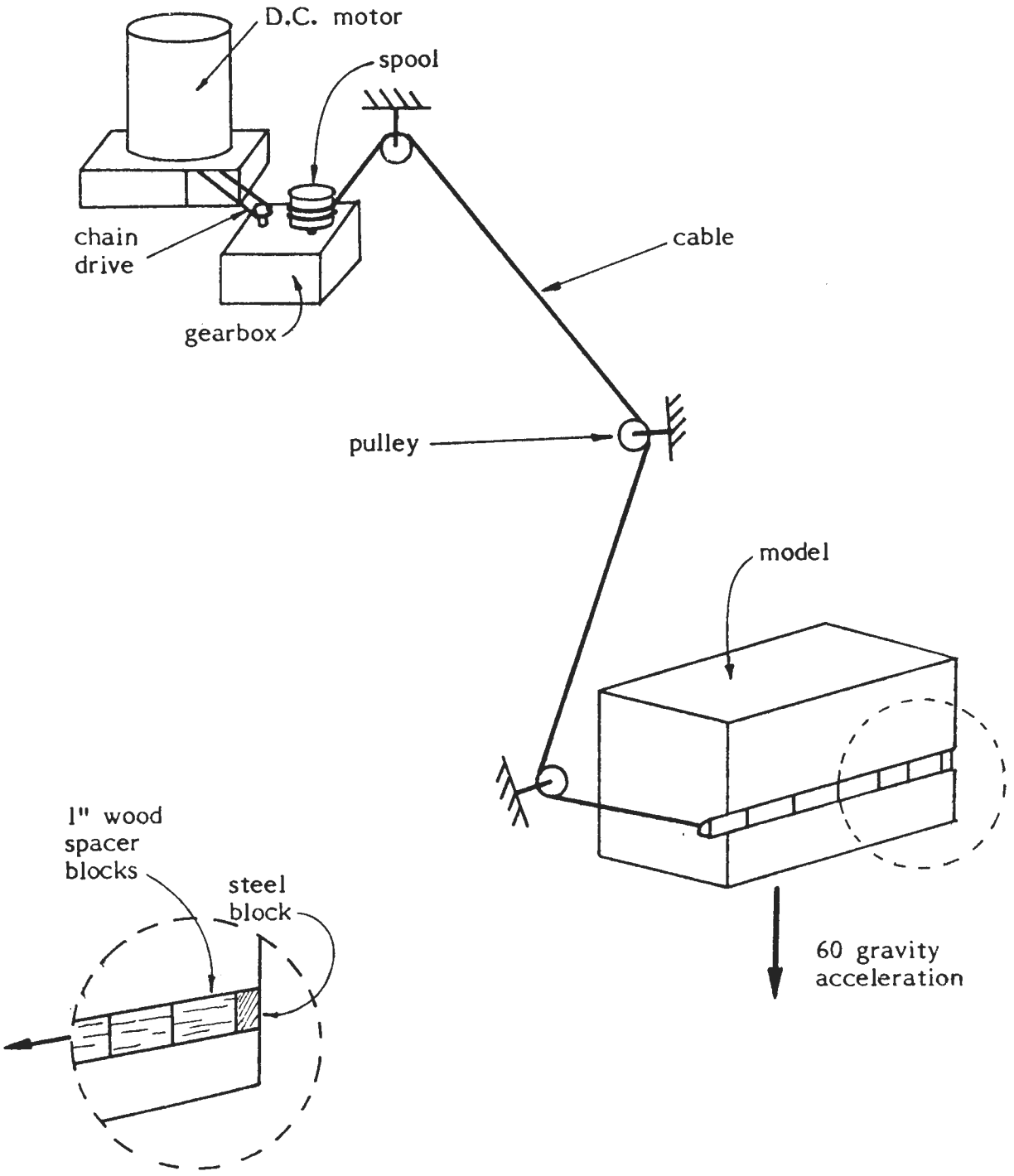

Fig. 34 - Excavation system

The wood and steel spacer blocks are one inch in diameter with three-eighth-inch slots for the cable.

Pulley geometry was designed to minimize the danger of yielding in the supporting eyehooks. Constraints in the design included: 1) the strength of eyebolt material, 2) the positions of existing threaded holes in the fixed bucket, and 3) the size of the eyehooks (less than or equal to the fixed bucket's threaded holes).

The minimum safety factor computed against yielding at the base of any eye-bolt was 2.74 at 100 g. A load test of the system was done using a calibrated spring to measure cable tension. The cable was tensioned up to 438 pounds before a connecting clip broke. No yielding of the bolts or any other part was found. Since the expected maximum tension in actual tests is only 100 pounds, the system elements are quite adequate.

C) Measurement Systems

Instrumentation of the models gave records of in-flight soil deformation on the ground surface and above the tunnel centerline. In addition pre- and post-flight measurements of surface elevation were taken.

Centerline deformations were recorded with a remote-controlled Canon F-1 35 millimeter camera mounted on the centrifuge web. Short intervals between photos were used during the excavation and longer intervals after in order to obtain a deformation "history" during and after the excavation. The deformation was shown with white pinheads placed in the soil on a one-inch grid. Some measure of standup time, the relative period of time before the tunnel is unmanagably deformed, could be obtained from these measurements. Events within the tunnel, including block progress and "fallout" (where a section of the crown falls into the tunnel) can be seen in the still photos.

Surface deflections were measured during flight with a system made especially for this research. Normally, distance measurements are made with linear variable differential transformers (LVDTs). However, LVDTs are unsuitable for measuring soil deflections in the centrifuge because their extensible cores become so heavy that they punch into the soil. A light-weight low-cost transducer, utilizing a light-sensitive element, thin rod, and wide footing (Fig-35) was developed for use in the centrifuge. In addition, a computer-based data acquisition system, utilizing a Radio Shack TRS-80 computer, was used to periodically sample and reduce transducer readings. In-flight surface elevations would be used to determine the time rate of subsidence, the amount of consolidation settlement, and the amount of elastic rebound occurring when flight was stopped.

A video-camera system was used during the test to observe the model. Design and fabrication of a special bracket was required so that the motor, gearbox, still camera, and video camera could all fit on the centrifuge web.

Surface measurements were taken by hand using a rod, a scale, and the grid made for placing pinheads on the centerline. Since surface measurement was rather tedious, and since it was necessary to release the fixed bucket, only two measurements were taken. The first was taken after the centrifuge was run for 30 minutes to consolidate the sample, and the second after the test was completed. It is useful to measure both total and differential settlements as they are main causes of building damage in tunneling.

Fig-36 shows the pictures of various components of the centrifuge used in the study.

5.2 Testing Procedures

In order for results to be of value in analysis, the material properties and stress histories of models must be identical from test to test. Therefore,

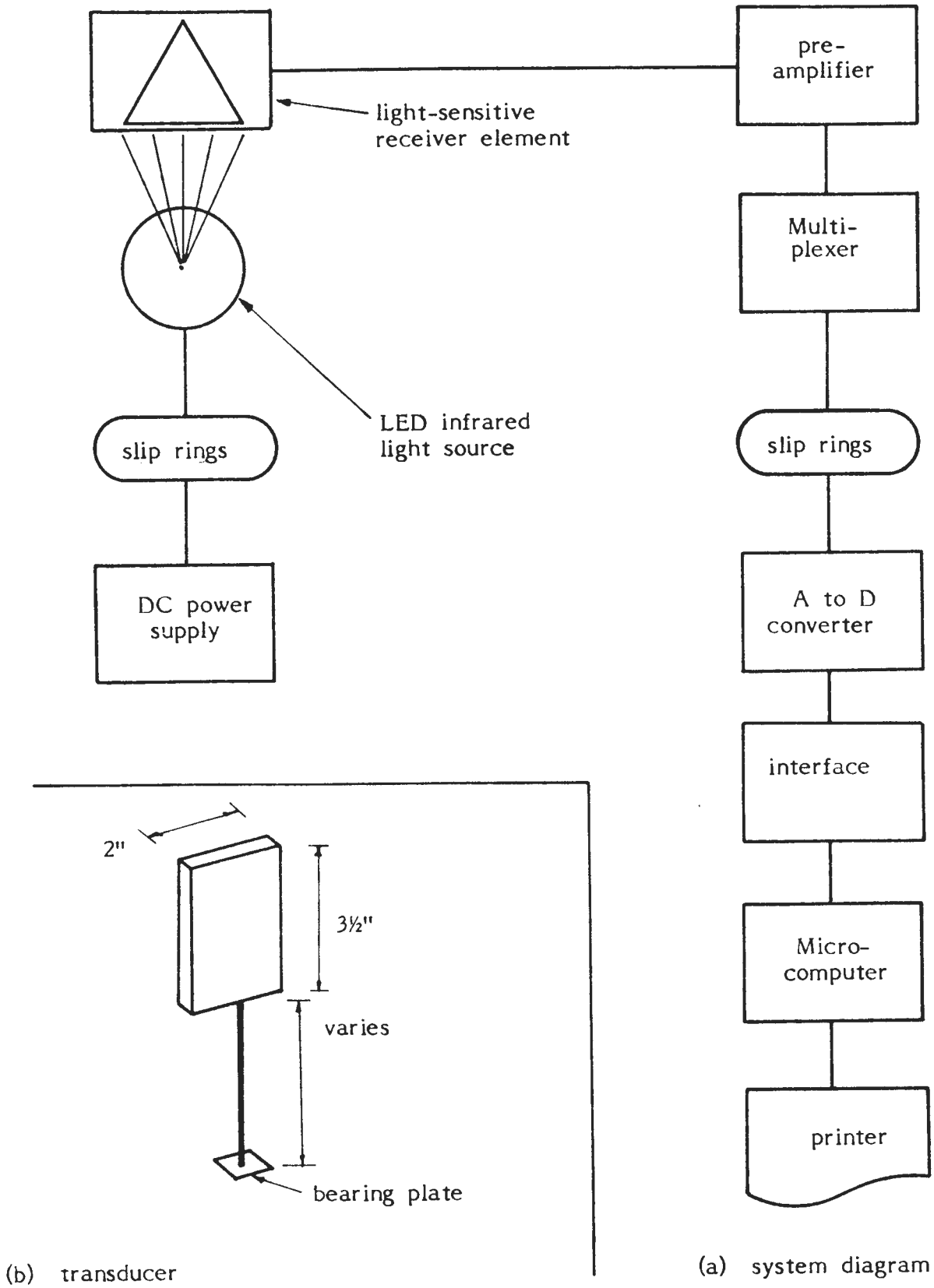

Fig. 35 - In-flight surface measurement system

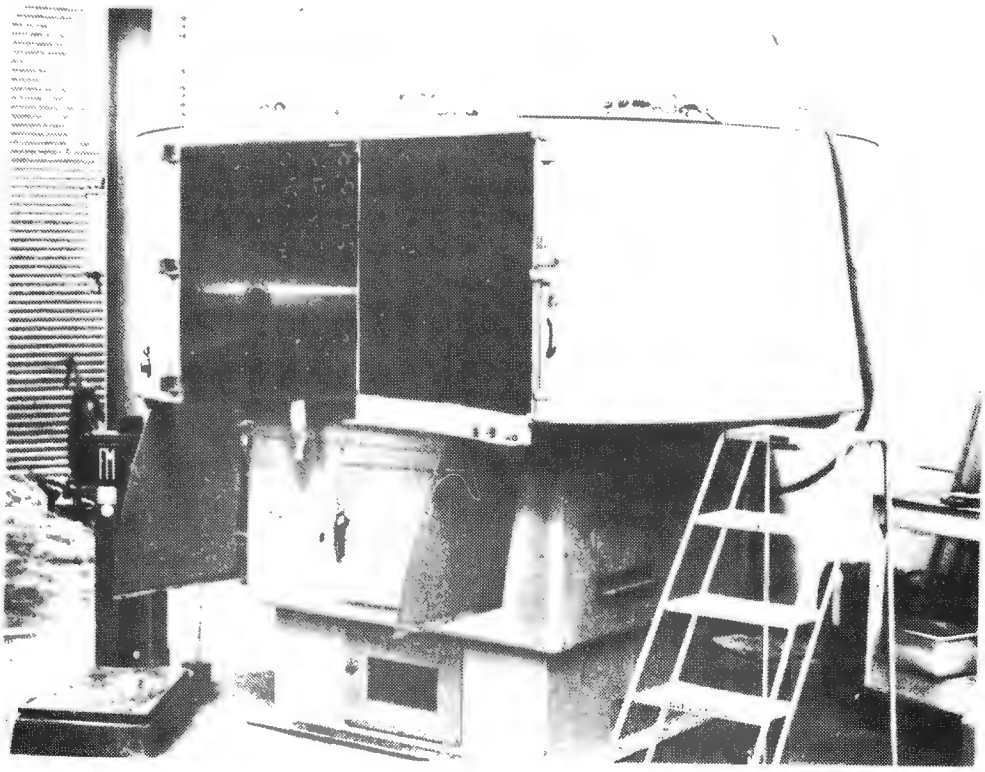

A. centrifuge

B. control panel

Fig-36. Various Components of Centrifuge

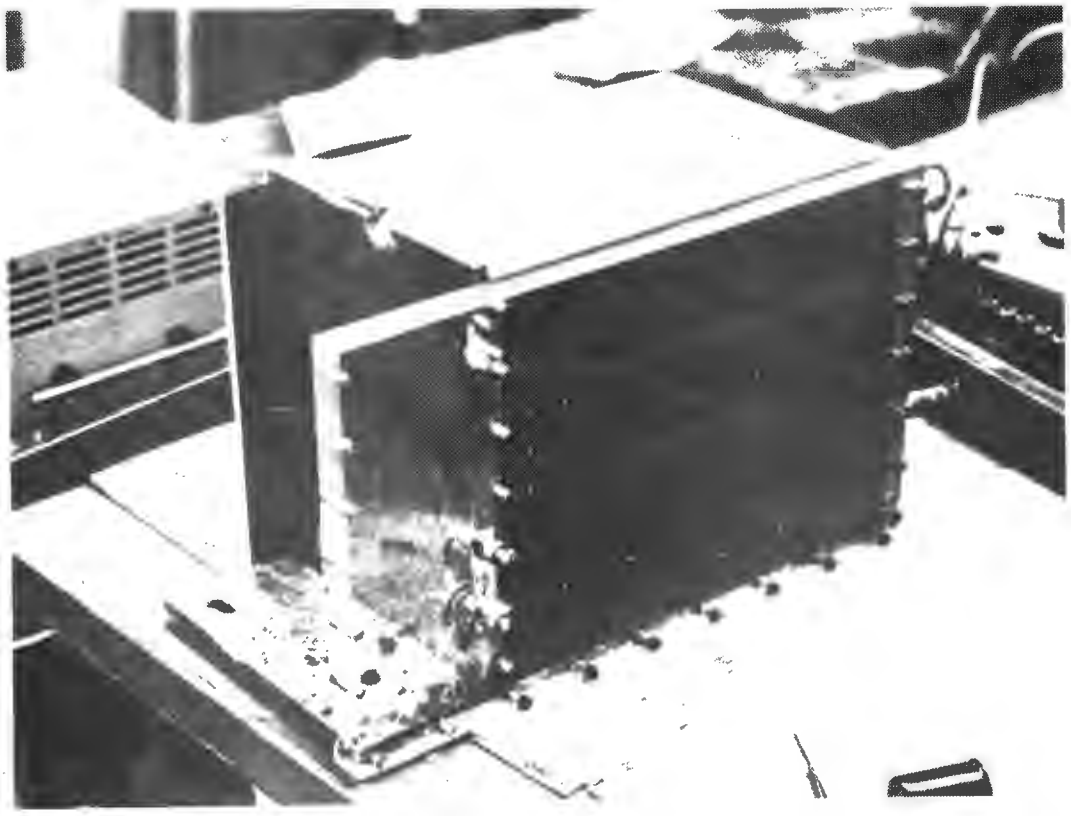

c. model with plexiglas

Fig-36 continued

procedures were established for preparing the soil, building the model, excavating the tunnel, and measuring deformations.

A) Soil Preparation

The soil used was the Yolo Loam, a sandy, silty clay of moderate plasticity. Before use in models the clay was crushed and passed through a #40 sieve to remove coarse sand and occasional gravel. When the soil was to be used in a sample it was wetted with de-ionized water to approximately the water content desired; then a water content test was performed and more water was added if necessary to reach the right content. De-ionized water was used to prevent the buildup of ions in the soil over time. Before the soil was compacted, it was cured for three to five days to allow the sample to become homogeneous.

A water content of 21.5 percent was found, in preliminary tests, to be the most suitable for modeling at 60 g.

After each test the compacted soil was cut from the sample box, put in a pan, soaked for three days, oven-dried, rewetted, and crumbled by hand to reduce the loss of fines found to occur in machine crushing. It was then used in another test.

B) Compaction

One or two days before the model test the sample was statically compacted with a Tinius Olson compression/tension testing machine. The soil was placed in the sample box in lifts of set volume ("four small scoops") and spread evenly by hand. The rate of compression was controlled so that models were alike from one test to the next. At first, since the soil was very soft and loose, the strain rate was held at a hydraulic valve setting of 30. When the compressive force reached 1000 pounds, the valve setting was reduced to 10. This setting was held until the force reached 2000 pounds. Each compacted soil layer was slightly less than one inch thick.

The plexiglas side of the sample box was first protected from scratching by a metal plate between it and the soil. However, it was found that a thin mylar sheet, along with careful removal of the compression plate (which pushes the soil down), could prevent damage to the plexiglas. Mylar sheets were also placed on the side plates to reduce boundary friction during compaction and testing.

If there was a curing period between compaction and testing, a small cup of water was placed on the surface of the model and the sample box was sealed with a top plate and taped to prevent moisture loss.

C) Tunnel and Spile Construction

After compaction the plexiglas plate and the mylar facing were removed from the sample box to expose the soil face. A one-inch diameter model tunnel was sculpted at the proper depth (about 3.5 inches from ground surface to tunnel centerline) in such a way that the spacer blocks would fit snugly. A wooden rod cut from the same round stock as the blocks was used to check the fit.

After the tunnel cavity was made, spiles were installed. Spacings were marked with a scale and a spatula, and angles were controlled with a small drafting triangle. The spiles were pressed into the soil until the end was about 1/16 in. beneath the tunnel face. This negated the possibility of spiles catching on a spacer block as it passed.

Originally, spiles were made by putting a piano wire (for tensile reinforcement) in a nail hole; the hole was then filled with injected aluminum sulfate grout. Although this process simulated actual practice, on this small scale, it was found to give stiff, large, ill-shaped spiles, in addition to being very tedious. Next, epoxy-and-sand coated finishing nails were tried. They had the advantage of being reusable, easily inserted, and uniform, but were still relatively

stiff and too large. The spiles actually used were made from epoxy-and-sand coated number 4 insect pins. Their flexural stiffness is not large, but since the dominant mechanism of spile reinforcing is axial force, they are suitable. The epoxy-and-sand coating was used to give a good frictional bond between the spile and the soil.

D) Installation

First, the motor, gearbox, and spool were installed in the centrifuge and anchored very firmly to the centrifuge web. Then the model bucket, containing the model and the 45° mirror, was lifted into position. Next, the still camera was loaded with film and put in its jig. The video camera was moved to the tall bracket and installed so as to rest on the still camera jig and a spacer plate. When the video camera bracket was bolted down, it pressed on the still camera jig. Both cameras had to be adjusted to give a proper picture before they were bolted down.

Since the model, box, and bucket may rotate at up to 335 rpm, a counterbalance bucket must be used to reduce cyclic forces on the centrifuge rotor shaft and bearings. Normally, swing-up buckets were used with the University of California, Davis centrifuge, so a dynamic balance was required to compensate for the center of gravity change as the buckets swing up during rotation. The cohesive soil used for these tunnel experiments made it possible, however, to use the fixed buckets, which made only a static balance necessary. This was because all the components of both the model side and the balance side remained in the same position before, during, and after rotation. The use of static balance simplified and shortened the installation process.

To perform a static balance, all the requisite equipment were installed; allowed the web to "float" by releasing four 3/4 in. bolts that connected the rotor shaft to the web; and set the web up on its "knife edges" that acted as fulcrums. Then weights were added to one bucket or the other until balance was achieved. When the operator was satisfied that the arms were in balance, he released the knife edges, clamped the web to the rotor shaft, and then ran the test.

E) Running the Test

When all parts and pieces were secure, the centrifuge was started. The rotational speed was adjusted upward until a centrifugal gravity resultant of 60 g acted on the model in the radial direction, away from the center of the rotor. The 60 g acceleration simulated a tunnel of 60-inch diameter with its centerline at a depth of 225 inches (18.75 feet) and 195 inches (16.25 feet) of cover above its crown. The model was held at 60 g for a 30-minute "consolidation" period that caused a natural stress distribution. After the consolidation period the centrifuge was stopped, surface elevations were measured, and the model was inspected. This took about 45 minutes.

After another safety check the model was again accelerated up to 60 g. Excavation was started after another consolidation period of 10 minutes. During both the 30- and 10-minute consolidations, still photos were taken to monitor consolidation settlements. Data from these photos could be used to separate settlement due to tunneling from that due to consolidation, so a true picture of the behavior could be obtained.

To date, the rate of excavation has been one inch in 40 seconds. Still photos were taken at these intervals during excavation. After the

tunnel was entirely excavated the time between photos was extended to reflect the anticipated slowdown in settlement as time passed. The excavation process, including the 10-minute consolidation, the excavation itself, and the observation period, was about 50 minutes.

F) Dismantling and Data Reductions

After each test all equipment must be removed to make way for the next test. The first task in dismantling the test is to remove the model and measure the post-flight surface elevations. Both fixed buckets are then removed and next the motor and cameras.

Surface measurements were taken as soon as possible after the test to minimize the chance of accidental damage or shrinkage due to moisture loss. After the centrifuge was cleared, the model was "dissected" to visually examine qualitative aspects of its behavior. When the dissection was complete, the soil was broken up into small (about 2 inch) chunks, placed in a pan, and soaked with de-ionized water in preparation for its next use. The equipment, including the sample box, was cleaned and otherwise put in order.

Surface elevations before and after the excavation were reduced to yield the total settlement at 96 points on a one-inch grid. After reduction, contours could be drawn to show the pattern and magnitude of settlements.

No data reduction was necessary for the in-flight surface measurements, since the computer-based data acquisition system did the task automatically. A plot of settlement versus time could be made from the measurements in order to show how the surface deformed as excavation progressed. These data could also be compared to the total settlement data as a check for pattern and elastic rebound.

Still photo negatives were used to print enlargements at the Civil Engineering photo lab. The enlargements could be used to compare settlement from one time to the next. A settlement history could be prepared for analysis by tabulating and plotting the positions of pinheads over the entire duration of the test.

5.3 Preliminary Tests

A) The Necessity for Preliminary Models

Fourteen preliminary models were built and tested as the apparatus and procedures were being developed. The preliminary tests were necessary to determine:

1) the best compaction method,
2) the best water content for tests,
3) the stability of different spiles,
4) the excavation rate,
5) methods for obtaining and reducing data, and,
6) the adequacy of the measurement program and systems.

B) Description of Tests

The fourteen model tests run to date are summarized in Table-10. The information presented includes the water content of the soil, the acceleration (g-level), spile configuration, and remarks significant to the development process.

5.4 Observations and Summary

A) Observations

Thus far, the preliminary model test results are qualitative in nature. They provide valuable information as to how the spile reinforced soft-ground

TABLE-10

Preliminary Centrifuge Model Tests

Model No.	Water Content (%)	Gravity Level (g)	NxLxSxA*	Remarks
1	Dry	1	-	Cake Compaction. Crumbles easily.
2	Wet	1	-	Cake compaction. Compaction model.
3	11.9	60	4xl"xl"x45° 0x0x0x0	Pre and Post-flight surface elevations = 6 in. Settlement on unreinforced side is 2-3 times that on reinforced side.
4	14.7	90	1xl"xl"x90° 2xl"xl"x45°	Post-flight surface measurements. Settlement with vertical spiles about twice that for angled ones.
5	14.7	90	-	Calibration test for consolidation
6	14.0	1	-	First try with excavation system. Failed due to faulty motor controller
7	14	1,60	0x0x0x0	Excavation system failed at 1 g when eyehook pulley supports ruptured. System was redesigned, then was OK in tests at 1 g and 60 g.
8	14	60	5x.9"x0.8"x30° 0x0x0x0	3-penny nails used as spiles. Mylar sheets used on boundaries. No excavation; post-flight surface measurements.

*No. of spiles x length of spile x axial spacing x inclination angle.

Table-10 continued

Model No.	Water Content (%)	Gravity Level (g)	NxLxSxA*	Remarks
9	29	60	same as 8	Very wet; reinforcement seemed to have no effect; consolidation large; too wet for meaningful results. Flow into tunnel filled it immediately. Excavation at 40 sec/in.
10	24.8	60	same as 8	Tunnel closed rapidly. Spiled section seemed to close slower. Time-dependency question makes still camera essential. Excavation at 40 sec/in.
11	20	60	5x.9"x1/2"x30° 0x0x0x0	Insufficient difference between spiled and unspiled sections. Excavation at 40 sec/in. Test may have been too brief to show different behavior.
12	21.4	60	5x.9"x1/4"x30° 5x2"x1/2"x30° 0x0x0x0	Distinct difference between spiled and unspiled sections. Excavation at 40 sec/in. Use 21.5% in future tests. Long spiles gave least tunnel deformation.
13	21.5	60	0x0x0x0	First use of still camera. Excavation at 40 sec/in. Tunnel closed entirely about 15 minutes after excavation.
14	21.5	60	5x2"x1/2"x30°	Good surface measurements and still photos. 40 sec/in. excavation. Settlements smaller than in Model 12, and occurred at much slower rate.

*No. of spiles x length of spile x axial spacing x inclination angle.

tunnel system can be meaningfully modeled and tested in the centrifuge. Furthermore, additional observations were made of the models to relate the surface depression and possibility of tunnel opening deformation to the installation of reinforcement. These are illustrated as follows:

1. Pattern of surface deformation

Surface settlement was largest directly above the tunnel as expected. Furthermore, the profile transverse to the tunnel axis approximately corresponds Gaussian error function with a constant component, i.e.

$$S = S_c + S_{max} e^{-nx^2}$$

This distribution has some theoretical justification and has been observed in actual construction (11). The constant component corresponds to consolidation settlement, which was quite large in the wet models. This expression may be fitted to the test data by a combination of least-squares and bounding numerical methods for comparison of tunnels reinforced differently. Fig-37 shows the example of the surface deformation measurements obtained during the test.

2. Deformed tunnel

In dry samples the crown failed by "fallout" which corresponds to spalling or loosening. In wet samples soil flowed into the tunnel cavity, but rather than flowing from the crown, the plastic soil flowed from about the upper quarter point. Another puzzling feature of the wet models is the presence of single deep cracks at the side and running parallel to the tunnel. Fig-38 shows the deformed shapes of the tunnel openings with and without spiling reinforcement.

3. Tension cracks

One surprising feature of the preliminary tests was that tension cracks appeared both above and below the tunnel. Such cracks had been expected above, but not below. The wetter models showed more evidence of cracking, and in very

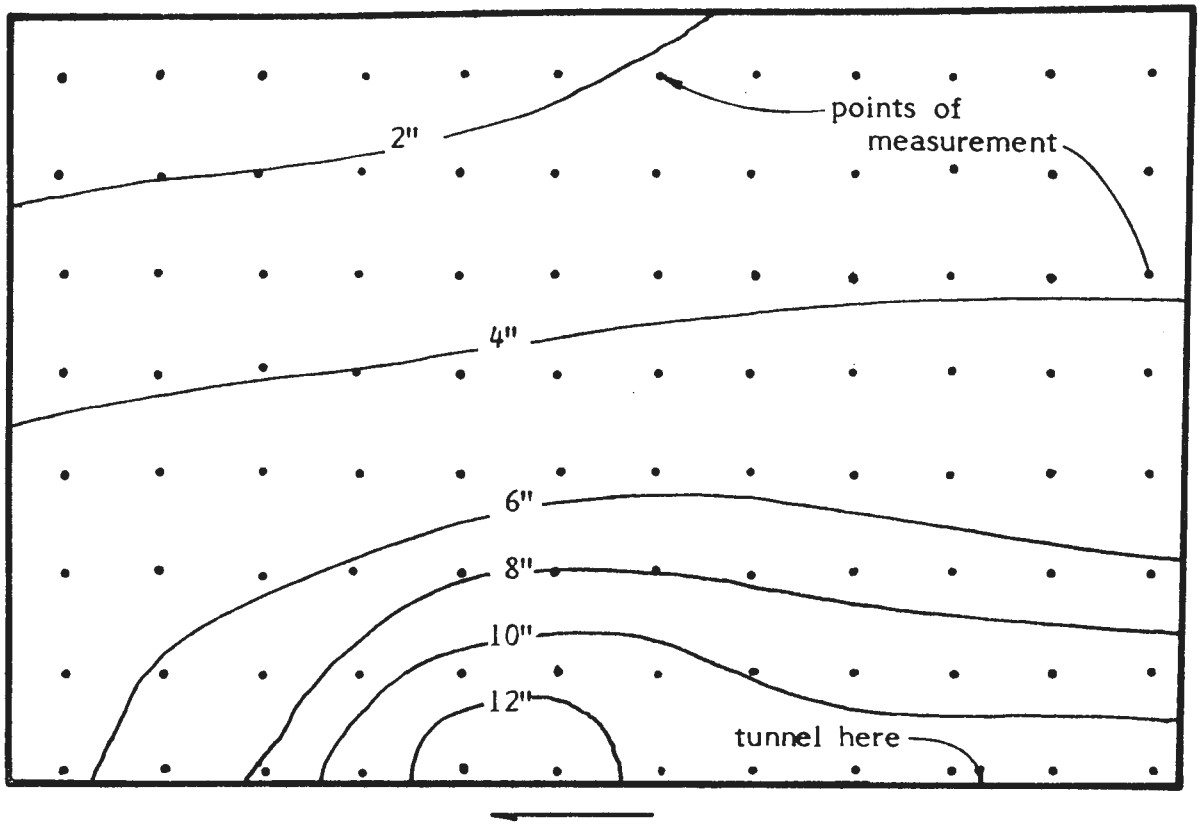

(a) surface settlement (scaled)

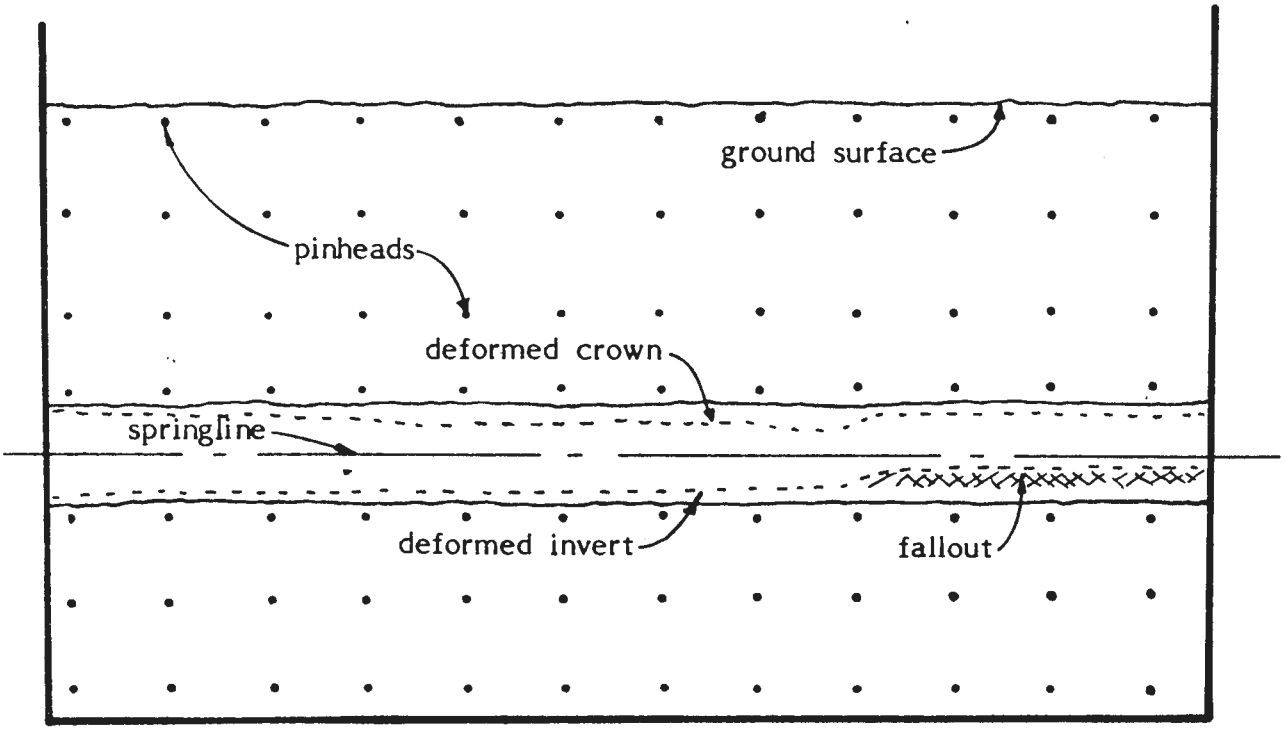

(b) elevation

Fig. 37 - Model 13 (scale: 1" = 2")

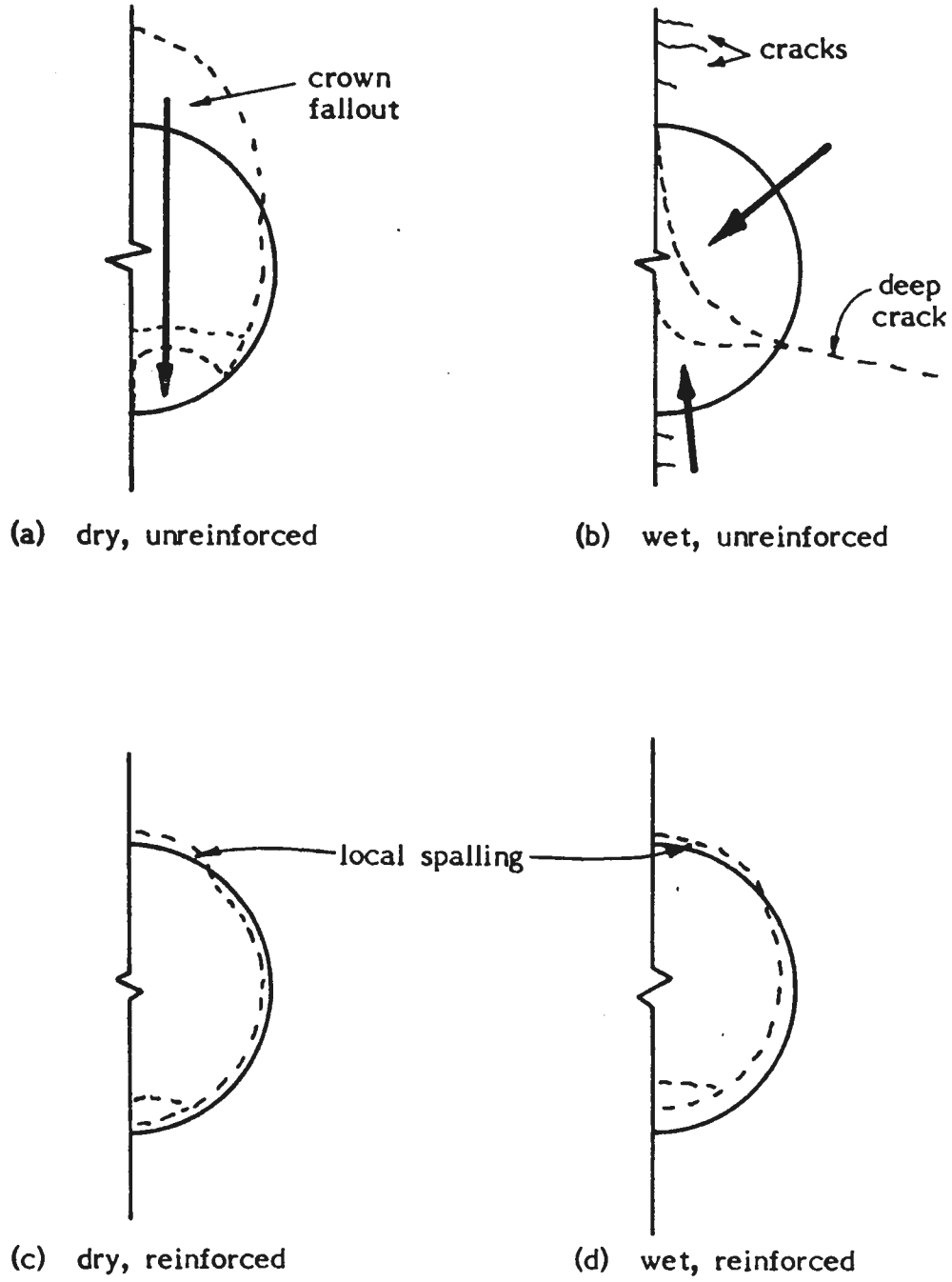

(a) dry, unreinforced

(b) wet, unreinforced

(c) dry, reinforced

(d) wet, reinforced

Fig. 38 - Deformed tunnel section

wet samples cracks appeared on the ground surface. Models 12 and 13 had the same water contents (21.5 percent) and excavation histories but were reinforced and unreinforced, respectively. Model 13 had an extensive mesh of fine cracks, whereas model 12 showed no evidence of cracking whatsoever.

B) Summary

Druing the course of the study, the soft-ground tunneling research carried out at University of California, Davis, has involved,

1) the conception, design and manufacture of apparatus to be used in centrifuge model testing. These include the sample box, excavation system, and the measurement system.
2) a series of 14 preliminary centrifuge model tests to develop the optimum conditions needed for soil compaction, moisture content and the installation of spile reinforcement.
3) a basic understanding of the modeled soft ground tunnel behavior. and
4) the development of numerical data reduction schemes.

These accomplishments are vital to the detailed quantitative centrifuge model tests to check the developed analytical models described in Chapter II.

CHAPTER VI

CONCLUSION AND SUMMARY OF WORK

This report presents the results of the preliminary investigation of the spiling reinforcement system in soft ground tunneling. It provides a synthesis of principles and knowledge, and a plan for developing and testing design procedures to enhance prospects of the system for implementation in the field.

The development of the generalized plane strain finite element method of analysis, including the composite element for the modeling of reinforced soil elements and the membrane element for the modeling of the shotcrete concrete lining, the results of the comparison of the behaviors between the spile reinforced tunnel and the unreinforced tunnel, the major findings from the parametric study, and the development of the centrifuge model testing program, including the modeling process of tunneling and spiling reinforcement, and the simulation of the excavation procedure in flight, are described in this report.

The validity of the developed analytical models however must be verified through the comparison with the centrifuge model tests and/or the field instrumentation. It may then be possible to make extensions and modifications of the developed analytical models. Once the analytical models are found to be successful, the results can then be used for the formulation of the design method of the spiling reinforcement system in soft ground tunnels and the formulation of the ground surface settlement prediction.

REFERENCES

1. Bang, S., "Analysis and Design of Lateral Earth Support System," Ph.D. Thesis, University of California, Davis, 1979.

2. Bang, S., C.K. Shen and K.M. Romstad, "Analysis of an Earth Reinforcing System for Deep Excavation," Transportation Research Record, No. 749, 1980.

3. Breth, H., "Tunneling in Soft Ground," Special Session 2, 9th ICSMFE, Tokyo, 1977.

4. Cording, E.J., and W.H. Hansmire, "Displacements Around Soft Ground Tunnels," Proc. 5th Panamerican Congress on SMFE, Session IV, Nov., 1975.

5. Duncan, J.M., and K.S. Wong, "Hyperbolic Stress-Strain Parameters for Non-Linear Finite Element Analysis of Stresses and Movements in Soil Masses," Report No. TG-74-3, Univ. of California, Berkeley, 1970.

6. Grant, R., J.T. Christian, and E.H. Vanmarcke, "Differential Settlement of Buildings," ASCE, Vol. 100, GT9, 1974.

7. Korbin, G.E., and T.L. Brekke, "A Model Study of Spiling Reinforcement in Underground Openings," Tech. Report MRD-2-75, Missouri River Div., Corps of Engineers, Apr., 1975.

8. Korbin, G.E., and T.L. Brekke, "Field Study of Tunnel Prereinforcement," ASCE, Vol. 104, 1978.

9. Muller, L., "Soft Ground Tunneling Under Buildings in Germany," Vol. 1, 9th ICSMFE, Tokyo, 1977.

10. O'Rourke, T.D., E.J. Cording, and M. Boscardin, "The Ground Movements Related to Braced Excavation and Their Influence on Adjacent Buildings," Report No. DOT-TST-76T-23, Aug., 1976.

11. Peck, R.B., "Deep Excavation and Tunneling in Soft Ground," 7th ICSMFE, State-of-the-Art report, 1969.

12. Polshin, D.E. and R.A. Tokar, "Maximum Allowable Non-Uniform Settlement of Structures," Proc. 4th ICSMFE, Vol. 1, 1957.

13. Pordovan, G., and Pigorini, B., "The Olympia Tunnel on the Autostrade dei Trafori: Consolidation Under Difficult Conditions," Proc. of the Int. Tunnel Symposium, Tokyo, 1978.

14. Romstad, K.M., L.R. Herrmann, and C.K. Shen, "Integrated Study of Reinforced Earth - I," ASCE, GT5, May, 1976.

15. Skempton, A.W., and D.H. MacDonald, "Allowable Settlement of Buildings," Proc. Instn. Civil Engrs., Part 3, Vol. 5, 1956.

DOT/RSPA/DMA-50/83/15

REQUEST FOR FEEDBACK TO
The DOT Program Of University Research

This booklet is intended to serve as a reference source for transportation analysts, planners and operators. Your comments will be reviewed by the persons responsible for writing and publishing this material. Feedback is extremely important in improving the quality of research results, the transfer of research information, and the communication link between the researcher and the user.

YES	NO	
☐	☐	Did you find the report useful for your particular needs? If so, how?
☐	☐	Did you find the research to be of high quality?
☐	☐	Were the results of the research communicated effectively by this report?
☐	☐	Do you think this report will be valuable to workers in the field of transportation represented by the subject area of the research?
☐	☐	Are there one or more areas of the report which need strengthening? Which areas?
☐	☐	Would you be interested in receiving further reports in this area of research? If so, fill out form on other side.

Please furnish in the space below any comments you may have concerning the report. We are particularly interested in further elaboration of the above questions.

Cut Out Along This Line

COMMENTS

Thank you for your cooperation. No postage necessary if mailed in the U.S.A.

RESEARCH INTEREST

PLEASE CHECK YOUR AREAS OF INTEREST. YOU WILL BE NOTIFIED AS NEW REPORTS ARE PUBLISHED.

TRANSPORTATION

- ☐ Air
- ☐ Highway
- ☐ Maritime & Ports
- ☐ Mass Transit
- ☐ Pipeline
- ☐ Rail

ECONOMIC REGULATION

- ☐ Air Carrier
- ☐ Motor Carrier
- ☐ Railroads

TRANSPORTATION STUDIES IN SPECIAL AREAS

- ☐ Advanced Technology
- ☐ Energy
- ☐ Environment
- ☐ Facilities & Terminals
- ☐ Hazardous Materials
- ☐ Safety
- ☐ Tunnelling
- ☐ Construction, Rehabilitation & Maintenance
- ☐ Efficiency, Productivity & Innovation
- ☐ Elderly, Handicapped & Disadvantaged
- ☐ Freight, Goods Movement & Commodity Flow
- ☐ Modeling - Demand, Supply & Traffic
- ☐ Rural Development, Planning & Policy
- ☐ Urban Development, Planning & Policy

☐ OTHER (PLEASE LIST) _____

_____

_____

U.S. DEPARTMENT OF TRANSPORTATION
Research and Special Programs Administration
Washington, D.C. 20590

NO POSTAGE NECESSARY IF MAILED IN THE UNITED STATES

BUSINESS REPLY MAIL
FIRST CLASS Permit #14561 Wash., DC
POSTAGE WILL BE PAID BY RSPA

Dr. Lloyd J. Money, DMA-50
Director, Office of University Research
U. S. Department of Transportation
400 7th Street, S. W.
Washington, D. C. 20590

PLEASE LIST YOUR NAME AND ADDRESS.

NAME _____

TITLE _____

ORGANIZATION _____

STREET _____

CITY, STATE, ZIP CODE _____